ASPECTS OF SHEAR STRAIN IN THE EAST RAND BASIN

BY

PAIGE ANNE PITTS

Dissertation undertaken in fulfillment of the requirements

for the degree

MASTER IN THE NATURAL SCIENCES

in

GEOLOGY

in the

FACULTY OF NATURAL SCIENCES

at the

RAND AFRIKAANS UNIVERSITY

Supervisor: Prof. C. Roering

Co-supervisor: Prof. J. Barton Jnr.

May 1990

"... it is clearly prudent to determine shear criteria at a local scale, then to approach the regional kinematics by sampling at close intervals, so as to be able to detect variations and integrate them accordingly."

Cobbold and Gapais, 1987.

"... it is indeed too arduous, for the effort must be invariably so much greater than the possible achievement."

Joseph Conrad, 1920.

- for the long-suffering loved ones of all geologists ever possessed by the demon of the East Rand Goldfield!

ABSTRACT

Rocks of the Witwatersrand Supergroup in the northern portion of the East Rand Goldfield have been examined on surface and in underground exposures in an attempt to establish the chronology, movement vectors, amount of strain and displacement associated with bedding parallel faults. It was found that more than one age of movement occurred along most of the non-bedding parallel fault planes with normal, reverse and strike-slip senses of motion. The ductile bedding plane faults are manifested in all lithologies, but the shale units have, in particular, acted as a locus for shearing and it is suggested that they should be regarded as phyllonites.

Bedding parallel faults are generally characterised by the presence of quartz veins and the development of phyllosilicates. They are categorised as mylonitic quartz schists. Syntectonic fault restricted quartz veins generally parallel the foliation, developed in the plane of flattening, and aided the movement of overlying strata during fault formation.

Kinematic indicators imply a broad northerly updip movement on the bedding parallel faults; implying they are thrust faults. Directionally specific kinematic indicators display at least two directions of thrust movement in the Central Rand Group, one to the NE and a second to the N to NW. The second group may represent two overlapping directions of movement. Only NE thrust movement are indicated in the West Rand Group. The NE thrust

event occurred after emplacement of Ventersdorp dykes and before deposition of the rocks of the Black Reef Quartzite Formation. The N thrust fault event occurred after deposition of the Black Reef Quartzite Formation and before deposition of Karoo age rocks. A possible third event of Bushveld Igneous Intrusion age may be manifested as thrust faults towards the NW.

The contact between the Central and West Rand Groups has acted as a major décollement during the N thrust event. The folds in this region may initially have been the result of thrust faulting towards the NE. Tilting of the fold axes during the postulated NW event is possible.

The resultant displacement in this region arising from the thrust faulting is estimated as ± 9km.

SAMEVATTING

Gesteentes van die Witwatersrand Supergroup in die noordelike gedeelte van die Oos Randse Goudveld is aan die oppervlak en in ondergrondse blootstellings ondersoek in 'n poging om die kronologie, bewegingsrigtings, hoeveelheid van vervorming en verplasing wat met die laagvlak verskuiwings geassosieerd is, vas te stel. Daar is vasgestel dat meer as een ouderdom van beweging langs meeste van die nie laagvlak verskuiwings vlakke plaasgevind het. Hierdie bewegings het langs op-, af- en wringverskuiwings plaasgevind. Die rekbare laagvlak verskuiwings kom voor in al die litologieë, maar veral die skalies het as n lokus vir skuifskeuring gedien dat hulle eerder as filloniete beskou moet word.

Die laagvlak verskuiwings word in die algemeen gekenmerk deur die teenwoordigheid van kwartsare en die vorming van die fillosilikate. Hierdie gesteentes word as milonitiese kwartsskiste beskryf. Syntektoniese kwartsare, wat tot die verskuiwingssone beperk is, is meestal parallel aan die foliasie, het in die vlak van afplatting ontwikkel, en het bygedra tot die beweging van die oorliggende strata tydens verskuiwing.

Bewegingsrigting-aanwysers dui in die algemeen n noordelike bewegingsrigting aan. Hierdie rigting is teenoorgesteld aan die hellingsrigting van die verskuiwingsvlak. Dit beteken dat

hierdie strukture oorskuiwings is. Daar kan ten minste twee rigtings van oorskuiwing in die Sentrale Rand Groep geindentifiseer word, een na die NO en 'n tweede in 'n N tot NW rigting. Die moontlikheid bestaan dat laasgenoemde bewegingsrigting twee verskillende rigtings verteenwoordig wat mekaar oorvleuel. Slegs verplasing na die NO is aangedui in die Wes Rand Groep. Oorskuiwing in die NO rigting het na die indringing van Ventersdorp gange en voor die afsetting van die gesteentes van die Black Reef Kwartsiet Formasie plaasgevind. Die oorskuiwings in 'n N rigting het egter na die afsetting van die Black Reef Quartzite Formasie en voor die van die Karoo gesteentes plaasgevind. Die moontlike derde rigting van oorskuiwing, wat in 'n NW rigting is, is waarskynlik van Bosveld Stollingskompleks ouderdom.

Die kontak tussen die Sentrale en Wes Rand Groepe het as n skeidingsvlak opgetree tydens die oorskuiwings in n N rigting. Plooie wat in die omgewing voorkom kan oorspronklik as gevolg van oorskuiwing na die NO onstaan het. Die orientasie van die plooi-asse het moontlik verander tydens die beweging na die NW.

Die uiteindelike verplasing in hierdie gebied, as gevolg van die oorskuiwings, word as 9km beraam.

TABLE OF CONTENTS

1. INTRODUCTION

The re-opening of old mines together with the need to increase the existing structural data base of the East Rand portion of the Witwatersrand Goldfield, have generated renewed geological research in the East Rand Goldfield. The Goldfield was previously mapped by Mellor (1915a), Kassner (1933) and Smith (1964) (Figure 1). The Mellor and Smith maps agree and indicate limited outcrop of rocks of the Witwatersrand Supergroup in the greater Benoni area. On both these maps, a major structural discordance between West and Central Rand Group rocks is evident, the origin of which had not, until this study, been satisfactorily explained. The economic potential of this area may well be underestimated if the effects of this discordance and associated bedding parallel thrusts, which have not previously been seriously investigated or regarded as being of any significance, are not considered in any re-appraisal of the viability of mining in the East Rand Goldfield.

The position of the East Rand Goldfield further makes it imperative that the deformational evolution of this area be determined in order to facilitate future modelling of the entire Witwatersrand Goldfield.

1.1 Aims and Purpose of this Study

The area studied is generally referred to as the East Rand "Basin", lying adjacent to the Central Rand "Basin" in the W and the Far East Rand "Basin" in the SE. The aims of this study were to:

.1 Examine aspects of shear strain in the East Rand Goldfield as evidenced in the rocks of the Witwatersrand Supergroup.

.2 Define the number and nature of faulting events affecting this area.

.3 Establish the movement vectors associated with the various generations of displacement which took place on planes parallel to the bedding.

.4 Estimate the shear strain related to bedding parallel faults.

.5 Determine the reason for the presence of structural discordances.

Extensive literature about this area has been published as mining has been conducted since the early 1900's. The vast majority of this literature, however, was published prior to 1970 and, as such, has not included the use of current structural techniques. This has necessitated a re-examination of this Goldfield to clarify the structural events and processes which have affected it.

1.2 Location of Study Area.

The "East Rand Goldfield", as studied, is the previously named "East Rand Basin", and does not include the Far East Rand or southern portions of the Witwatersrand Goldfield, as applied by Pretorius (1980) and de Jager (1986). The area investigated lies approximately 25km ESE of Johannesburg (Figs. 1,2), and is delimited by Atlasville in the W, Putfontein in the N and

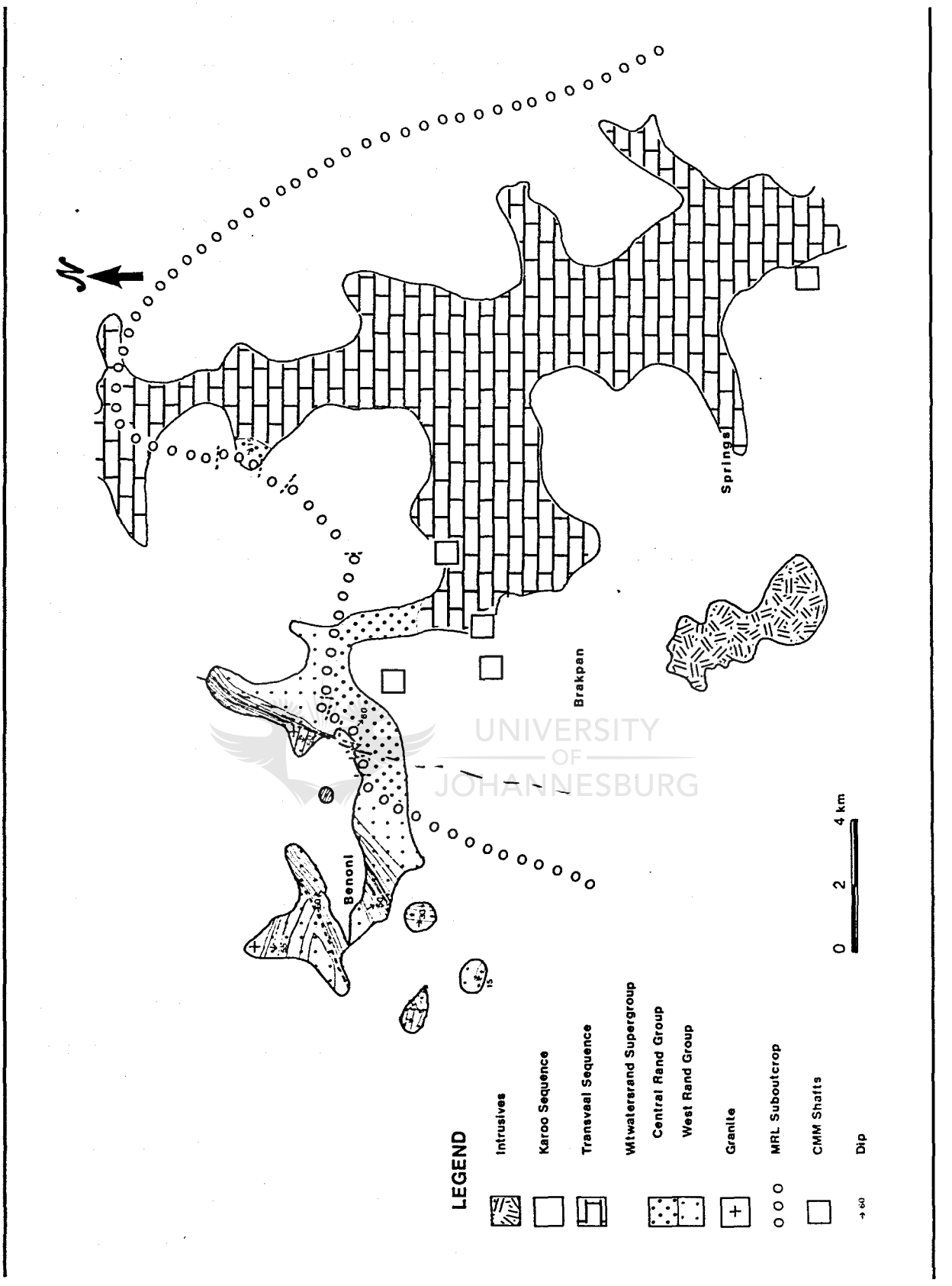

Figure 1: Geological map of the East Rand Goldfield, compiled from Mellor (1915a), Smith (1964) and this investigation.

Springs in the SE (Map 1, Fig 2). Exposures are in Modderfontein and greater Benoni. The area is almost entirely covered by urban development and soil, thereby precluding the possibility of using broad regional mapping to unravel structural complexities. Although the area investigated is 200km^2, the outcrops available for detailed mapping cover a total of 25km^2 (only 13%) and, therefore, a significant amount of the data used in this thesis was collected underground on Consolidated Modderfontein Mines (1979) Ltd. (CMM). CMM comprises all, or part, of the previously named Van Ryn Gold Mine, New Modder Gold Mine, Modderfontein Deep Gold Mine, Government Gold Mining Areas, New Kleinfontein Gold Mine, Brakpan Mines, New State Areas Gold Mine, Geduld Gold Mine, East Geduld Gold Mine, Springs Gold Mine, Daggafontein Gold Mine and East Daggafontein Gold Mine (Figure 3). An in-depth study of the Number 1 Circular and Number 14 shafts was conducted and specific features on Number 7, North Eastern Properties (NEP) and Springs-Dagga (SD) shafts examined.

1.3 Methods of Study and Data Collection

The surface area was mapped in detail using 1: 10 000 orthophotographs and Mellor's 1:60 000 published map as bases. Mesostructures were examined and mapped both on surface and underground to determine their chronology, movement vectors and amount of strain related to a particular event in the structural history of the rocks. Several profiles were mapped on surface and underground to supplement the mesostructural data. Petrographic work was conducted on material from a small number of dykes to determine their character. The relative age of these dykes could thus be ascertained by comparison of their

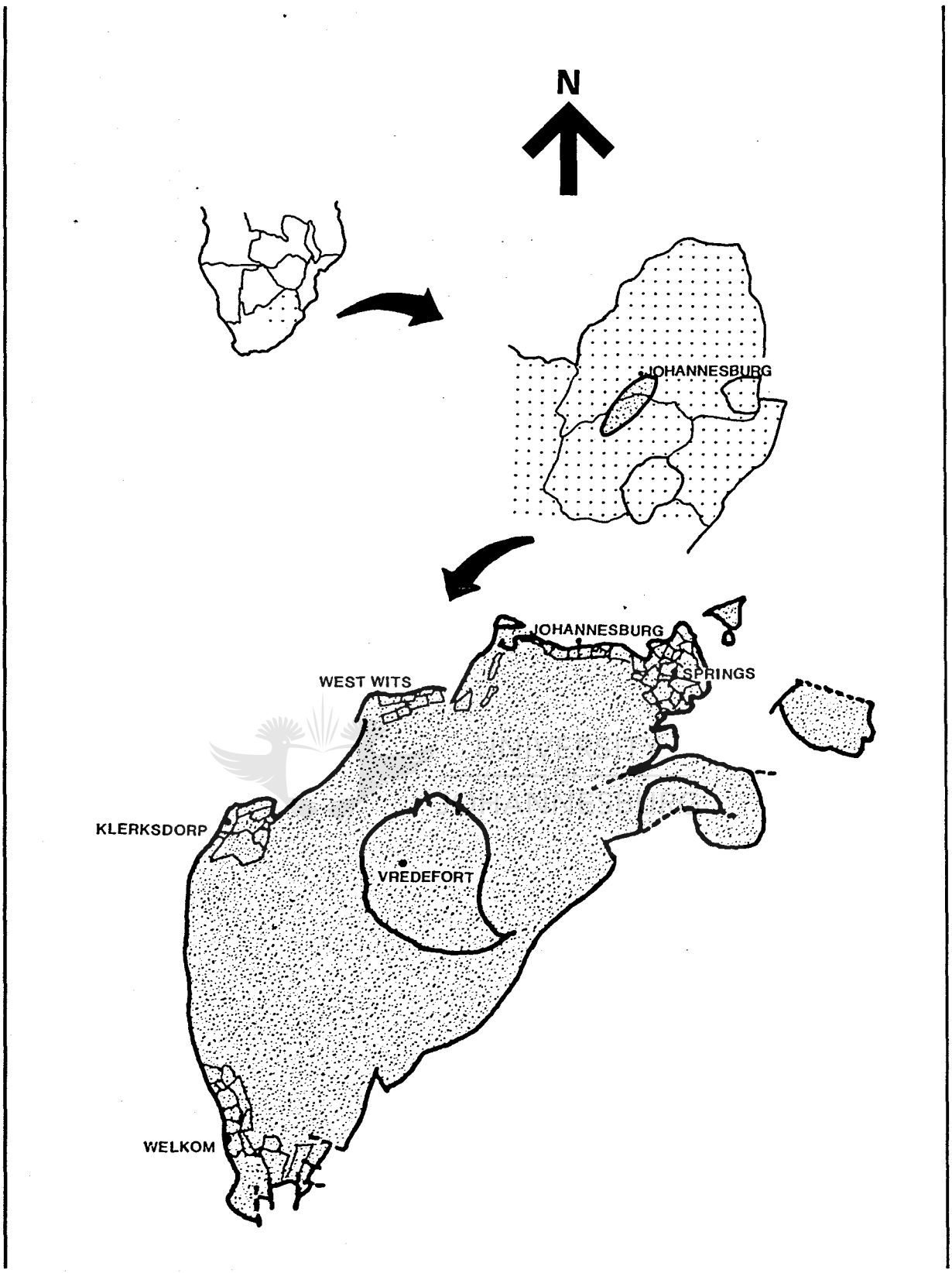

Figure 2 : The position of the Witwatersrand Goldfield. The locality of the present study is the eastern portion of the Goldfield around Springs.

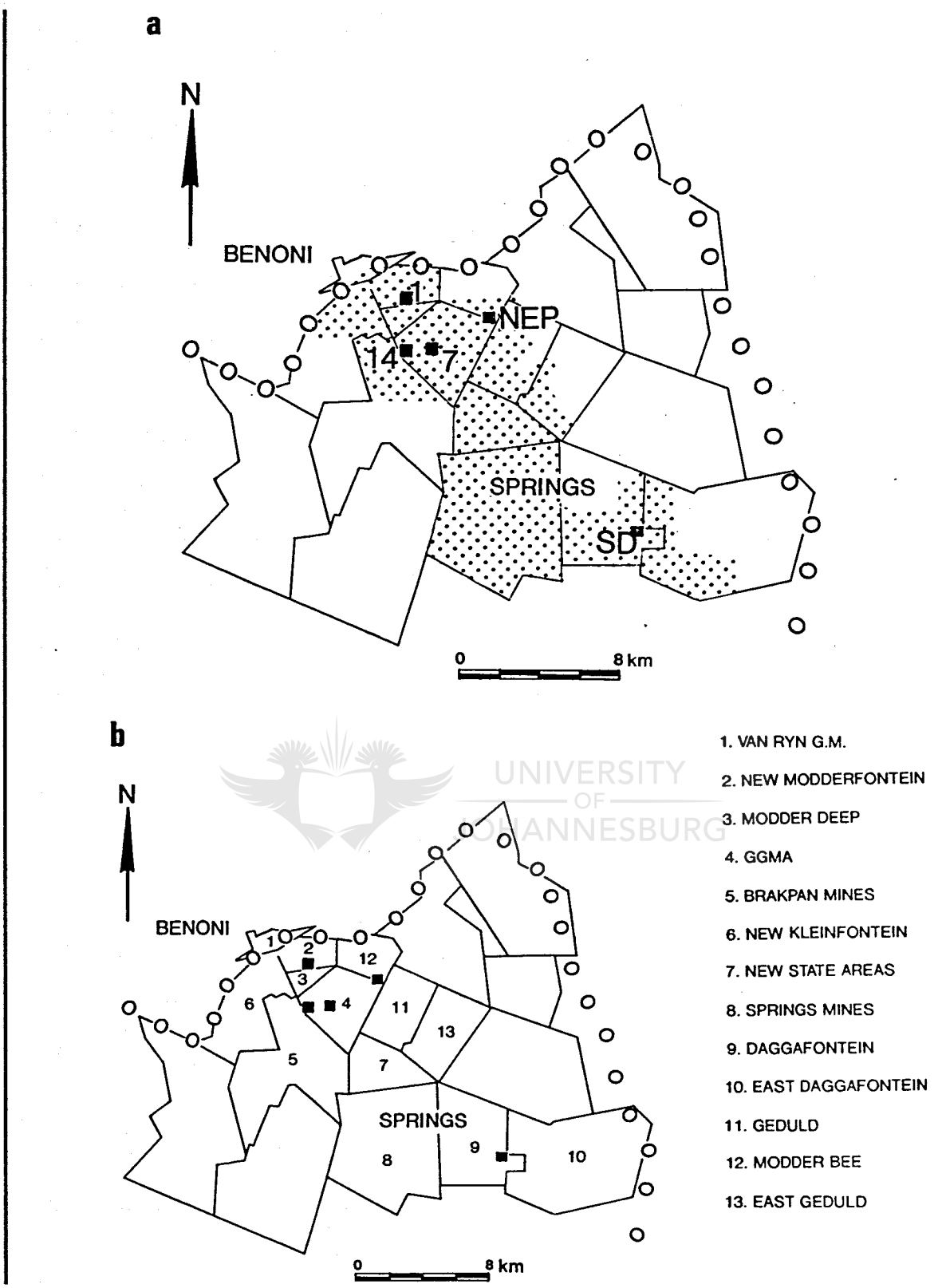

Figure 3 : a) The positions of the shafts investigated on CMM. The speckled area indicates the mining areas held by CMM.
b) Boundaries of the old mines as at 1964. The names of these mines, as generally referred to in the literature, are indicated.

petrographic nature with that documented for dykes of known relative age.

1.4 Terminology

The implications attached to various geological terms have changed with time. For this reason the following terms used in this thesis are defined:

- "East Rand Goldfield" replaces the previously used East Rand Basin. This is done to avoid the (incorrect) genetic suggestions made by the use of the word "basin". It is now widely accepted that the Witwatersrand Goldfield cannot be simply regarded as a basin in the sedimentological sense (e.g. Roering *et al.*, 1990) since later tectonic activity has substantially modified the distribution of the lithologies. This is equally true for this eastern remnant, which has long been considered as a structural feature (Pretorius, 1964).

- The broad stratigraphic subdivision of the Witwatersrand Supergroup proposed by SACS (1980) has been adhered to, insofar as this subdivision describes the preserved lithological packages (Fig. 5). However, the presence of two major unconformities, one at the base of the Central Rand Group and another within the Turffontein Subgroup, together with the evidence presented in this work for shearing along lithologic contacts, suggests that this does not represent the stratigraphy *sensu stricto* of the area.

- As no definitive work on the correlation of the lowermost reef of the Central Rand Group in the East Rand Goldfield with those

of the Central Rand Goldfield has, as yet, been published, this reef is referred to in this thesis as the Main Reef Leader, based on personal observation of this reef by the author.

- The "channels" underlying the Central Rand Group in this area are termed the "Footwall Reef Beds", to eliminate any genetic inference, and to indicate that they are multilithologic in nature, in contrast to the terms "footwall reef channels" or "Footwall Reef Quartzite Beds" (Whiteside, 1950; Kupisiewicz, 1954-1956; Antrobus and Whiteside, 1964).

- Foliation is regarded as a planar fabric produced in the rocks in response to tectonic and related metamorphic processes.

- The term "fault" is used in a non-genetic sense, as recommended by Wise *et al.* (1986), and does not indicate the relative ductility of the deformation zone.

- Despite the fact that the rocks examined have all undergone metamorphism, many sedimentary and igneous names are employed as no viable alternative terminology has, as yet, been developed for low grade rocks of this type.

Geochronological ages used in this thesis refer to those quoted and reviewed by Walraven *et al.* (1990), and quoted by Roering *et al* (1990):

- the Dominion Group underlying the Witwatersrand Supergroup, ± 3060 Ma,
- the overlying Ventersdorp Supergroup rocks, ± 2700 Ma,
- the Transvaal Sequence, ± 2500-2080 Ma,
- the Bushveld Igneous Intrusion, ± 2060 Ma.

2. PREVIOUS LITERATURE

The first mines to come into production on the East Rand were the Van Ryn Gold Mine and Nigel Mine in 1888. The majority of the other mines which operated in the area had opened by the early 1920's (de Jager, 1986). The development of geological knowledge of the East Rand Goldfield could be chronologically summarised as: - surface mapping and correlation, - stratigraphic and sedimentological studies, - the development of gold value and structure contour plans, - classification and determination of relative ages of intrusives, - the discovery and investigation of footwall beds. Although much work was done on the supposed stratigraphic sequence in this area, few workers appeared to recognize the importance of the bedding parallel faulting evidenced. The review papers by Antrobus and Whiteside (1964) and de Jager (1986) provide an adequate overview of the existing literature, for this reason, only specific observations and statements of relevance to this work in a limited number of papers are highlighted here.

Attention must be drawn to the confusing correlation of the lowermost economic reef in the East Rand Goldfield with reefs in the Central Rand Goldfield. Hatch and Corstophine (1909 *in* Mellor, 1915b) were among the first to correlate the Nigel Reef with the South Reef and Van Ryn Reef. The lowermost economic reef became commonly referred to as the "Main Reef", implying correlation with the Main Reef of the Central Rand. Mellor (1915a,b) similarly correlated the Nigel Reef and Van Ryn Reef, and concluded that the Brakpan Reef and Van Dyk Reef were equivalents. He, however, correlated these with the Main Reef

Leader of the Central Rand, and the channelised Bastard Reef of the East Rand with the North Reef of the Central Rand. Sharpe (1943) followed the same correlation, but included the Main Reef of the Central Rand in the correlation of the Footwall Reef Beds. Whiteside (1950) named this lowermost reef on the East Rand the Composite Reef, as he believed that it was the result of the combining of the Main Reef, Main Reef Leader and the South Reef. Ellis (1943) reverted to the common mining usage of the name "Main Reef", as did Ralston (1953) and Cluver (1957). Again, Antrobus and Whiteside (1964), de Jager (1964) and Cousins (1965) alternatively referred to this reef as the Main Reef Leader or South Reef. It is important to bear in mind this multitude of names and to realize that all the authors are referring to the same reef, which lies on the unconformity at the base of the Central Rand Group.

Krause (1913) pointed out that the width of the lower Witwatersrand succession from the Central Rand to, and across, the East Rand was extremely variable, and attributed this to duplication of strata through faulting and anticlinal folding, although he was unable to identify the faults responsible for this.

Mellor (1915a), first drew attention to structural discontinuities in the West Rand Group of the East Rand Goldfield. He noted that the rocks of the Orange Grove Quartzite Formation abut against those of the Government Group in the Van Ryn area, the rocks of the Hospital Hill Subgroup abut against themselves in the Homestead Dam region, and the distance between the granite and Main Reef Leader was extremely variable. In addition, he noted that the thickness of the Bird

Amygdaloid varied, and that, where present, it may occur at several horizons in the Central Rand Group.

In a paper discussing upper Witwatersrand lithologies (1915b), Mellor described the "very sharply defined character of the parting at its (the Main Reef Leader's) foot" and noted its schistose, talcose, exceptionally finely grained siliceous or slaty nature at various, widely separated localities. Towards the Central Rand this footwall was generally associated with numerous quartz veins parallel to the bedding. In the East Rand Goldfield, this footwall was often composed of "channelised" coarser sediments termed the "Bastard Reef" which were, in turn, intimately associated with slaty beds. He reported the same variety of rocks as forming the footwall to the Kimberley Reefs.

Sharpe (1943), after encountering a significant thrust fault displacement on Government Gold Mining Areas during a stratigraphic examination of the rocks of the Central Rand Group and associated lithologies, warned that "where major thrust faults occur, duplicate intersections in economic horizons may be obtained and premature stopping of drilling may result in a loss of information". In his description of the Upper Kimberley (UK) beds, he recorded "soft talcose zones of shear" within the stratigraphy and fracturing of pebbles in the UK9A unit parallel to bedding. He also wrote of the possibility of the channels in the footwall to the Main Reef Leader having been folded prior to the deposition of the hanging wall.

Whiteside (1950) similarly proposed that many of the Middle Kimberley (MK1) puddingstone "channel" shaped sections he had observed represented remnants of truncated synclinal folds, and

were usually covered by a blanket of chloritoid shale. The variations in the thickness of the MK1 puddingstone and the MK2 in the Daggafontein area were interpreted as arising from folding only because he could see no displacement in the UK9 beds.

Du Toit (1954) reported the possibility of thrusting on a considerable scale during and following Ventersdorp volcanism. Footwall Reef Beds hosted in the Jeppestown Shales have a channelised form, and Carleton-Jones (1936) expressed the opinion that these reefs filled hollows caused by erosion and folding.

"Tear faults" began to feature prominently in the literature after Ellis (1943) discussed a strike-slip fault in the East Geduld region. This post-Transvaal, left-lateral tear fault strikes ± E-W, dying out laterally, particularly W. Younger horizontal faulting on a NNW orientation was regarded as having two phases of movement on it. Folding observed on Grootvlei Mine, which Ellis (1943) recorded as oriented at approximately 45° to the NNW-SSE tear, was initiated prior to tearing and continued after the cessation of tear movement. Whiteside (1944) described a further two tear faults. The "Vogel's Tear" in Vogelstruisbult Gold Mine Areas Ltd. extended E-W into adjacent mines and moved left-laterally. The second, running NW-SE through Brakpan and West Springs Mines displays right-lateral movement. Although quite certain about the post-Ventersdorp (post-2700 Ma), pre-Bushveld (pre-2060 Ma) age of the Vogel's Tear, he had no clear evidence for the timing of the second fault.

In addition to the tear faults, Ellis (1946, 1947) studied many of the intrusive events represented in the East Rand, and deduced their relative age relationships. His examination of the Marievale Granophyre led him to conclude that it was metamorphic in origin. The apparent granophyre is generally found in or within metres of the contact between the West Rand and Central Rand Groups, and rises and falls with this contact. Upon considering the relationship of the granophyre to this contact and the different ductilities of the shales of the Jeppestown Subgroup and the Main-Bird Quartzite, he suggested that the contact was "a locus of concentration of directed stress and therefore flowage". Although he found no evidence of displacement along the contacts of the granophyre, he did observe changes in strike and/or dip of the Main Reef across the granophyre. Age relationships were unclear, and he assumed the granophyre to be post-Transvaal (2500 Ma - 2080 Ma).

Ralston (1953) disputed the metamorphic origin proposed by Ellis (1947) for the Marievale Granophyre, and interpreted it to be igneous in origin. He suggested that its emplacement had resulted in sillimanite grade metamorphism of the shales of the Jeppestown Subgroup along their contact with these intrusives.

In a series of unpublished mine reports, Kupisiewicz (1954-1956) described the structure affecting the footwall "channel" features unique to the East Rand Goldfield (the Footwall Reef Beds). These features are hosted within the shales of the Jeppestown Subgroup and are commonly sites of high gold concentration. Through his examination of these channels and the overlying Main Reef Leader, he was able to distinguish two phases of folding in this region, one which occurred after the

deposition of the West Rand Group and before the deposition of the Central Rand Group, and the other after the deposition of the Central Rand Group, probably during the deposition of Ventersdorp rocks. Axial traces of both phases of folding lie essentially on the same NW-SE orientation. Bedding within the channels is commonly steepened upwards away from the bottom of the channel, and may even be overturned. These beds generally strike E-W and dip to the SSE. In addition, where this steepening of beds is not present, the units are significantly thinner. He attributed this phenomenon to the folding and shortening of the beds in response to the same compressive forces which produced the flat bedding parallel faulting he reported in the underlying shale units and within the channels. The strike of this faulting parallels the strike of the beds and consists of numerous small scale stacked faults.

Kupisiewicz (1954-1956) similarly noted two distinct generations of strike-slip faulting in this area, one of Ventersdorp (2700 Ma) age and the other of post-Bushveld (2060 Ma), pre-Karoo (300 Ma - 200 Ma) age. The Ventersdorp aged faults are predominantly left-lateral, and the post-Bushveld faults are right-lateral. The scale of these features, their orientation and their relative ages led Kupisiewicz (1954-1956) to suggest that they are a manifestation of the release or relaxation of the compressional forces which gave rise to the deformation of the channel beds.

Cluver (1957), like Mellor (1915b), drew attention to the large scale faulting of the beds of the West Rand Group, and noted that these faults were not manifested in adjacent rocks of the Central Rand Group. He also particularly studied the anticlines

manifested in the Main Reef Leader and concluded that there are four major anticlines whose axes all strike NW-SE and have a shallow plunge. The southwestern flank of one of these anticlines does not end in a trough, but in a "wide, slightly undulating plane". The same flank of another flattens in dip to the N. Cluver (1957) was largely restricted to examining the Main Reef Leader, where he observed that pay shoots trend across the anticlines and are not influenced by the folds, an observation later disputed by Greenberg (1963). He therefore concluded that - the deformation which produced the folds only commenced after the deposition of the Witwatersrand Supergroup, - it was most likely post-Ventersdorp and pre-Transvaal in age, - and the pressure responsible may have come from the SW and resulted in "the whole area underlain by the Witwatersrand System" having been "moved to the NE and that the northeastern portion of this huge mass was folded". He also presented an alternative scenario, which he personally favoured, in which a horizontal couple arising from SW to NE compression resulted in folding and a tear motion on E-W faults.

Antrobus and Whiteside (1964) interpreted the morphology of the footwall quartzite channels (as discussed by Kupiesiwicz, 1954-1956) as resulting from "slumping or compression", and noted that the beds within the channels are sometimes overturned in the N. They remarked upon the fact that the quartzitic shales of the Jeppestown Subgroup are "green and sheared near their contact" with the overlying rocks of the Central Rand Group, and that the angular unconformity which this contact represents is "often masked by shearing and quartz veins". Like de Jager (1964), they were of the opinion that both the Main Reef Leader and Upper Kimberley Reef lie on erosional surfaces which have

truncated footwall anticlines.

Although they did not see evidence for repeated movement on old faults, Antrobus and Whiteside (1964) noted recurrent movement on the Springs Monocline (which is even "reversely faulted"), repetition of earlier folding of Witwatersrand and Ventersdorp rocks in post-Transvaal times, and they acknowledged the existence of "some inconsistencies" in the chronology of structural events they proposed.

The presence of authigenic chloritoid and/or rutile together with sericite in the various shales, argillaceous layers and impure quartzites was interpreted by de Jager (1964) as arising from "stress metamorphism". He also noted quartz-sericite bodies of pre- strike-slip faulting ages. These bodies are of low angle and appear to occupy SW-NE fault planes and are the result of replacement of quartzites and shales along these planes. It is interesting to note the appearance, on a section he compiled at Vogelstruisbult Mine, of a fault parallel to the bedding in the plane of the section.

Brock and Pretorius (1964a), contrary to Antrobus and Whiteside (1964), noted more than one phase of movement on many faults in the Witwatersrand Goldfield and in particular along the preserved edges of the strata, where even reverse fault duplication of strata was recorded. They postulated movement between the granite and the overlying Orange Grove Quartzite Formation to explain the overturning of strata on the Rand.

The "asymmetrical feature with nothing to balance it" which forms the Springs Moncline was regarded as a "reflection of a

deep-seated fault, a suspicion which is strongly enhanced by the bifurcation (of the structural contours) of a monocline in what is characteristically a fault pattern" by Brock and Pretorius (1964a). They observed that the Vogel's Tear dips at 45°. This is shallower than expected for a tear fault, and may have arisen from the same forces which formed the monoclinal feature, and be tectonically related to an "overthrust" in the East Rand Goldfield. Although of the opinion that this "late stage compression" did not have a large impact on the structural development of this area, Brock and Pretorius (1946a) did concede that it was "not fully understood" and that it may also have reactivated basin edge structures.

Strike-slip faults in the East Rand were considered by Brock and Pretorius (1964b) to be of "post-basining age" and to have utilized pre-existing fault planes. "In many cases they are of a scale that allows them to be explained as adjustments between adjacent fault blocks". These authors felt, however, that the horizontal movement on these strike-slip faults was of lesser importance than the relative vertical movement. Pretorius (1964) made direct reference to strike-slip and reverse faulting and "overthrusting" on an E-W strike in the Central Rand Goldfield.

The unconformity below the South Reef acted as a décollement in the Randfontein Estates area as seen by the presence of pebbles on this contact, which have been cut in half. (Cousins, 1965).

The maps compiled by Armstrong (1968) show the right-lateral, NE-SW Jeffrey's Tear of Daggafontein stopping against the left-lateral, E-W Vogel's Tear, but he was unable to resolve age

relationships between the two.

Lenthall (1972), based on a study of heavy mineral compositional variations of the Witwatersrand rocks of the greater East Rand area, concluded that the anticlinal features were active during sedimentation.

Wagener (1975) concluded that the structural pattern of the East Rand Goldfield was established prior to or early in the deposition of the Witwatersrand succession and influenced the deposition of even the Transvaal Supergroup.

In the Central Rand Goldfield, Grohmann (1989) studied the sub-surface geological structure. Using the effect of events on dykes of known age, he concluded that there were multiple events of different ages present, and that many of these events reactivated older faults. Of particular interest is his identification of early Ventersdorp left-lateral tearing and associated thrusting, late Transvaal bedding plane movement and simultaneous reactivation of earlier thrusts, and the both westerly and northerly thrust movement on bedding planes during Bushveld times.

2.1 Summary of features previously recorded

Prior to 1964, manifestations in the rocks of deformation parallel to bedding were recorded by most workers in the East Rand Goldfield. The fault within the West Rand Group which is exposed on surface in the Van Ryn area, and its absence in the Central Rand Group, was noted by a number of workers. Strike-

slip faults, of a number of different ages and orientations were recorded. Folds on a broadly NW-SE orientation were recorded, but their origin and age were not widely agreed upon. Metamorphism of lower greenschist facies was documented on a regional scale, and amphibolite grade metamorphism was noted on a local scale on Marievale Gold Mine. Sillimanite grade of metamorphism was been recorded in the Jeppestown Subgroup adjacent to rocks of (disputed) intrusive origin on mines adjacent to Marievale Gold Mine. The reactivation of fault planes within the Goldfield has been proposed by several authors, although this suggestion has not always been widely accepted. In the early 1960's, however, observations relating to manifestations of the bedding parallel deformation began to dwindle in number, and this line of investigation ceased entirely after 1964. The significance of these observations have, to date, not been fully appreciated.

3. GEOLOGICAL SETTING

3.1 General Geology

An E-W section across the East Rand Goldfield is concave upward (Fig. 4). The Goldfield in fact forms the N-S striking eastern limb of a broad NW plunging syncline in the Witwatersrand Goldfield. The western limb strikes E-W and comprises the Central Rand Goldfield (Pretorius, 1964). An attenuated sequence of the Central Rand Group type section is present, with the beds thinning markedly towards the SE. This has been attributed to the transgressive peneplanation of the land

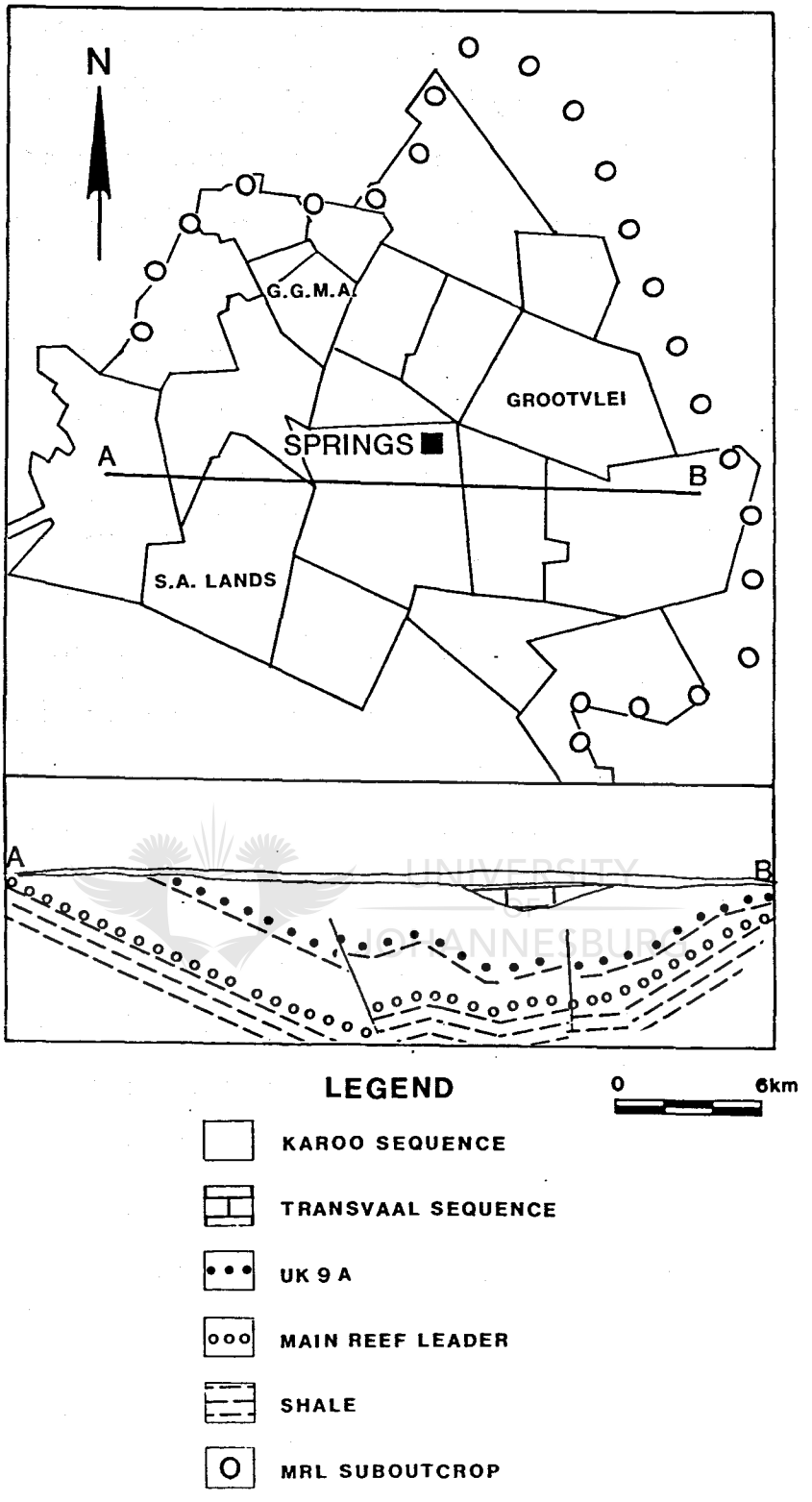

Figure 4 : A schematic cross-section through the East Rand Goldfield displaying its concave upward nature. (After Lurie, 1981).

surface prior to and then later during the deposition of the rocks of the Central Rand Group. The two resulting unconformities are overlain by the Main Reef Leader and Kimberley Reef (UK9A) and are underlain by erosion channels and synclines. It has been assumed that the anticlines were eroded away (Sharpe, 1949; Antrobus and Whiteside, 1964).

The lower portion of the Witwatersrand Supergroup is dominated by argillaceous beds, and the upper portion by arenites with localised well-developed conglomerate bands and shales. The lower portion has been interpreted as representing deposition in a shallow shelf environment (Pretorius, 1974). The upper portion is characterised by cyclical sedimentation (Sharpe, 1949) and is regarded as having been deposited in alluvial fan environment data (Pretorius, 1974), local palaeocurrent data (Armstrong, 1968) is used to substantiate this.

Rocks of the West Rand Group crop out in the northern sector of the East Rand Goldfield where they are cut by major NE-SW faults. The limited exposure of the Central Rand Group shows the beds to be broadly folded (Fig. 1). Numerous apparent strike-slip faults are exposed in underground workings, belonging to at least two ages with distinct directions of displacement (Ellis, 1943; Whiteside, 1944; Kupisiewicz, 1954-56).

The area is traversed by various generations of dykes generally considered to be of Ventersdorp, Bushveld and Karoo ages. (Ellis, 1943,1946,1947; Brandt, 1950; Ralston, 1953). Metamorphism, as seen in the development of phyllosilicates and rutile is of lower greenschist facies (de Jager, 1964; Lenthall,

1972), but locally may attain amphibolite (Ellis, 1945) or sillimanite grades (Ralston, 1953).

3.2 Stratigraphy

Rocks of the Witwatersrand Supergroup and Transvaal and Karoo Sequences are represented in the East Rand Goldfield. The type sections of the West and Central Rand Groups of the Witwatersrand Supergroup are essentially present in attentuated form (Fig. 5), but erosion or coalescence of beds resulted in the absence of certain markers at the base of the Central Rand Group. Rocks of the Ventersdorp Supergroup are not present, except possibly as dykes. Rocks of the Transvaal Sequence are generally accepted as almost fully developed, and crop out over a considerable portion of the area. The upper portions of the Karoo Sequence are absent due to erosion.

Although the subdivision of the Witwatersrand Supergroup as proposed by SACS (1980) has been employed for the West Rand Group in this study, it should be borne in mind that this may not represent the stratigraphy *sensu stricto* of the area. The Central Rand Group division has been adhered to to subgroup level only. Underground exposures are primarily of the Turffontein Subgroup, with limited exposures of Johannesburg Subgroup units available underground and in subsurface stopes. The detailed structural examination of, in particular, the rocks of the Kimberley Formation (Turffontein Subgroup) necessitated the use of a more rigorous stratigraphic subdivision than that proposed by SACS (1980). Since that of Sharpe (1943) was developed for these beds on the previously named Government Gold

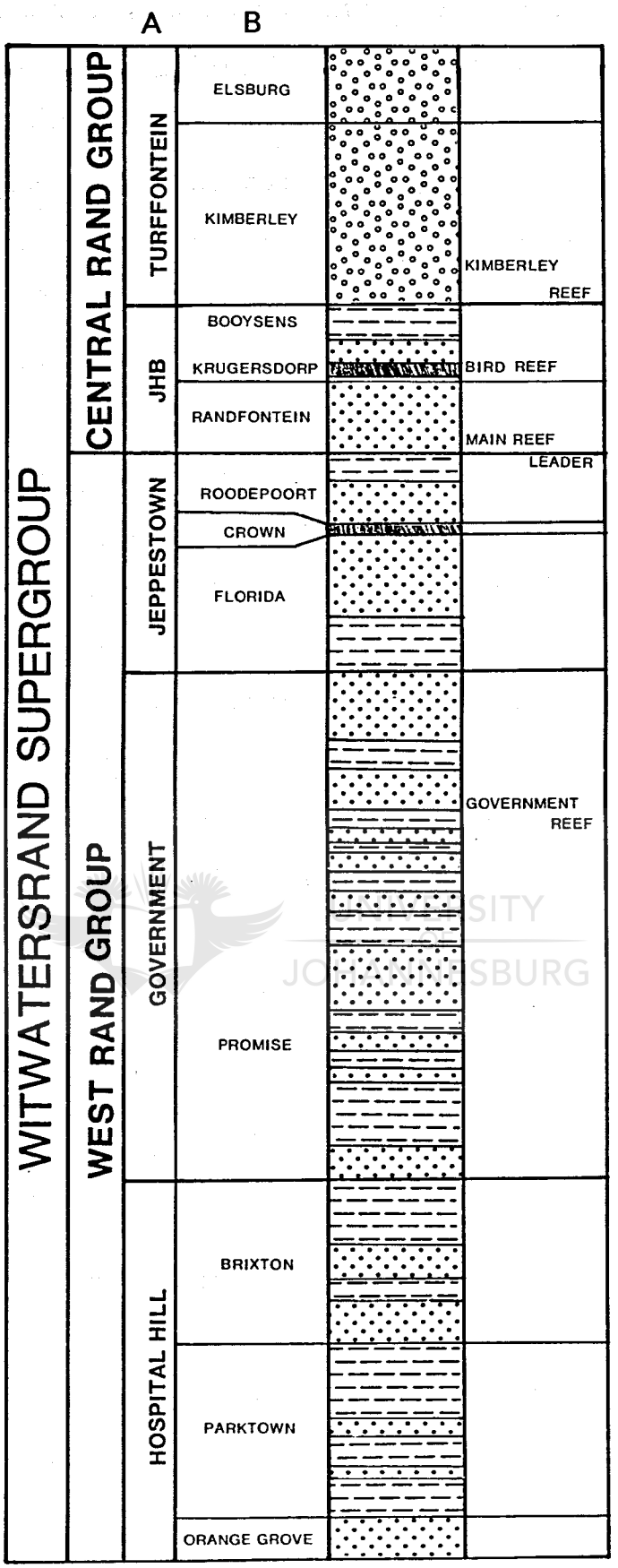

Figure 5 : The stratigraphy of the Witatersrand Supergroup in the East Rand Goldfield. (After SACS, 1980; Tankard, *et al*, 1982). A = Subgroup. B = Formation.

Mining Areas (GGMA) (now incorporated into CMM), and is in current usage on these shafts, it has also been used in this study (Fig. 6). Similarly the more detailed division and lithological description of the Johannesburg Subgroup (previously known as the Main-Bird Series) constructed by Antrobus and Whiteside (1964), (Table 1), has been applied in the strain analysis.

Sharpe's (1943) examination led him to divide the Kimberley Series, as it was then known, into three packages: the Lower, Middle and Upper Kimberlies. These were lithologically further

subdivided and named using numbers in ascending order from the top of each unit downwards. He included in the Lower Kimberlies (LK) the LK2 and LK1 units, termed by SACS (1980) the Booysens Shale and Doornkop Quartzite Formations respectively.

3.2.1 Lithological descriptions

Descriptions are limited to those beds on which detailed strain analyses were conducted, i.e. the Central Rand Group. The nomenclature of Sharpe (1943), where it applies to these rocks, is used; that of SACS (1980) then appears in brackets.

Johannesburg Subgroup (Main-Bird Series of Antrobus and Whiteside (1964))

The break-down of the lithologies in this subgroup as represented on the East Rand Goldfield can be seen in table 1.

LK2 (Booysens Shale Formation) This unit forms the footwall to

the Turffontein Subgroup over the entire area studied. It is a grey-black argillaceous mudstone which becomes progressively more arenaceous upwards. The point at which the mudstone has graded up to a quartz arenite is regarded as the base of the Turffontein Subgroup (SACS, 1980). At many localities in this goldfield, however, this contact represents a local unconformity.

LK1 (Doornkop Quartzite Formation) These beds comprise distinct, fine-grained, glassy, grey-green quartz arenites. They may be absent towards the SE, and up to 50m thick in the extreme western portion of the area.

Lithology	*Approximate preserved thickness in metres*
Quartzites	67
Bird Reef Marker	3
Quartzites	6
Bird Amydaloidal Diabase	46
Quartzites	6
Bird conglomerates	21
Quartzites	46
Argillaceous quartzites	30
Quartzites	46
Fine-grained green quartzites	30
Quartzites	46
Upper leaders and quartzites	18
Main Reef Leader	0.6
UNCONFORMITY	

Table 1 : The Johannesburg Subgroup as present in the East Rand Goldfield. (After Antrobus and Whiteside, 1964).

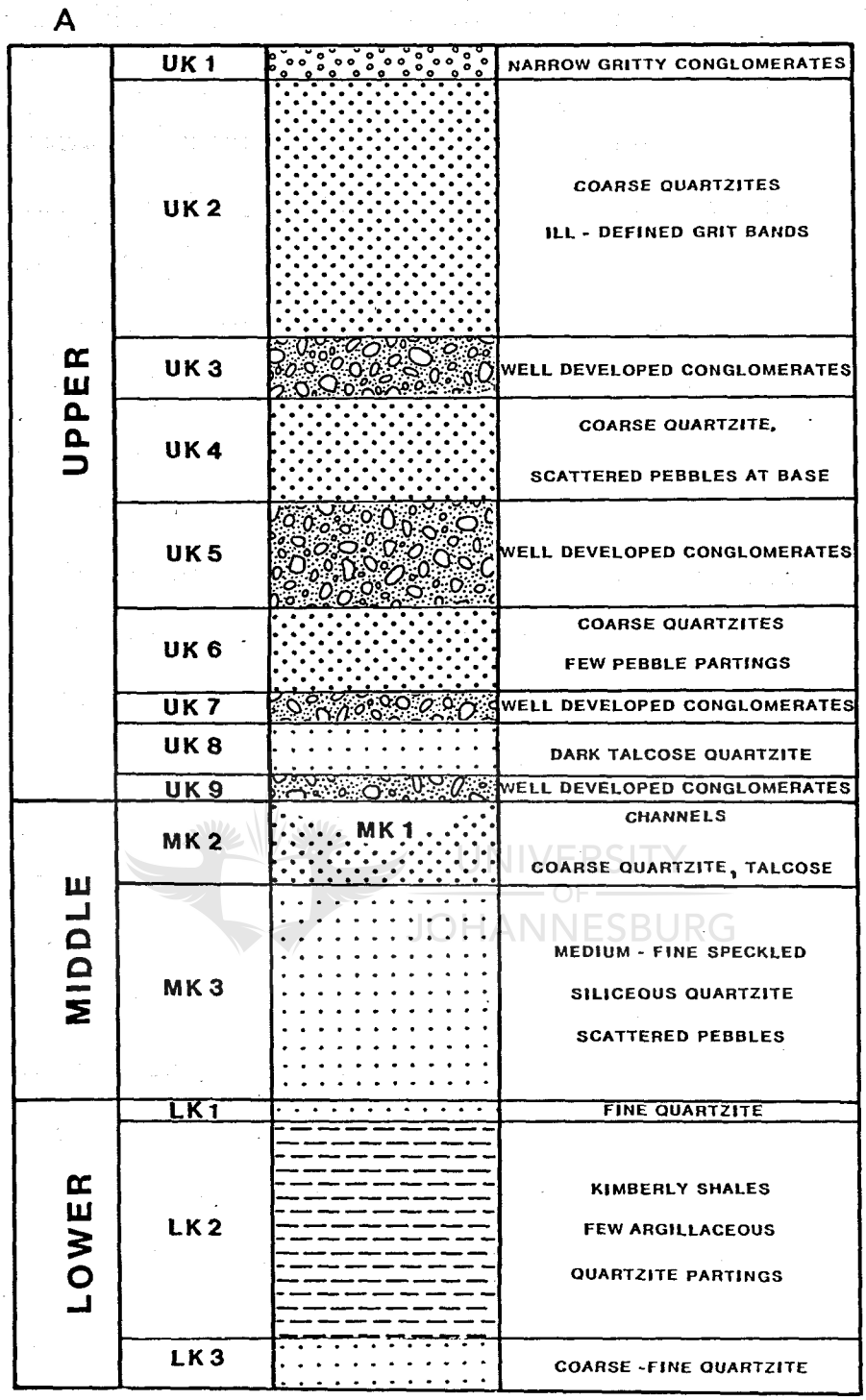

Figure 6 : The stratigrapic subdivision of the Kimberley Formation in the East Rand Goldfield. (After Sharpe, 1943). A = Member.

MK3-UK3 (Kimberley Quartzite Formation) The base of this group of beds is regarded as the point at which the beds begin to contain scattered pebbles, or - where present - at which the first pebble layer appears. As the overlying quartzites are exceedingly difficult to distinguish from those of this group in the East Rand Goldfield, the top of these units is not here as readily definable as it is to the west of this area (Auchterlonie, 1987).

The MK3 is predominantly a green protoquartzite with scattered angular chert and rounded quartz pebbles. The chert pebbles include black and banded varieties. Rare lenticular pebble bands are present. The rock contains scattered angular black chert fragments of a few millimetres in length which give it a speckled appearance.

The MK2 is characteristically a coarse quartzite with subordinate narrow bands of conglomerates. Pebbles are, on average, 2cm in length, decreasing in size upwards and are generally composed of chert and vein quartz. The matrix is medium-grained grey, glassy orthoquartzite.

The MK1 comprises a complex sequence of channelised beds which include shales, conglomerates, argillaceous, proto- and orthoquartzites and poorly sorted argillaceous diamictites. The shales are generally dark green to grey in colour and are commonly chloritoid bearing. Many of the thinner (< 75cm) shale beds and argillaceous partings are, in fact, talc-sericite or quartz-chlorite schists. The clasts in the conglomerates

consist of angular chert and rounded quartz pebbles (Viring, 1986).

The MK1 is unconformably overlain by the UK9 reefs. These reefs are of major economic importance and are made up of four subunits:

a) UK9C = a quartzite characterised by thin bands of large quartz vein pebbles, scattered, infrequent shale clasts and buckshot pyrite,

b) UK9B = a package of clast-supported, vein quartz conglomerates and quartzites,

c) UK9A = narrow clast supported conglomerate zone containing white vein quartz pebbles and pyrite mineralization,

d) UK9A marker = a fine-grained, green, siliceous quartzite.

The overlying UK8 is a dark, often olive green medium to coarse-grained protoquartzite with numerous talcose partings. The green hue is regarded as resulting from the presence of chlorite. Scattered small pebbles or single pebble bands are present.

The UK7 comprises numerous medium to large pebble conglomerates with intervening bands of coarse grey-green orthoquartzite. Argillaceous partings are common.

The bulk of the UK6 unit is formed by medium to coarse-grained orthoquartzites with scattered black chert fragments. Thin inconsistent pebble bands, fine-grained orthoquartzites and argillaceous partings (now interpreted as schists) are present on a lesser scale.

The UK5 is readily distinguishable by the well-developed conglomerate zones it contains. These zones are separated by a thick layer of coarse-grained orthoquartzite (Sharpe, 1943).

In contrast the UK4 comprises light grey medium-grained orthoquartzites with scattered quartz and chert pebbles, and has a thin argillaceous layer at its upper contact (Sharpe, 1943; Auchterlonie, 1987).

The UK3 package is a dark grey medium to coarse-grained orthoquartzite with scattered pebbles and pebble bands, and a well-developed conglomerate at the top.

UK2-Elsburg Quartzites (Elsburg Quartzite Formation) The Elsburg Quartzite Formation comprises the UK2, UK1 and Elsburg Quartzites of Sharpe's classification, although only the UK2 is commonly developed in this area. The UK2 is a medium to coarse-grained grey-green orthoquartzite containing scattered pebbles, grit layers and some fine-grained beds (Sharpe, 1943). The UK1 consists of narrow gritty conglomerate layers and thin pebble bands separated by bands of coarse quartzite and occasionally fine-grained orthoquartzite (Sharpe, 1943). These beds are unconformably overlain by the Black Reef Quartzite Formation (BRQF, Transvaal Sequence).

3. 3 Intrusives

A number of intrusive phases are represented in the East Rand Goldfield. The petrographic nature and relative age of each of

these phases has long been established (Ellis, 1943, 1946, 1947; Brandt, 1950; Ralston, 1953; Antrobus and Whiteside, 1964). Most of these dykes have, however, experienced considerable dynamic and retrograde metamorphism so that few of the original minerals are preserved (Antrobus and Whiteside, 1964; De Jager, 1964). The substantial chloritisation and epidotisation of most of these intrusives obscure their original mineralogy and may lead to misclassification if not taken into consideration. Despite this metamorphism, igneous terminology was used to name these dykes, and often refers to the appearance of the dykes rather than their true mineralogy.

Since the age of dyke emplacement and that of the formation of the fracture along which it is sited are not necessarily coeval, the use of the orientation of a dyke in order to establish its age has generally proved unreliable in this goldfield. For this reason, selected dykes were examined using petrographical and X-ray diffraction techniques. These dykes were thereby compared with the established dyke classification of the East Rand Goldfield to determine their relative age. Attempts at the geochemical classification of these dykes was hindered by the extreme alteration evidenced in many of them, and the lack of an established geochemical data base against which results on the dykes of this goldfield could be compared. Nevertheless, together with field relationships, the appearance of these dykes have been used in an attempt to determine the relative ages of some of the faulting events.

Four phases of dyke intrusion were identified in the study area. From youngest to oldest these are:

1. Relatively fresh dolerites containing twinned plagioclase and augite, in ophitic relationship, are evidenced on NEP Shaft. Some alteration of the augite to an amphibole and chlorite has occurred. Olivine, iron-oxides and iron, titanium oxides are present in accessory amounts. These dykes have been catergorised as Karoo - age dolerites.

2. A series of dyke exposures on 1 Circular Shaft display almost identical mineralogy and texture, differing only in grain size and orientation from one exposure to another, and may represent only two individual dykes cutting across the shaft. These fine-grained, dark green and speckled black rocks are sheared by later faults on orientations varying from 075° to 120°. In thin section, the foliation developed during this shearing is defined by a rough alignment of green - brown biotite. The rocks have a glomeroporphyritic texture; the groundmass comprises chloritised actinolite, feldspar, sericite and quartz. Epidote intergrown with secondary ilmenite is present, with the ilmenite commonly showing minor alteration to leucoxene. Albite microphenocrysts exhibit varying degrees of sericitisation, and rare remnants of augite present have experienced alteration to chlorite and epidote. Anhedral iron oxides and small blebs are scattered throughout the rocks. Secondary quartz and clinozoisite amygdales are present in one of the exposures. These characteristics are compatible with those attributed to "Green Syenite" dykes (Brandt,1950).

3. A second series of dykes are exposed on the same shaft. They are generally a lighter green than the "Green Syenites", and slightly finer grained. Thin sections reveal an epidote, chlorite, muscovite, quartz groundmass which is commonly

streaked by iron-oxides. Accessory green to brown biotite, ilmenite and leuxocene are present. Calcite appears to be rare, but as it is present as fine specks in the groundmass, its presence may be under-estimated. Magnetite dust sometimes clouds the epidotes, and replacement textures of a possible amphibole by a green chlorite and epidote is common. Skeletal to dendritic ilmenite has undergone a minor amount of alteration to leucoxene and is generally closely associated with the ubiquitous epidote. Indistinct relict plagioclase twinning textures are detected in the groundmass. The chilled margin of such dykes contain rock fragments from the host quartzite. Although the epidote and chlorite alteration is intense, it is possible to classify these dykes as belonging to the Ilmenite Diabase group as described by Antrobus and Whiteside (1964).

4. An isolated exposure bearing no known relationship to the other dykes on 1 Circular Shaft is light grey-green in hand specimen, and very fine grained. This dyke is strongly altered and comprises a fine grained mass of granular quartz, colourless chlorite, sericite and altered iron-oxides. Minor replacement textures after original plagioclase phenocrysts are present, and appear to define a vague trachytic texture. No epidote has been identified in this dyke. This dyke is therefore classified as a Ventersdorp Diabase (Ellis, 1946; Brandt, 1950; Antrobus and Whiteside, 1964).

4. STRUCTURAL DATA

4.1 Techniques

The lack of outcrop and limited available underground exposures necessitated the use of techniques other than surface mapping to elucidate the complexity of structure in this area. Movement vectors were determined using slickenside and slickenfibre orientations on most generations of faults. The bedding parallel faults were studied using kinematic indicators such as s-c fabrics (Lister and Snoke, 1984), bedding-cleavage relationships, movement directions on ramps, rotation of rigid bodies (Simpson and Schmid, 1983), boudinage orientation and intrafolial folds.

Data gathered from specific surface and underground areas were compared to discern both common trends and differences caused by localised disturbances. In addition, the field relationships of various structures were noted to attempt to resolve their relative ages.

4.2 Faults

4.2.1 Fault Orientations

Surface manifestations of the large scale faults, which are no longer exposed, are indicated by the effect these structures have on the regional outcrop pattern (Map 1). The strikes of these faults are thus inferred.

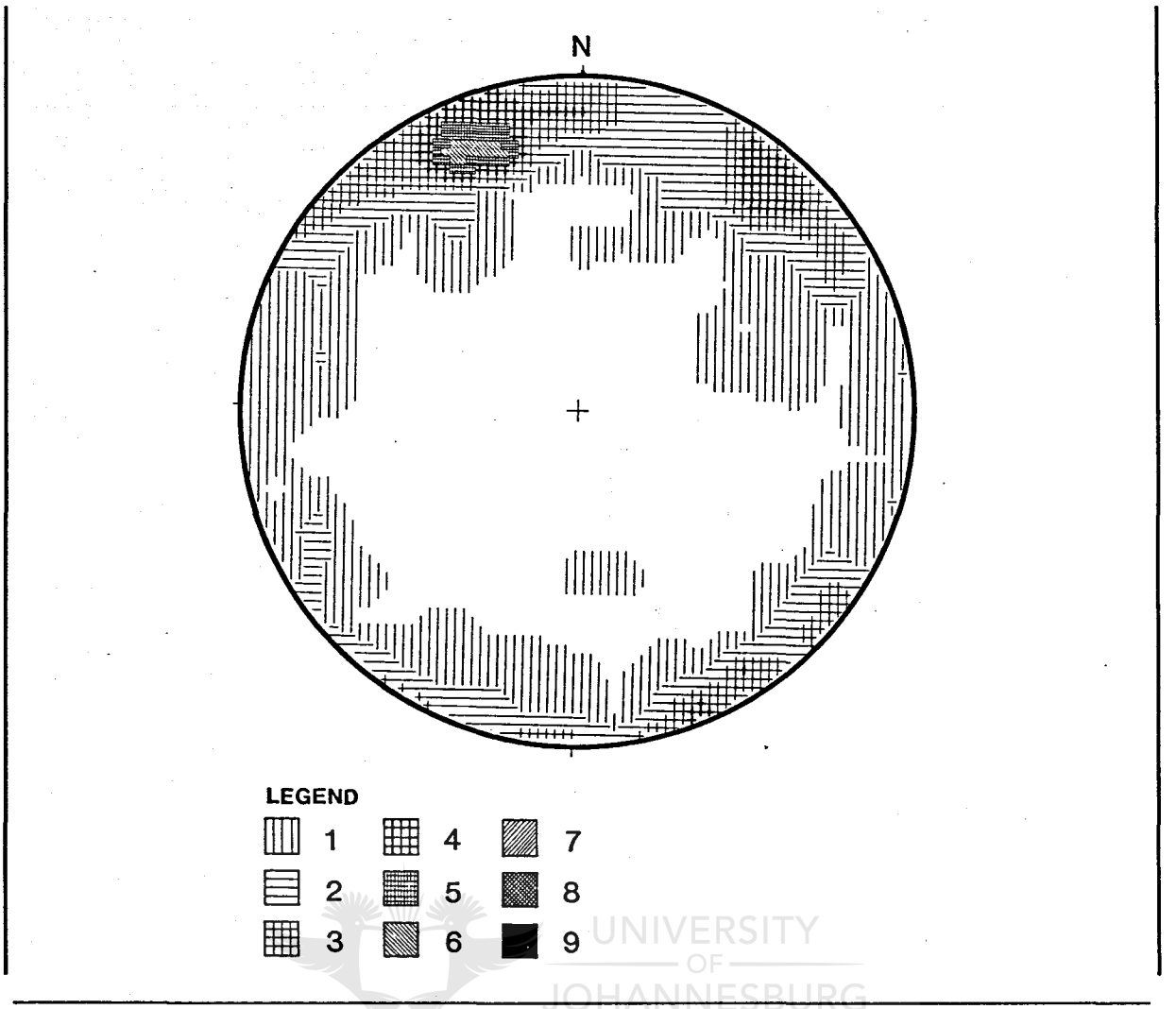

Figure 7 : Contoured plot of the orientation of the poles to fault planes of all non-bedding parallel faults measured within the Witwatersrand Supergroup rocks in the East Rand Goldfield. (Schmidt stereographic projection). Total number of readings = 251. Contoured at 1% level.

Numerous generations of non-bedding parallel faults have affected this area (Fig. 7). The major orientations are:

- striking NE-SW and steeply dipping
- striking NW-SE and steeply dipping
- a spread of smaller populations of moderate (± 45°) to steep dips on E-W and N-S at the 3% level.

In addition, a group of shallow to moderately S dipping, faults

exist (Fig. 8), which parallel the bedding (Section 4.3).

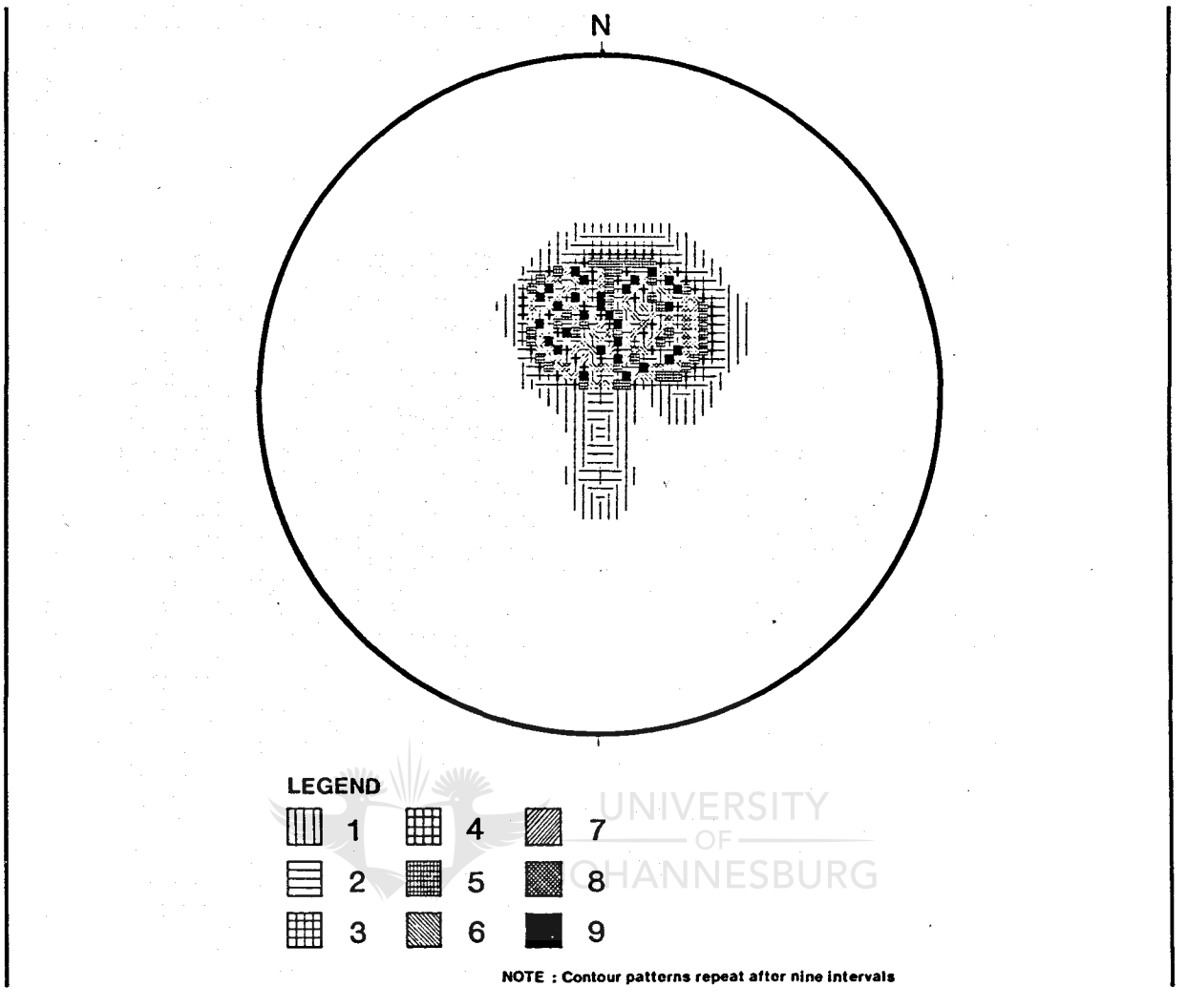

Figure 8 : Contoured plot of the orientation of the poles to fault planes of all bedding parallel faults measured in Witwatersrand Supergroup exposures in the East Rand Goldfield. (Schmidt stereographic projection). Total number of readings = 221. Contoured at 1% level.

The orientations of slickenfibre (Fig. 9) and slickenside data associated with each particular fault orientation have been plotted. The broad and multiple modes (in a statistical sense) derived from plotting these data on Schmidt stereographic projections does not arise as a result of later folding or re-orientation of these planes (see section 4.5). Some of the scatter in the readings may be due to the pre-existing

anisotropism of the rocks. The multiple generations of slickenfibre growth often witnessed on single planes suggest, however, that several phases of movement are responsible for the scatter rather than multiple orientations related to a single movement.

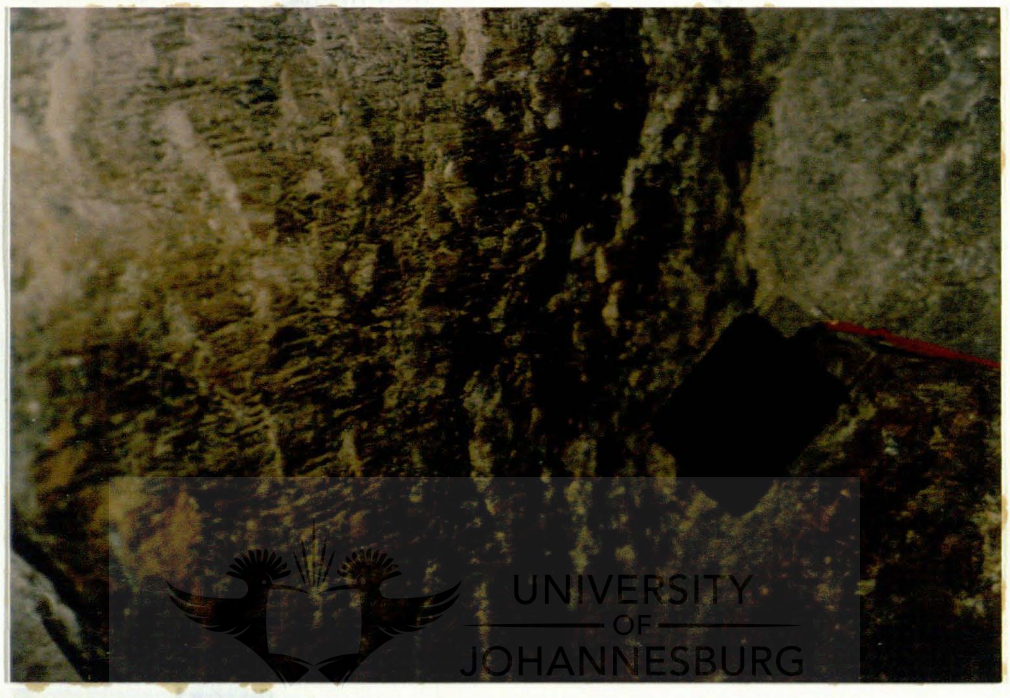

Figure 9 : Slickenfibres developed on a strike-slip fault as seen on 1 Circular Shaft.

The NW-SE striking faults show evidence of three distinct movement directions (Fig. 10) viz.:

- a steep to vertical movement,
- a moderate oblique movement,
- a shallow to horizontal strike-slip movement.

The steeper movement directions, as indicated by both stratigraphic and kinematic indicators, are usually normal faults, although reverse movement on these and the moderately dipping movement directions is not uncommon. Shallow

slickenfibres plunge to the NW and the SE, moderate fibres exclusively to the SE and the steep mode predominantly to the NE.

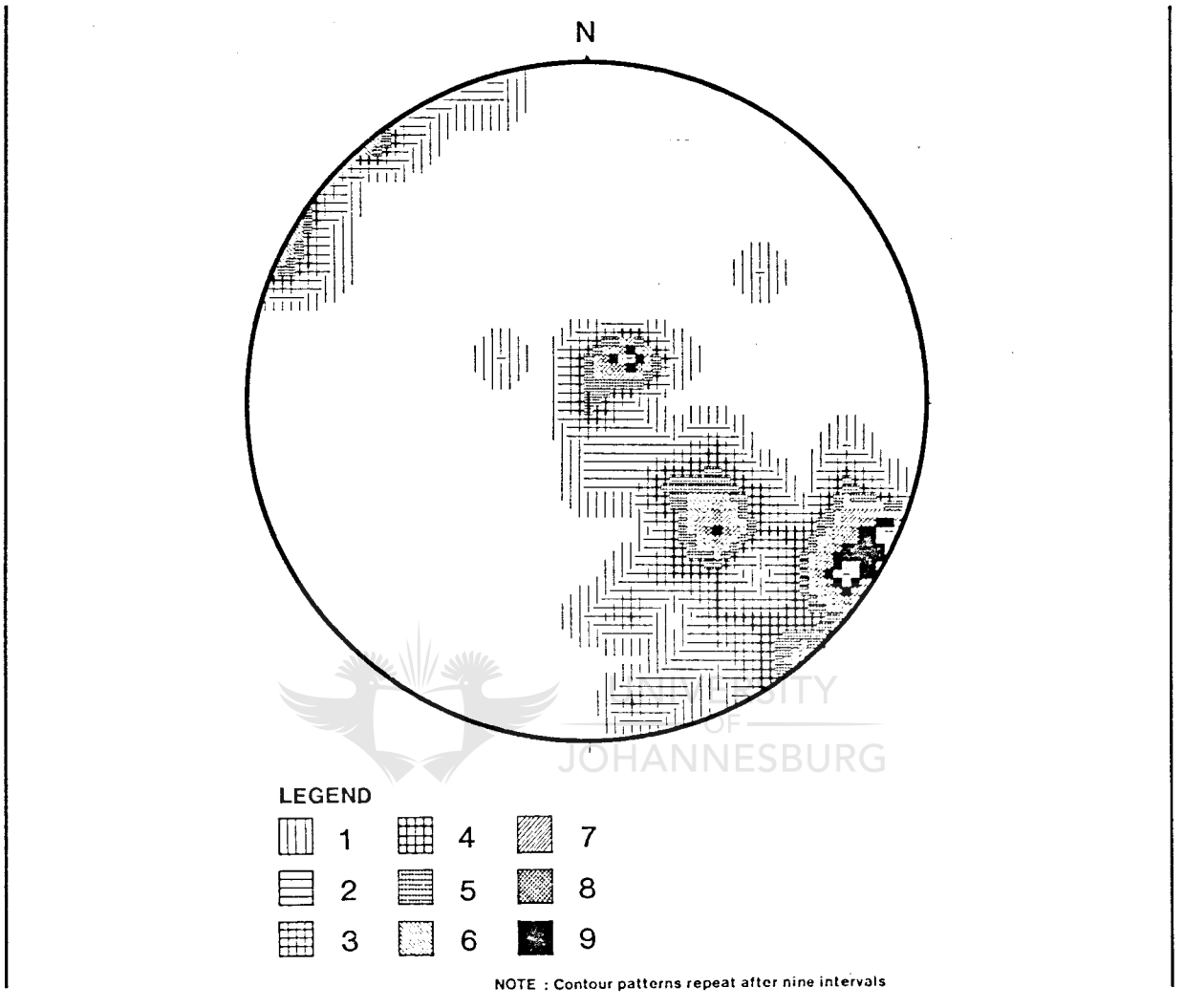

Figure 10 : Contoured plot of the orientation of slickenfibres developed on NW-SE striking fault planes (Schmidt stereographic projection). Total number of readings = 55. Contoured at 1% level.

NE-SW trending faults display a similar pattern of directional modes (Fig. 11). A very much smaller percentage have shallow to horizontal strike-slip motions. Moderate to shallow dipping slickenfibres plunge both to the NE and SW, whilst the steeper varieties plunge predominantly SE.

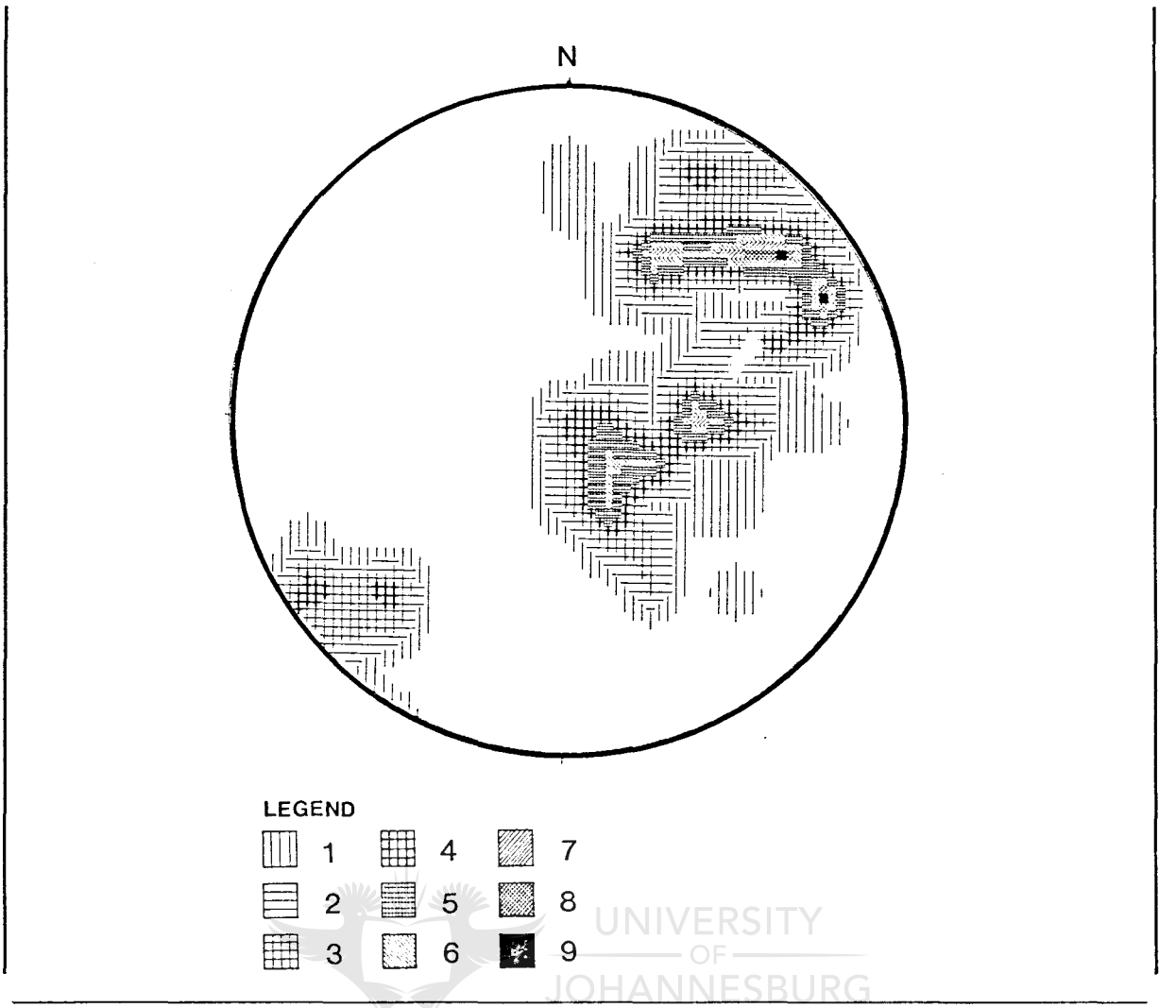

Figure 11 : Contoured plot of the orientation of slickenfibres developed on NE-SW striking fault planes (Schmidt stereographic projection). Total number of readings = 69. Contoured at 1% level.

Slickensides which plunge steeply to the N and S dominate the E-W striking fault planes (Fig. 12). These structures are generally normal faults. Shallow to moderate plunges for slickenfibres are also present, and are characterised by oblique normal and reverse to horizontal strike-slip movements.

The N-S trending faults do not display the same development of slickenfibres and, for this reason, the plot of these data has not been contoured (Fig.13). The individual points plotted show a wide range of orientations, but all plunge towards the E.

These planes represent both normal and reverse faults.

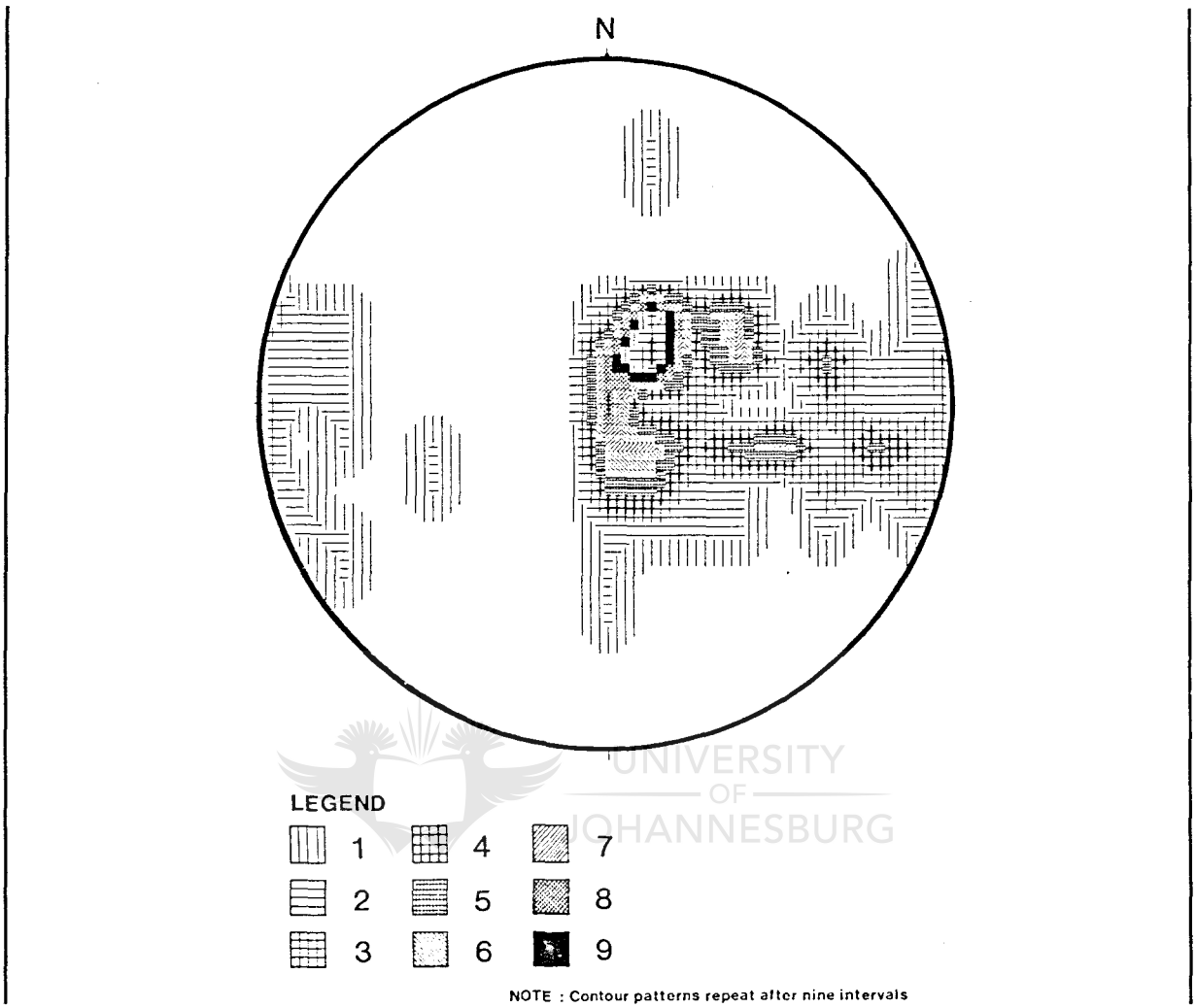

Figure 12 : Contoured plot of the orientation of slickenfibres developed on E-W striking fault planes (Schmidt stereographic projection). Total number of readings = 60. Contoured at 1% level.

Although strike-slip displacement of some magnitude has been recorded in the East Rand Goldfield (Ellis, 1943; Whiteside, 1944; Armstrong, 1968), no significant displacement was established on CMM in this study. One exception to this is the NE-SW right-lateral Jeffrey's Tear fault which passes through the underground workings on SD Shaft. Armstrong (1968) depicted this strike-slip fault on his map of the area, and attributed a

horizontal separation of over 900m to it. More recent development in this area now indicates that the horizontal separation is more likely to be approximately 380m along this fault (Sloman, per. comm. 1989).

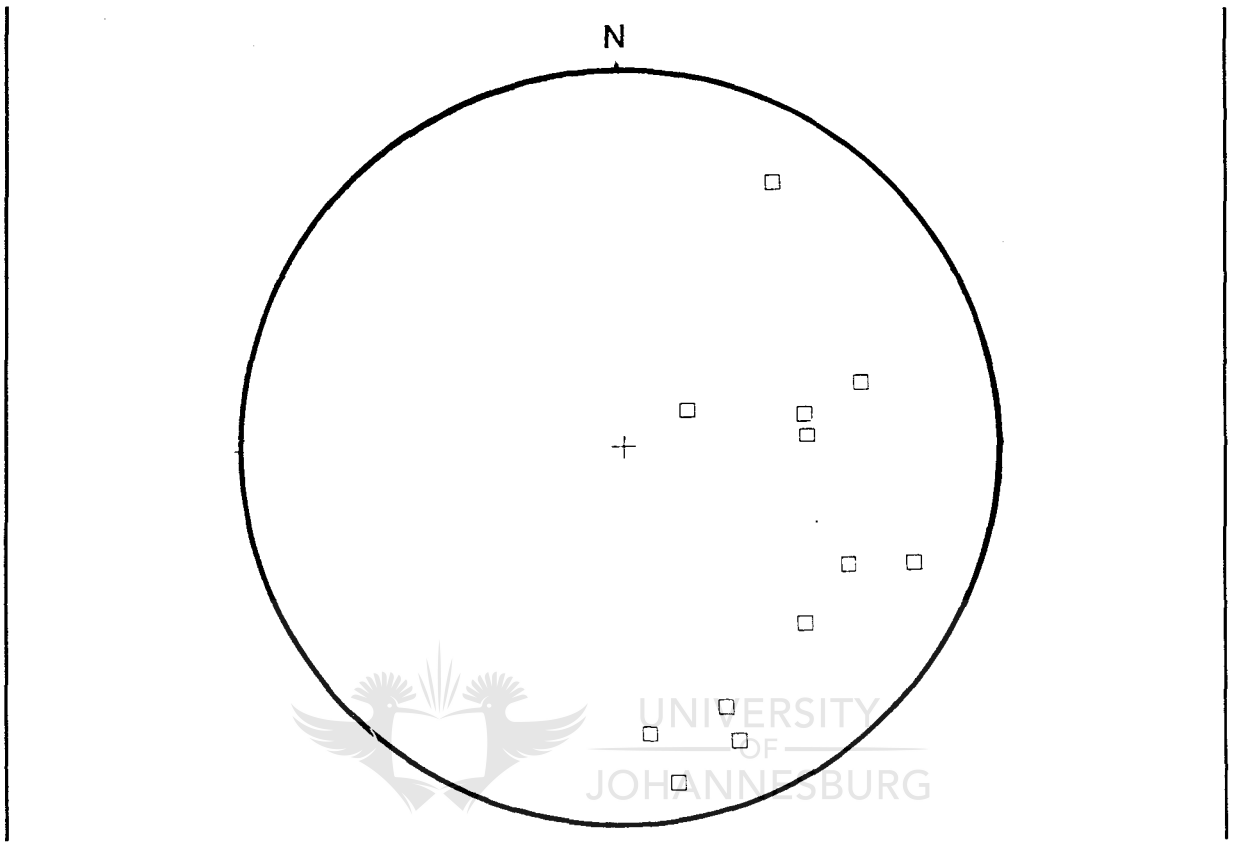

Figure 13 : Plot of the orientation of slickenfibres developed on N-S striking fault planes (Schmidt stereographic projection). Total number of readings = 12.

The presence of slickenfibres of varying plunge on essentially parallel planes within each group of faults suggests a complex history of deformation with repeated movement on most fault planes. The steep to vertical dips of the NW-SE, NE-SW and E-W fault groups might be inferred to indicate that they initiated as wrench faults. Shallow to oblique plunges of the slickenfibres on these fault planes confirms that many of them probably operated as wrench faults during their history, whereas

steep plunges are in agreement with the noted normal and reverse senses of movement.

The displacement on normal and reverse faults seldom exceeds tens of metres. All fault types are generally represented by zones of failure rather than individual displacement planes, and these zones typically comprise discreet failure planes spread over distances of tens of metres, which makes the resolution of displacement due to any one fault type difficult. This problem is further exacerbated by the problem of isolated repeated movement on individual planes within a zone.

4.2.2 Quartz veins

Quartz veins lying within and cutting across beds are common in all the quartzites in the study area. They also are present, less commonly, in the more argillaceous units. In terms of their shape and spatial relationship to structures, the quartz veins can be subdivided into three categories:

- sinuous and irregular massive forms (no consistent orientation)
- extension fractures
- fault related veins.

Veins of the first category are streaky or constitute irregular blobs, and exhibit both forms without any notable preference for one or other form in particular lithologies or structural environments. Such veins do not appear to be constrained in position or shape by fault or joint planes and are not characterised by a consistent orientation within the exposure, but follow random paths. Streaky veins are common in the

general vicinity of faults but do not exclusively appear in proximity to faults. In rare instances, these veins appear to progress from a sinuous, randomly oriented character to consistently oriented as they approach major structures.

The streaky veins resemble "braided" veins as described by Raybould (1975), although he does not discuss any occurrence of the more blocky to irregular, massive forms. These streaky or "braided" veins are also reminiscent of some "linked en echelon veins" of Nicholsen and Pollard (1982). They do not, however, consistently emulate either of these two forms, suggesting that their formation is not attributable to mere simple fracture filling or linking of en echelon arrays through deformation of bridges between en echelon veins.

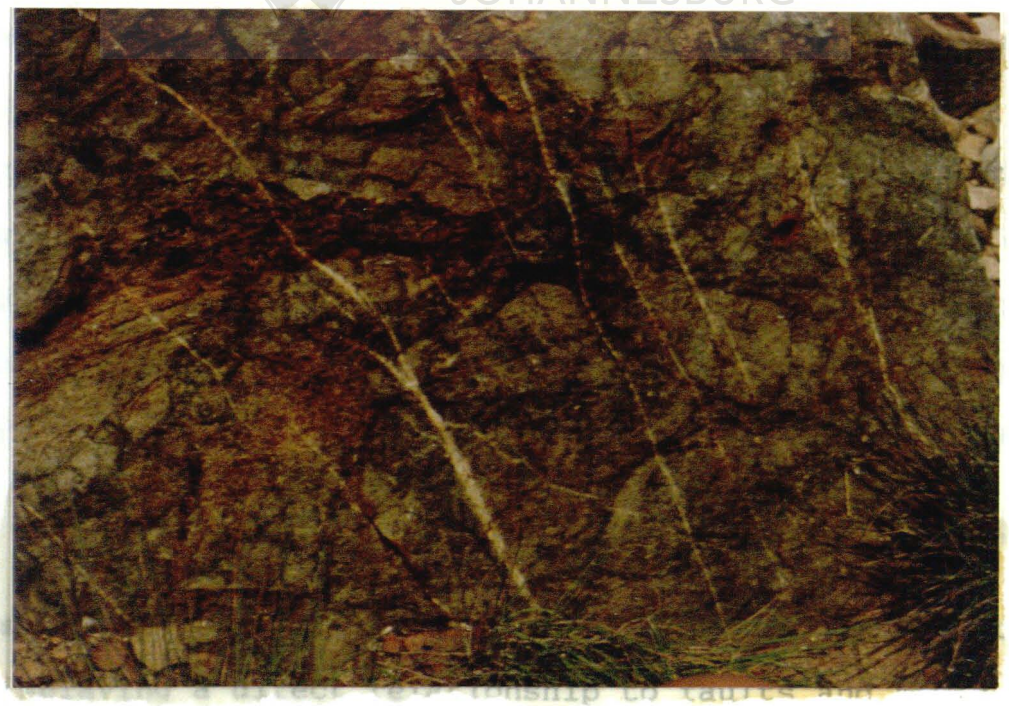

Figure 14 : Small, consistently oriented quartz veins in extension fractures within the Government Subgroup, Middle Lake. The view is 45cm across.

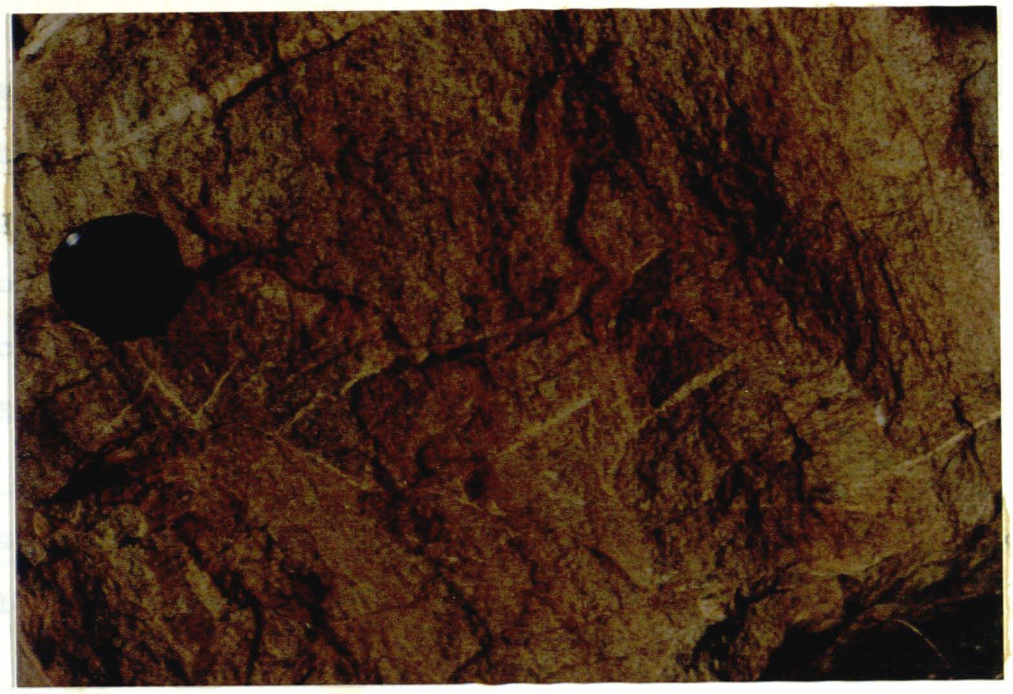

Figure 15 : En echelon, quartz vein-filled, extension fractures, as seen in the Government Subgroup at Middle Lake.

The second category of veins comprises those which form an infilling of extension fractures (Fig. 14). In some cases, the grains and crystals of the veins are fractured along the vein walls, but display no significant displacement. These veins occur in clusters, and form recognizable groups of joints following similar trends which can be measured throughout the East Rand Goldfield. Linking and braiding of these veins is rare, as those veins which follow parallel joints are generally too widely spaced for this to occur. An en echelon arrangement is common (Fig. 15). The thickness of these veins varies between 3mm and 20cm, but is commonly between 3mm and 50mm.

The classification "fault vein" relates specifically to those veins displaying a direct relationship to faults and fault zones in or adjacent to which they lie. These veins occur along vertical, sub-vertical and bedding-parallel faults. Such veins

are also present in very close proximity to faulted dykes.

In the vertical and sub-vertical faults, the quartz veins are essentially restricted to the fault zone and usually appear as strongly brecciated fault rocks. In some instances these veins show only fracturing. The latter are most common in the vertical and near-vertical fault generations striking N-S, E-W and NE-SW. The brecciation of the vein material within the fault indicates that reactivation of movement along these fault planes probably took place. Veins associated with bedding parallel fault zones are discussed in section 4.3.5.

4.2.2.1 Vein fibre data.

Whilst the sinuous and irregular vein forms rarely display oriented fibre growth, extension fracture veins generally exhibit good fibre development. These fibres are usually oriented at 90° (± 15°) to the strike of the vein walls. The trend of the length of the fibres has been measured, and the implied extension directions for each set of veins is tabled in Table 2. Where possible, their relative ages have been determined from field relationships, and indicate that more than one generation of veins has been formed on some orientations. The broad sequence of development of extension trends appears to be: E-W, NE-SW and NW-SE, N-S, and a final phase of fibres which rotate progressively from NW-SE through E-W to NE-SW as seen in individual veins bearing sigmoidally shaped fibres. Bedding parallel faulting in these West Rand Group localities does not displace this final phase of vein development.

AREA	LOCALITY	EXTENSION TRENDS
N of Homestead Fault		
	Atlasville	NW-SE NE-SW E-W N-S
S of Homestead Fault		
	Homestead Dam	ENE-WSW NNE-SSW ESE-WNW N-S
	Clinic	ENE-WSW NW-SE N-S NE-SW
	D Taljaard Park	NW-SE N-S NE-SW
	Korsmann's Pan	NW-SE E-W N-S
	Middle Lake	E-W N-S NE-SW NW-SE
	Benoni	N-S NW-SE E-W NE-SW
S of Van Ryn Fault		
	Van Ryn Dam	NE-SW ENE-SSW E-W

Table 2 : Extension directions obtained on fibred veins exposed on surface in the East Rand Goldfield.

4.2.3 Field relationships of non-bedding parallel faults.

The interaction of the non-bedding parallel faults was examined at their intersections. Faults of the steeply dipping N-S group displace moderately dipping NW-SE faults in, for example, the 1E4W cross-cut on 1 Circular Shaft. Within the same cross-cut,

however, a similar N-S fault is cut and disturbed by a NW-SE fault. Various examples of equally apparently contradictory relationships are also in evidence between the E-W strike-slip faults and the NE-SW normal faults, notably in the 1E5 footwall drive E on the same shaft. No cross-cutting relationships between the N-S and E-W groups were observed.

The majority of the non-bedding parallel fault zones consist of brecciated vein quartz, small amounts of talc and either rock flour or crushed quartzite. Most of these fault rocks can be classified as crush breccias or fault breccias. There are some faults, however, whose planes are occupied by dykes. Ilmenite Diabase dykes (see section 3.3) of post-Ventersdorp and pre-BRQF age, generally have faulted contacts. The faults associated with this shearing are the N-S moderately dipping, NW-SE strike-slip, NE-SW normal and steep E-W faults, but do not always cross-cut the dykes as the orientation of these dykes is variable. Younger WNW trending Green Syenites dykes are similarly faulted by moderate to steeply dipping NW-SE and E-W strike-slip faults.

Determination of the relative ages of the non-bedding parallel faults, and the resolution of their apparently contradictory cross-cutting relationships is partially resolved through the use of:

- fault planes which do not exhibit re-activation features, i.e. planes which do not bear more than one age of slickenfibre development, and whose fault rock does not include brecciated vein quartz material,
- their relationship to dyke intrusions
- their relationship to the BRQF. (See section 7.5).

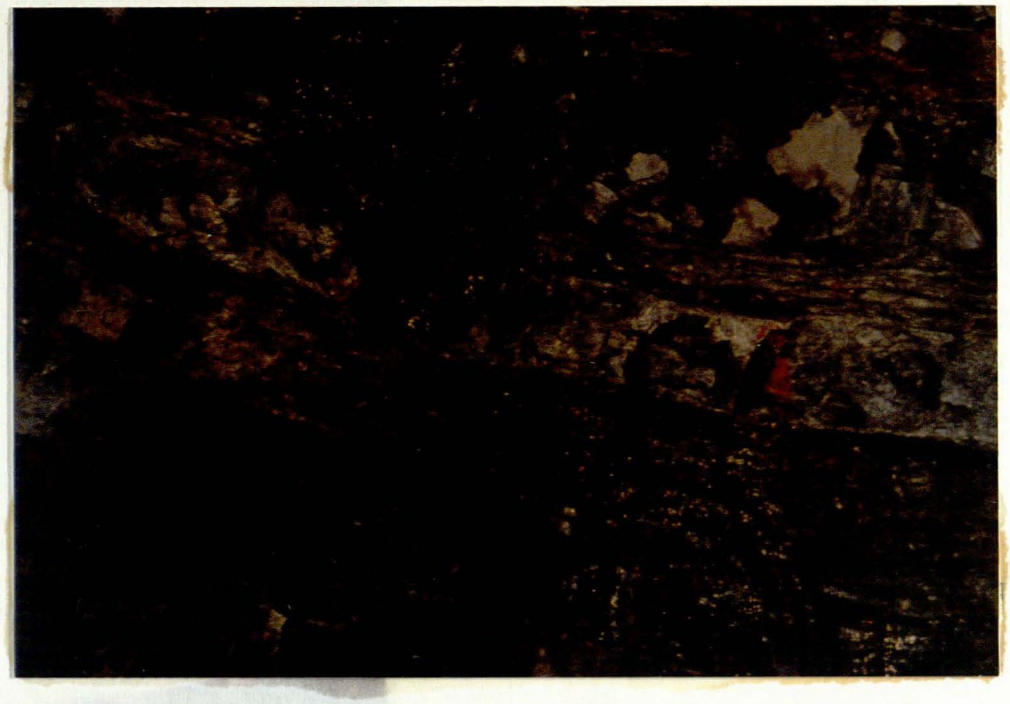

Figure 16 : Bedding parallel fault zones in the LK1 as seen at 1 Circular Shaft. The darker, apparently argillaceous beds represent high strain zones.

4.3 Bedding parallel faults

Bedding parallel faults are the most prevalent type throughout the East Rand Goldfield. As the name implies they are parallel to bedding such that their strikes (±E-W) rarely deviate from that of the bedding by more than 10° (Fig. 16). The vast majority of these faults are narrow (< 15cm) although exposures of individual faults up to 2m in thickness have been observed (Fig. 17). The faults are most commonly sited at lithological contacts (Fig. 16), although they may occur within a single bed (Fig. 18) or cut up through the stratigraphy.

Bedding parallel faults are ubiquitous within shale horizons, although they are often difficult to recognise. They are not restricted to these units, and are commonly observed within

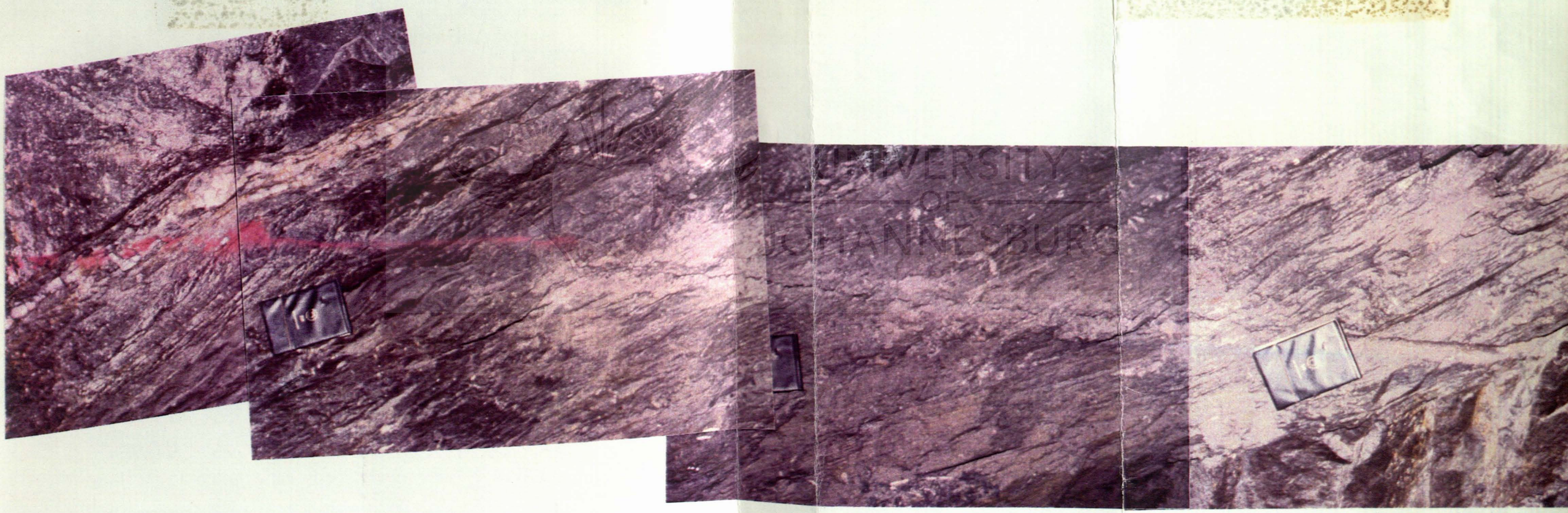

Figure 17 : Panoramic view of the bedding parallel fault zone commonly present in the vicinity of the MK2/MK3 contact, as seen at 1 Circular Shaft.

Figure 18 : A bedding parallel fault sited within a MK2 conglomerate band, 14 Shaft.

quartzites, conglomerates (Fig. 18) and even within the metamorphosed lavas of the Johannesburg Subgroup (Fig. 19). In the latter case, fault planes deviate from the usual angle of dip, and become steeper than the bedding overlying the lavas with distance from this contact.

Major lithologic contacts, such as that between the MK3 and MK2 are characterised by particularly broad (0.4 - 2.0m) faults or fault zones (Fig. 17). The contact between the Jeppestown and Johannesburg Subgroups, as seen in subsurface in the Van Ryn area, is completely obscured by a zone of green, fine-grained, altered mylonitic fault rock, which represents another such concentration of strain at a lithological contact.

4.3.1 Fault rock associated with bedding plane faults.

The bedding parallel faults are generally characterised by the

Figure 19 : Bedding parallel faults, Bird Lavas, NEP Shaft. The contact between the lavas and overlying quartzites is defined by a quartz vein (A). The thin faults parallel the contact adjacent to it, but steepen with distance to sub-parallel to it (B).

presence of quartz veins contained in or adjacent to foliated fault rock. The quartz veins often display bright green rims. Petrographic examination and XRD determinations reveal that these rims are mostly pennine with minor amounts of microcline. This rimming is generally accompanied by pyrite, chalcopyrite, siderite and even pyrrhotite (Figs. 20, 21).

The nature of the fault rock is dependent on the original undeformed lithology. Determination of the original lithology is complicated by hydrothermal alteration which has taken place within these zones, resulting in an apparently more argillaceous rock than the surrounding undeformed rock. This alteration is characterised by the development of phyllosilicates, particularly varieties of chlorite which lend a light, white-

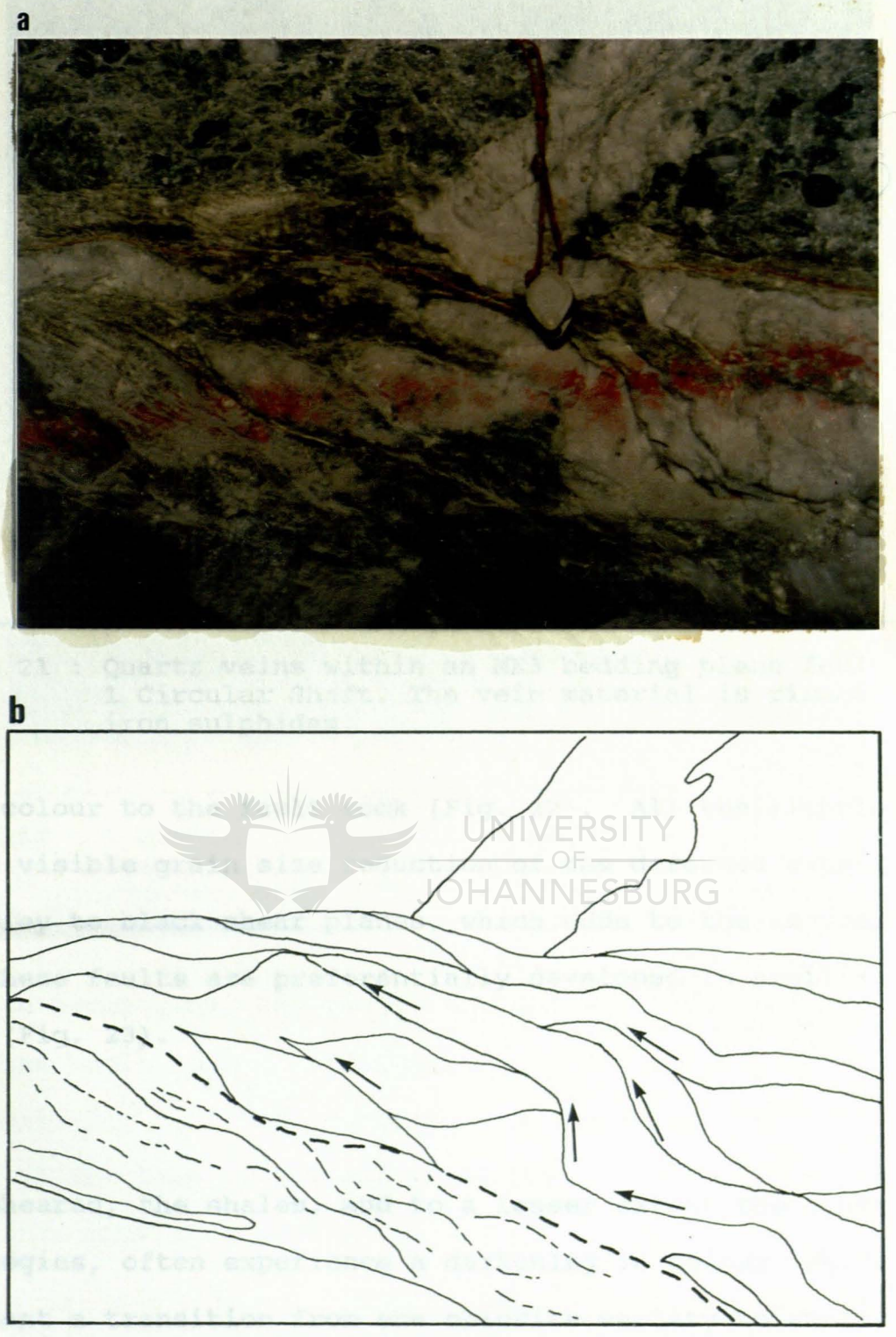

Figure 20 : a) Duplex and ramp structures indicated by faulted quartz veins in an MK3 bedding plane fault, 1 Circular Shaft. The deformed host to the veins is characterised by zones of substantial chloritisation. N is to the left of the photograph. b) Line sketch of above photograph. Solid lines outline horses, thin dashed lines incipient horses, and the thick dashed line a fault plane.

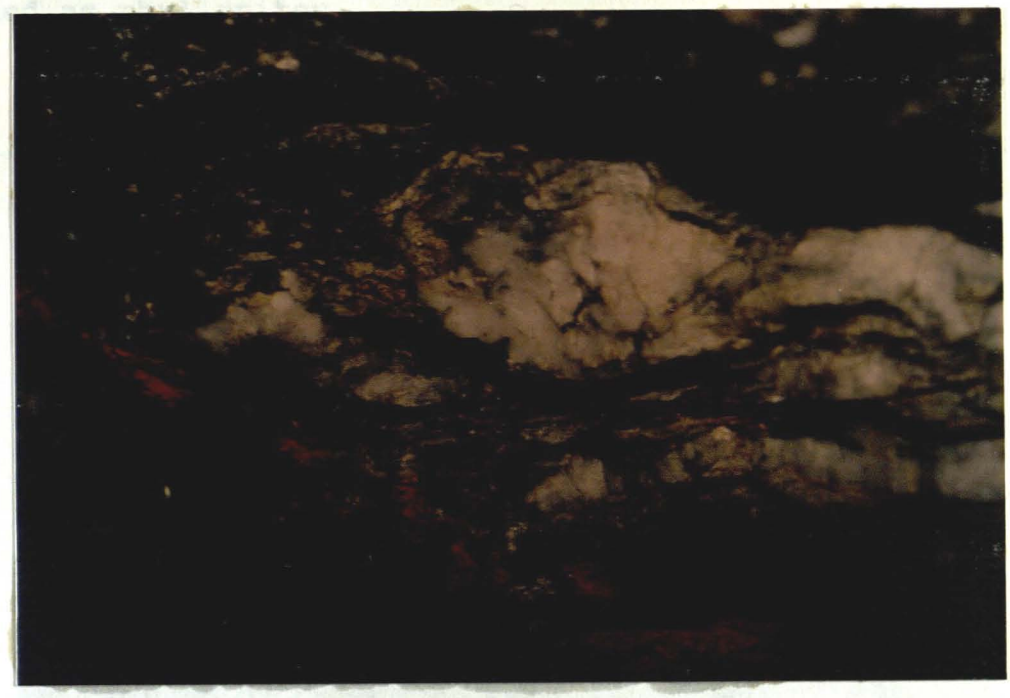

Figure 21 : Quartz veins within an MK3 bedding plane fault zone, 1 Circular Shaft. The vein material is rimmed by iron sulphides.

green colour to the fault rock (Fig. 22). All the lithologies show a visible grain size reduction of the deformed material, with grey to black shear planes, which adds to the impression that these faults are preferentially developed in argillaceous zones (Fig. 23).

Once sheared, the shales, and to a lesser extent the other lithologies, often experience a darkening in colour, which may represent a transition from one chlorite variety to another (Law, pers. comm., 1989). Where the shale is present in the footwall of major fault zones, as at SD (Figs. 24, 25), a transition from a dark green-grey undeformed shale to a black highly deformed shale is observed. The exceptionally fine-grained nature of the phyllosilicates in these shales, and the

pervasive shear deformation of them, implies that they should be regarded as phyllonites.

Figure 22 : A bedding parallel fault within an MK2 quartzite, as seen at 14 Shaft. The sheared material adopts a lighter, more intense white-green hue than the relatively undeformed surrounding quartzite.

With few exceptions, the fault rock appears to be mylonitic, using the fault rock classification of Roering, *et al* (in press). Two localities have been observed, however, where cataclasites occur: at the base of the MK1 at 1E7S on 1 Circular Shaft, and within the BRQF at 7 Shaft.

4.3.2 Slickenside movement data

Due to the predominantly ductile nature of the bedding parallel faults, few of them show any reasonable slickenfibre growth. A limited number of such fibres were measured up on shallow fault planes, however, and the resultant implied movement directions are plotted in Figure 26. Most slickenfibres plunge to the S,

Figure 23 : A bedding parallel fault in an MK1 quartzite, 14 Shaft. The sheared material progresses from grey along its contacts to black - grey in the centre. It may include small pebbles where immediately adjacent to the overlying conglomerate.

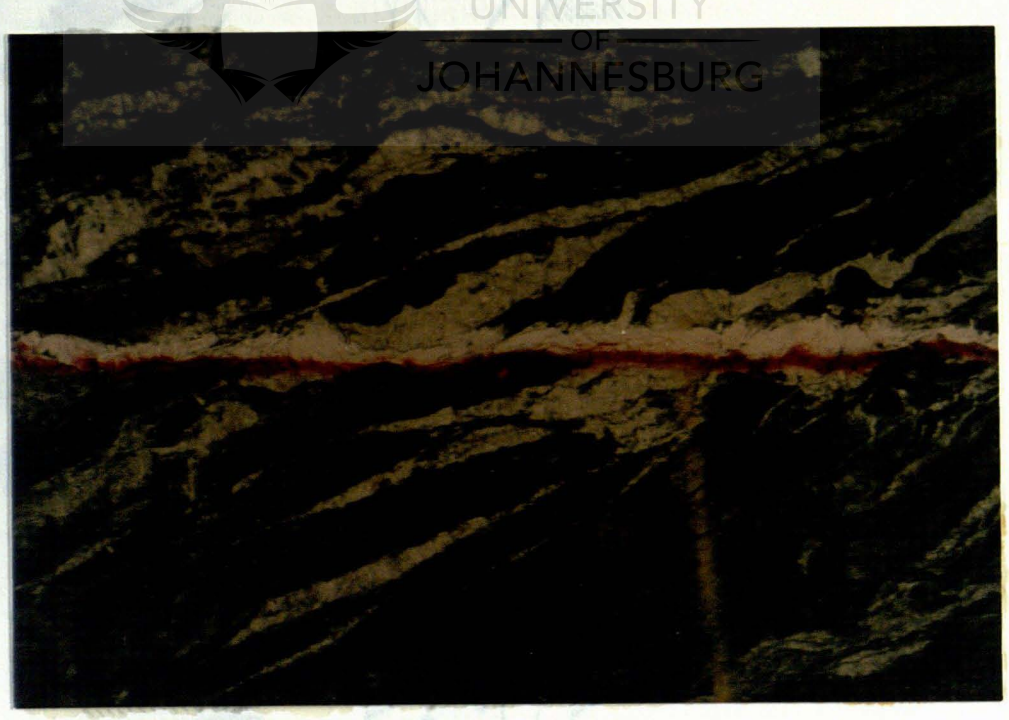

Figure 24 : The deformed footwall to the ramp in Figure 25. The footwall material progresses from black (A) close to the ramp to black-green with distance from the ramp (B). Note the differing degrees of deformation of the quartz veins.

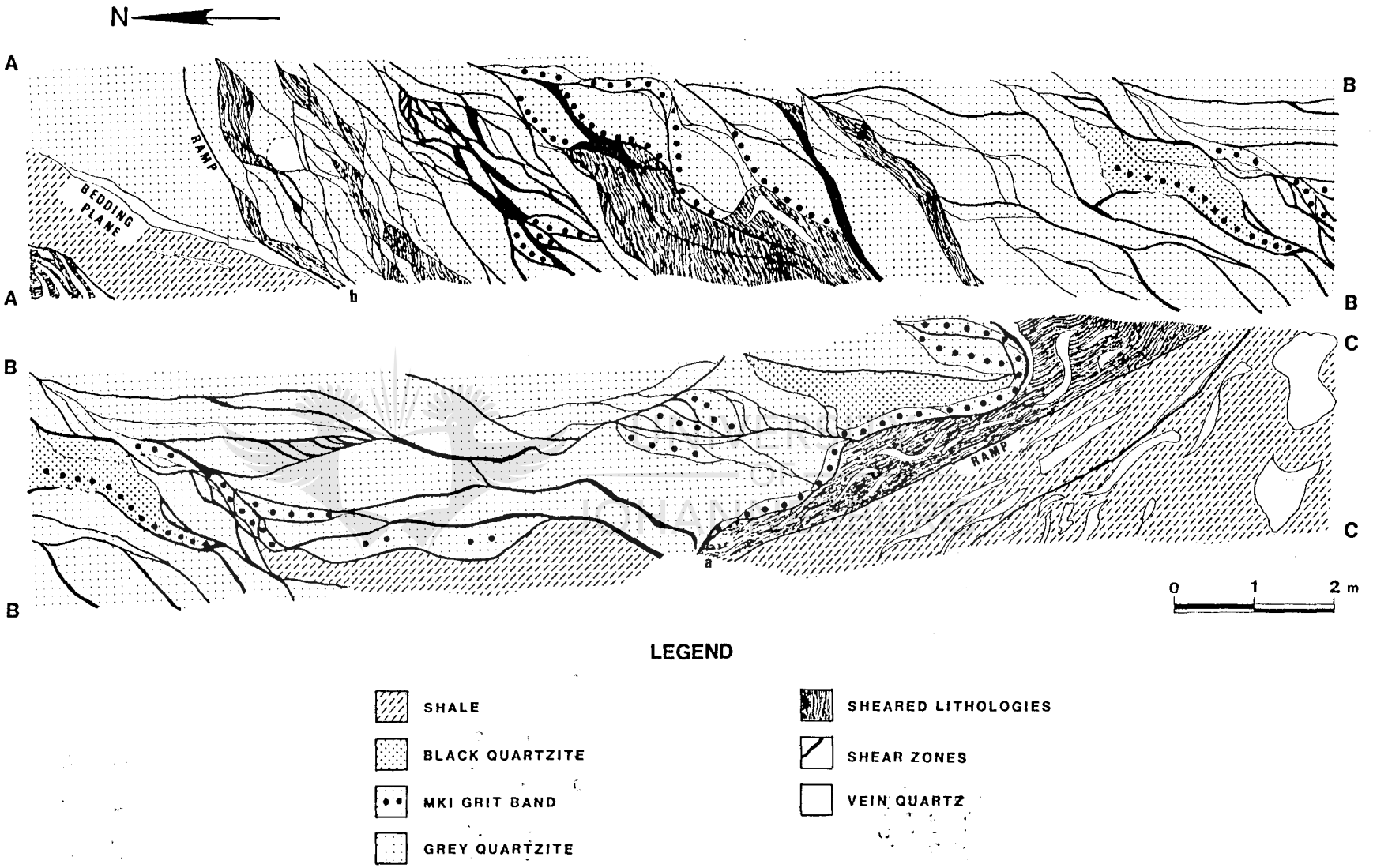

Figure 25 : Ramp and duplex structures on SD Shaft. The profile curves from left to right through 40°. MK1 conglomeratic bands can be seen to back-steepen and overturn against the ramp planes. All black lines between beds represent fault zones, drawn to scale.

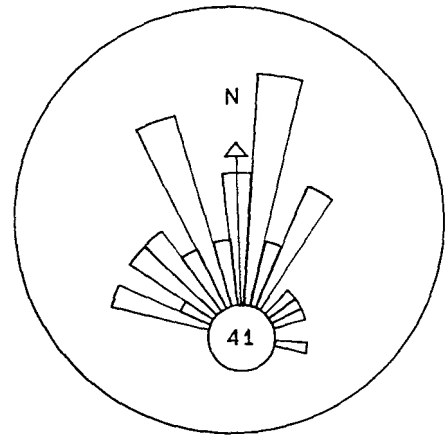

Figure 26 : Plot of the implied movement directions obtained from the orientation of slickenfibres developed on bedding parallel fault planes. Total number of readings = 41. Note there are several directional modes, this is true of all shafts.

but do so on a variety of orientations, ranging from slightly W of NW to NE. Readings falling into different modes have been measured on different planes within metres of each other. This does not appear to represent a broad scatter due to differing positions of the data points or irregular movement of the nappes, but rather, as will be shown later, reflects distinct modes of movement. Slickensides developed on bedding planes in the quartzites of the Hospital Hill Subgroup at the Clinic locality (Map 1) appear to plunge either sub-vertically (Fig. 27), or at shallow angles towards the W to NW (Fig. 28). Slickenfibres formed on steeper ramp planes are dealt with in section 4.3.4.1.

An attempt was made to derive the orientation of the stress axes associated with these faults by applying the method described by Aleksandrowski (1981) to the combined slickenside data from the flat and ramp planes of these faults. This method requires that the planes of movement related to a single event be oriented at

varying dips and strikes. In this study the variation in the orientation of these planes proved to be insufficient to produce a reliable solution.

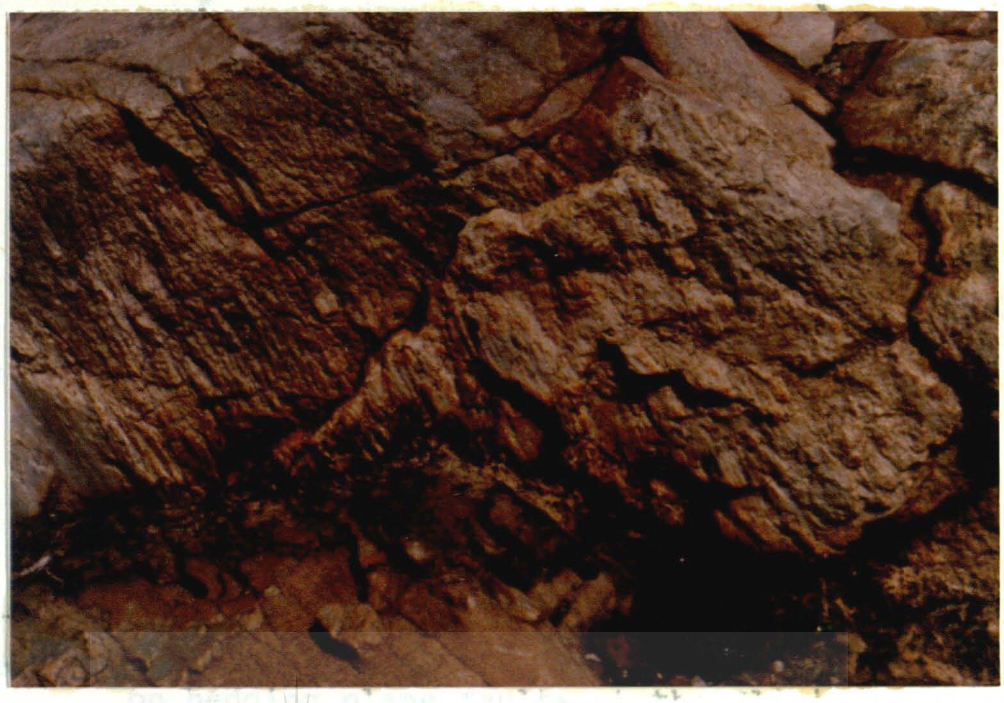

Figure 27 : Steeply plunging slickenfibres developed on overturned bedding plane faults at the Clinic locality, Benoni.

4.3.3 Foliations

The development of a tectonic foliation has occurred more readily within the shale units than within the quartzites and conglomerates. They are not absent from the latter two lithologies, but are restricted to fault zones and the deformed rocks in their immediate proximity.

The intersection of the shear and foliation planes produces a line which lies 90° to the movement direction in the plane of the fault (Roering and Smit, 1987; Lister and Snoke, 1987; Coward and White, 1988). Since the faults are parallel to

→ Orientation of the movement directions obtained from the angle between the cleavage and bedding. (Schmidt stereographic projection).
X = average pole to cleavage; ● = average pole to bedding.

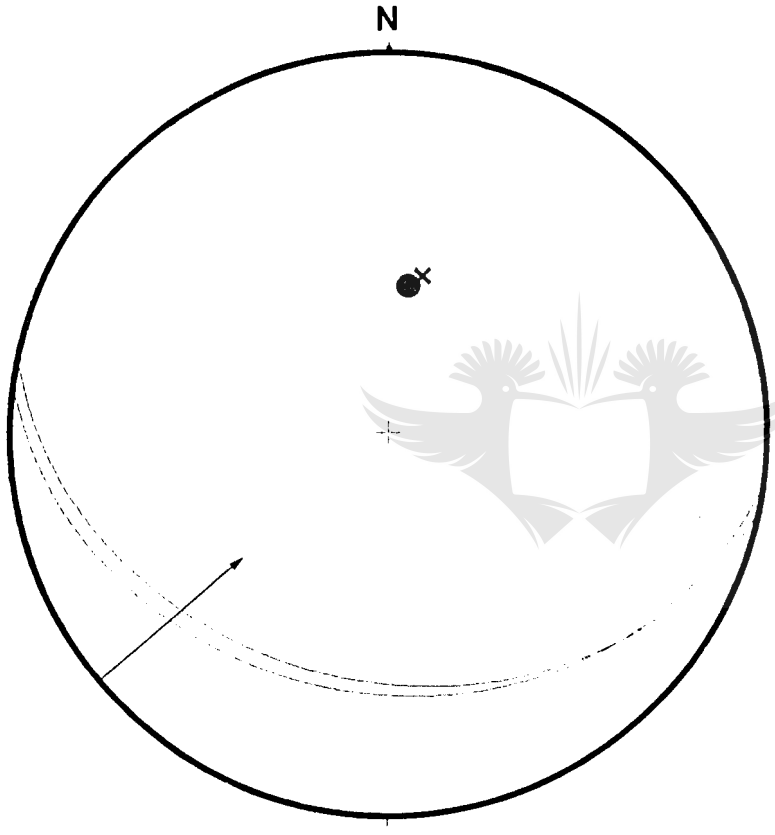

Figure 29 : Within the Jeppestown Sub -group, Heald Bridge.
Total number of readings = 40.

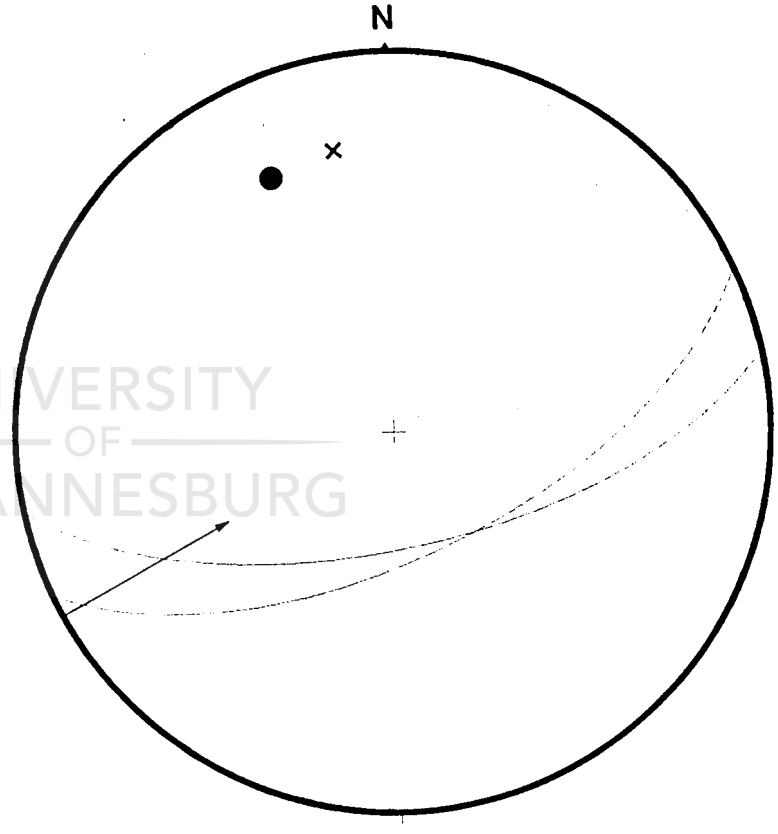

Figure 30 : Within the Jeppestown Subgroup, Danie Taljaard Park.
Total number of readings = 30.

the Van Ryn area (Map 1), a single set of asymmetric kink bands are developed in phyllonites in the Jeppestown Subgroup, and the highly deformed quartzitic footwall to the Main Reef Leader. The kink bands are short relative to the flat limb of the kinks and steeply dipping. Evidence of subsequent shear along these bands is present. The primary foliation is E-W striking and dips to the S. The "fold hinge" of the bands strikes NNE to NNW and the axial plane of the kink bands dips towards the W.

Tectonic foliations in the quartzites of the Government Subgroup at Middle Lake define a single group of moderate, S dipping, E-W striking planes. This relationship suggests that movement on the bedding planes was towards the NE (Fig. 31). In contrast, although foliations in the Rynfield Dam area also form a single mode, the planes are steeply N dipping on a NNE-SSW strike (Fig. 32). The beds in this area are, however, overturned and rotated, the timing of which has not been determined. Movement towards the NE is indicated.

The LK2 shales at 1 Circular and NEP shafts exhibit more than one mode of cleavages. A plot of the poles to the cleavage planes (Fig. 33) reveals at least two dominant orientations: a N or broad N to NW mode (which may represent overlapping N and NW populations) and NE. Additional scattered readings appear to be related to the faulting events discussed in section 4.2. There is little variation in the pattern of these orientations between the two shafts. Analysis of the intersection of each of these planes with the bedding suggests that at least two bedding parallel movements have occurred in this area, one towards the NE and the other towards the NW.

→ Orientation of the movement directions obtained from the angle between the cleavage and bedding. (Schmidt stereographic projection).
X = average pole to cleavage; ● = average pole to bedding.

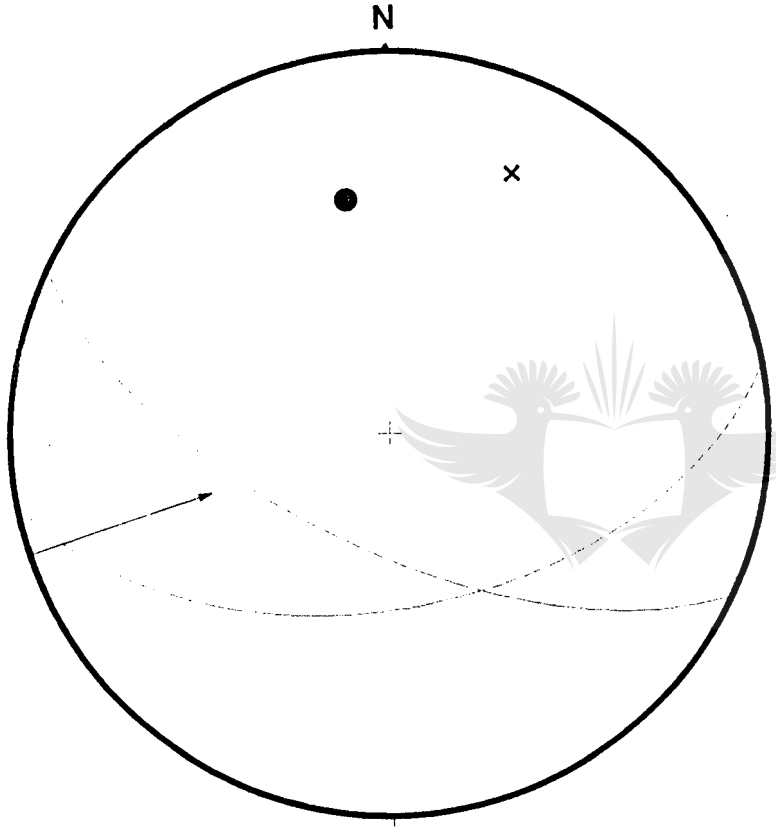

Figure 31 : Within the Government Sub -group, Middle Lake, Benoni.
Total number of readings = 45.

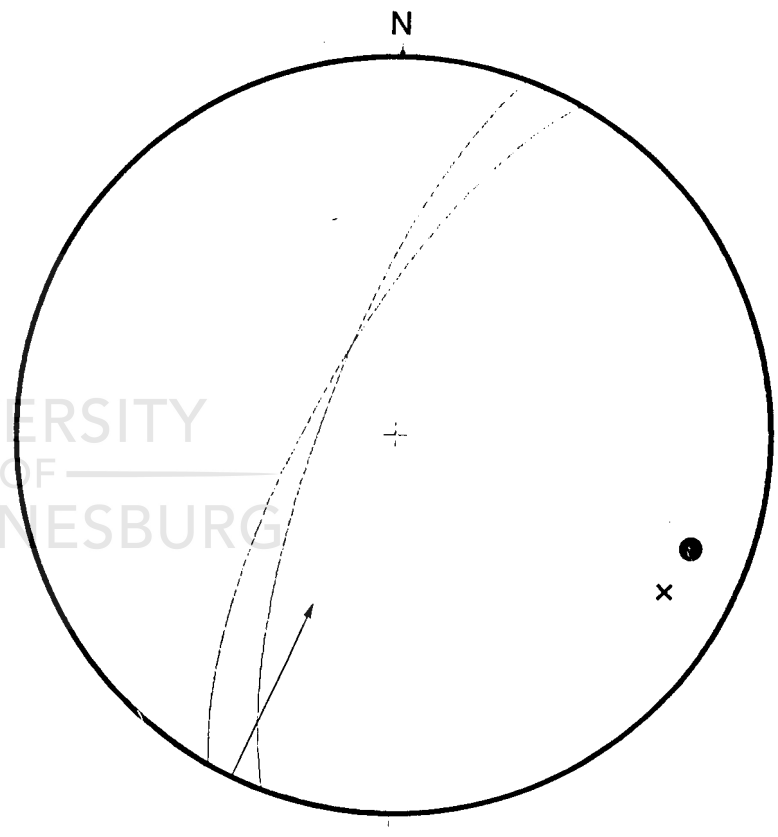

Figure 32 : Within the Government Subgroup, Rynfield Dam.
Total number of readings = 20.

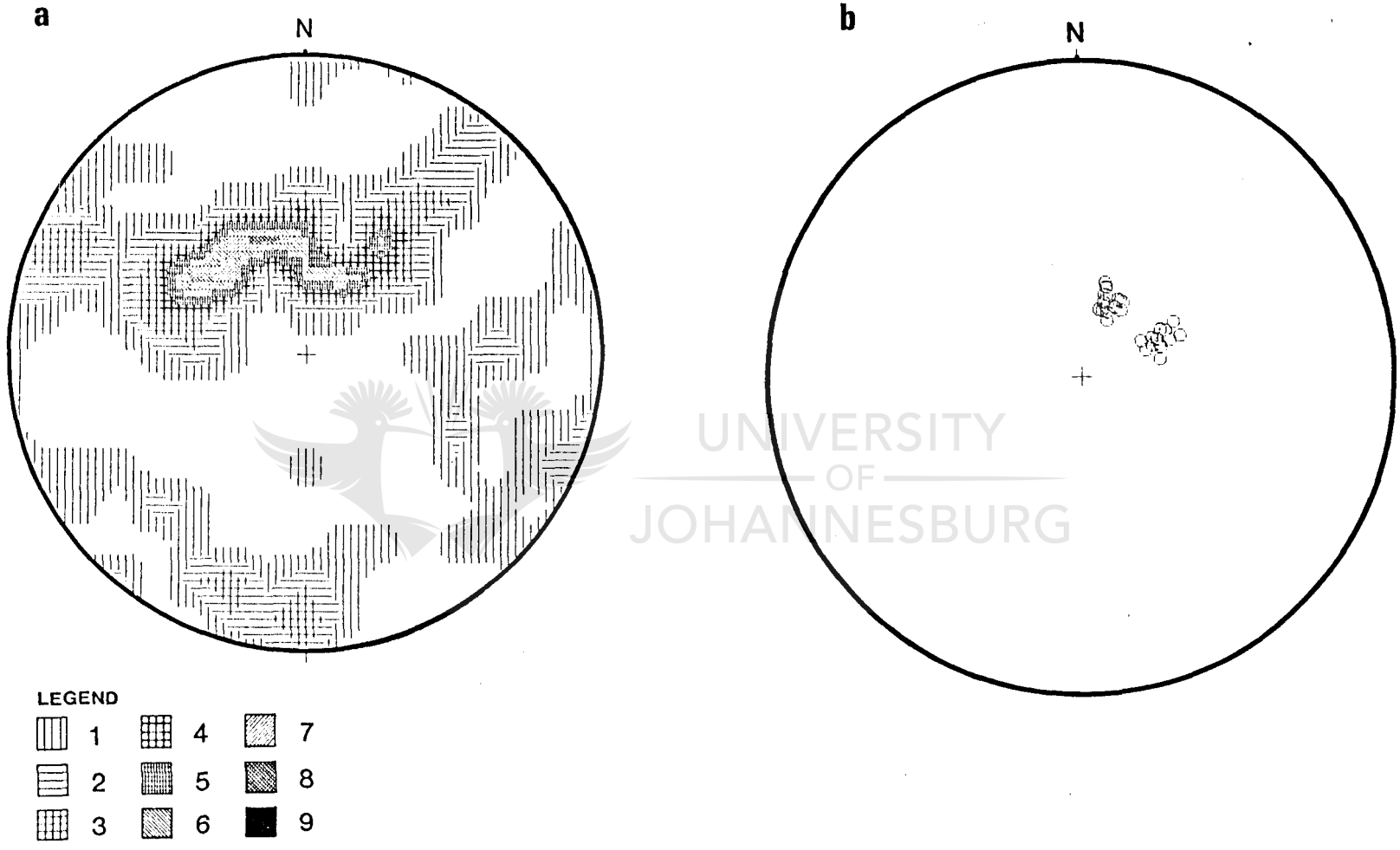

Figure 33 : Plot of the poles to cleavage planes developed within the LK2 shales on:
a) 1 Circular Shaft , total number of readings = 87. Contoured at 1% level. b) NEP Shaft, total number of readings = 35. (Schmidt stereographic projection).

The better exposed rocks of the Central Rand Group contain numerous zones of foliated rock. Within the zones of ductile shear, and along their boundaries, s-c fabrics, as defined by Lister and Snoke (1987) (Fig. 34), are present. These have been measured within quartzitic, conglomeratic, and argillaceous beds. Initial attempts to analyze these readings by the determination of average s and c plane orientations proved unsuccessful, as the s-planes orientations are broadly scattered and appear to define at least two populations. Individual pairs of s-c planes read at single points were, therefore, plotted and analysed (Fig. 35). The zones in which these measurements were taken, as well as the resultant movement vectors, are of shallow to very shallow dip and their restoration has little affect on the directions of movement obtained.

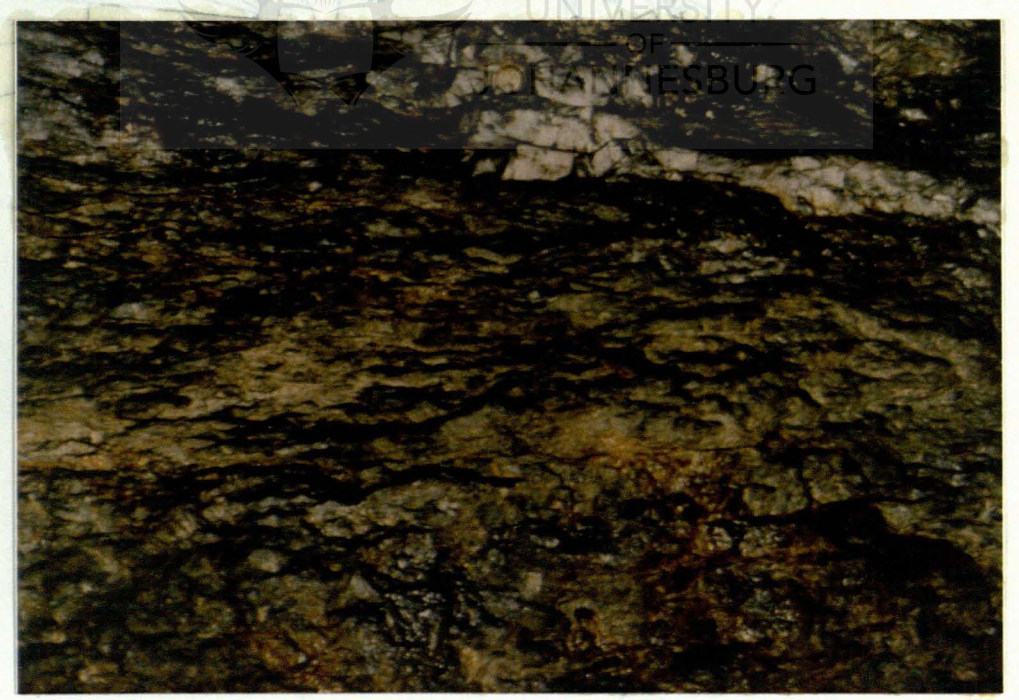

Figure 34 : S-C planes within a Kimberley Subgroup bedding parallel fault. These planes are often distinguishable by their darker colour. The c - planes lie E-W across the photograph and the s - planes lie NE-SW. The length of the photographed area is 9cm.

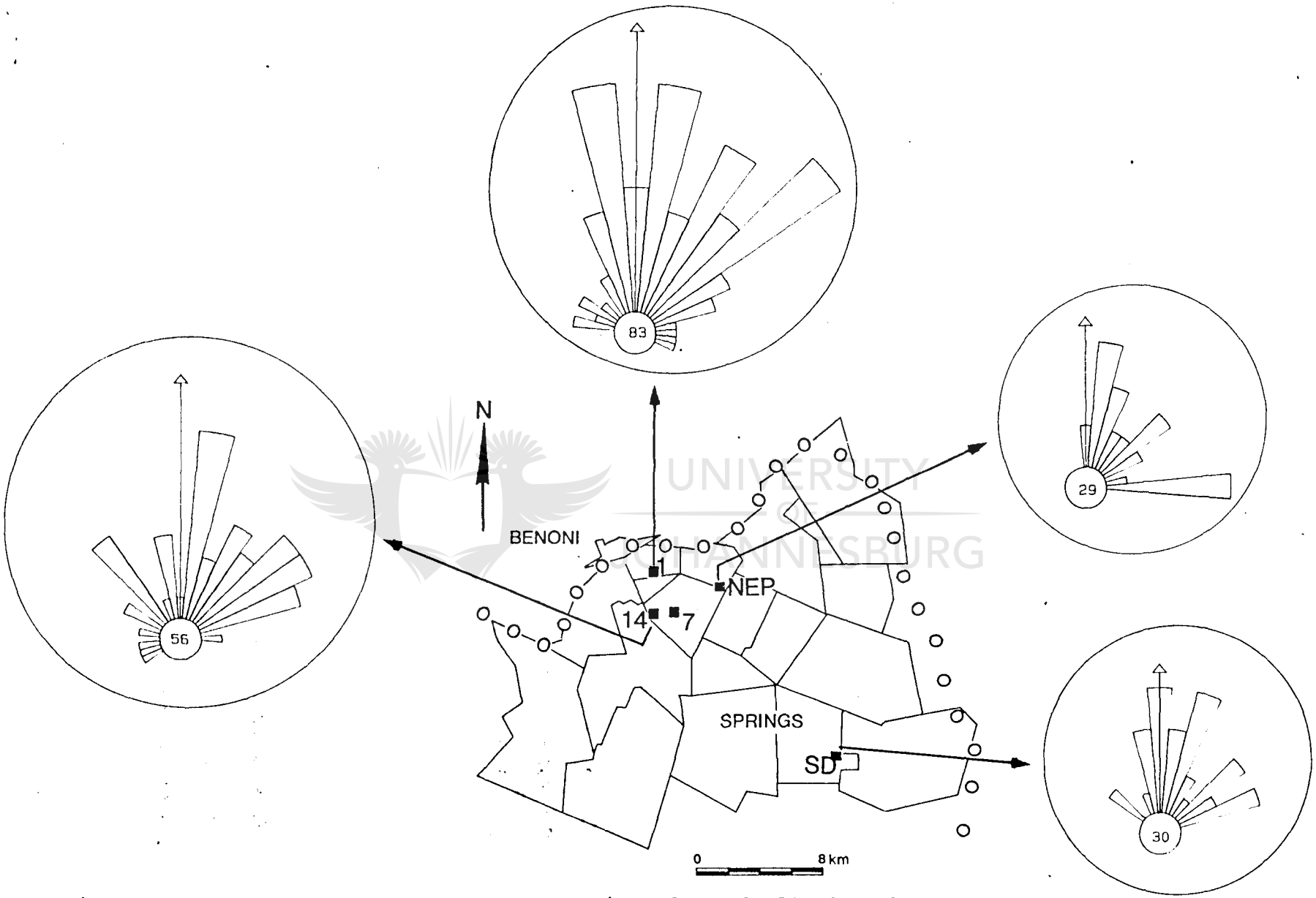

Figure 35 : The movement vectors on bedding plane faults based on s-c relationships in the Central Rand Group on each shaft of CMM.

The absolute position of each movement vector mode may be shifted as a result of the differing geographical position of the shafts around the broad gentle warp in the beds of this area, but at least two, and possibly three distinct senses of motion are obtained: NE and N to NW. An additional mode to the E is present at NEP shaft, but is less conspicuous at the other localities. This represents a small number of readings and does not appear to be significant.

4.3.4 Ramps and duplexes

Ductile bedding plane shear zones are characterised by variations in thickness and angle of dip of foliation. These variations are largely the result of the development of ramps and duplexes. The scale of such features ranges from that of the width of the foliation (< 2 cm) to several metres (Figs. 36, 37). Although the ramp planes are generally smoothly sigmoidal, staircase forms are also present. Relatively few back-thrusts were observed, but one is present in 18N10A cross-cut SE on 14 Shaft, where the Middle Kimberley units are thrust towards the S. Intraformational duplexes predominate in exposures of the Central Rand Group, but individual, isolated horses of up to several metres in length do exist throughout the rocks.

Large ramps which cut up through stratigraphy and the formation of duplexes behind these ramps are generally only distinguishable where reefs and other marker horizons are present. Multiple intraformational duplexes within fault zones occur on all scales (Figs. 36, 37). In certain instances it can be observed that a large horse within a duplex is in itself comprised of a number of smaller horses, and thus also forms a duplex boundary. (Figs.

20, 25, 37, 39). Such features may result in local thickening of zones by up to 200%.

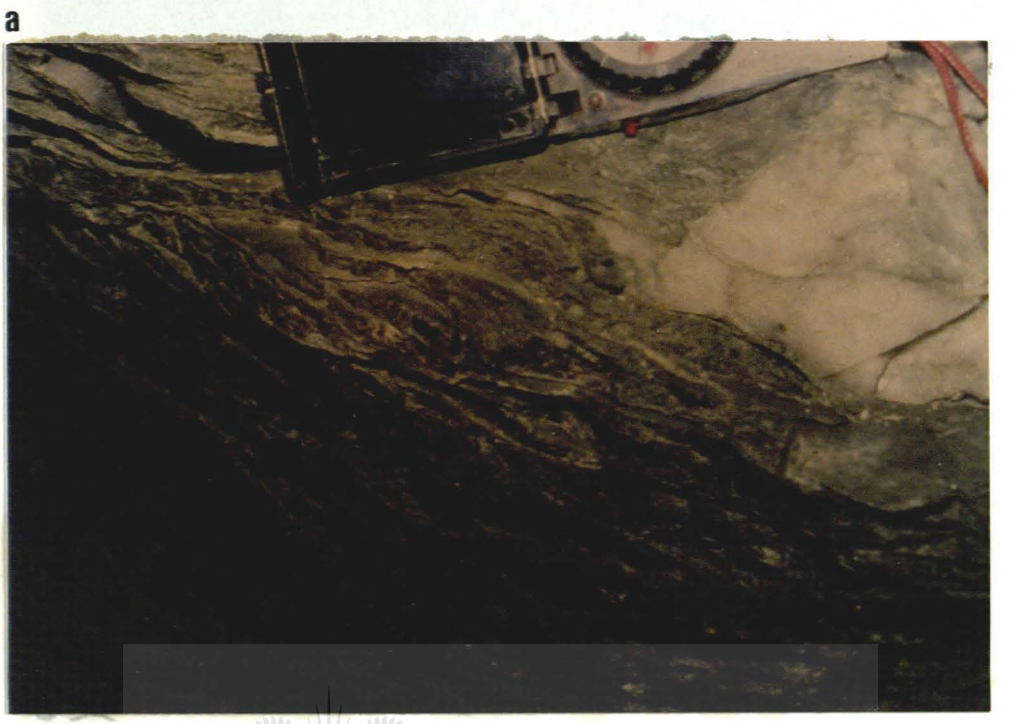

Figure 36 : a) Small scale duplexes and ramps within an MK3 bedding plane fault, 1 Circular Shaft. These duplexes utilize the plane of foliation for ramping. N is to the left of the photograph.
b) Line sketch of above photograph.

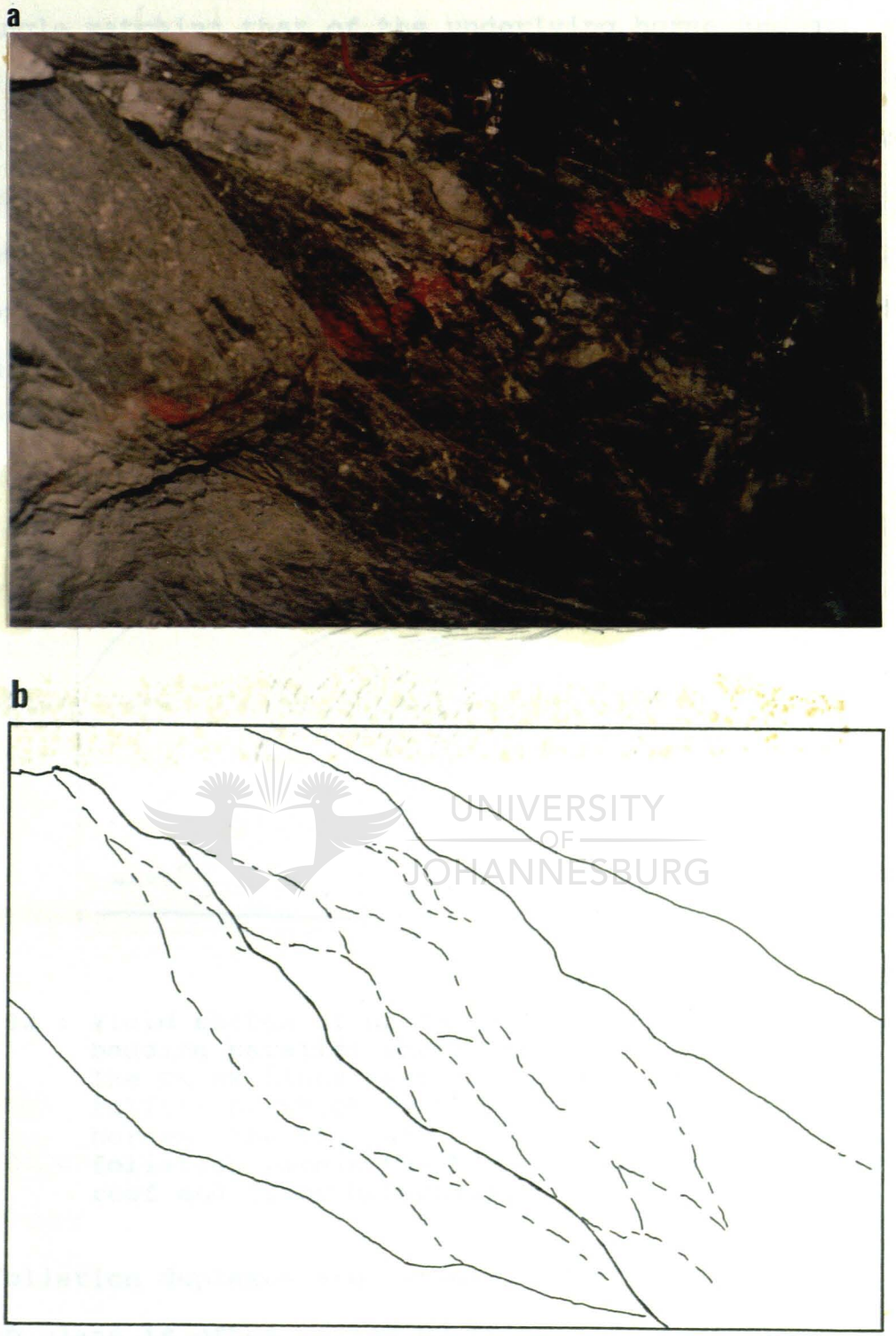

Figure 37 : a) Duplexes and ramps within a bedding parallel fault zone, NEP Shaft. Many horses utilize the plane of foliation for ramping. Smaller horses within the larger duplexes (defined by lithologies of contrasting colours) are barely discernible due to this phenomenon. N is to the left of the photograph. b) Line sketch of above photograph. Solid lines delineate large scale duplexes which ramp on the s-plane of the foliation. Dashed lines outline internal horses.

In the smaller zones, duplexes are often stacked in a highly uniform manner. Almost identically sized and shaped horses lie at an angle matching that of the underlying horse and are thereby constrained to the original thickness of the fault zone. This is most clearly demonstrated by foliation scale duplexes. Duplexes of this nature do not usually exhibit significant deformation of the hanging wall through anticlinal folding, but have roof and floor detachments which are almost parallel due to uniform thickening within the limits of the exposure (Fig. 38).

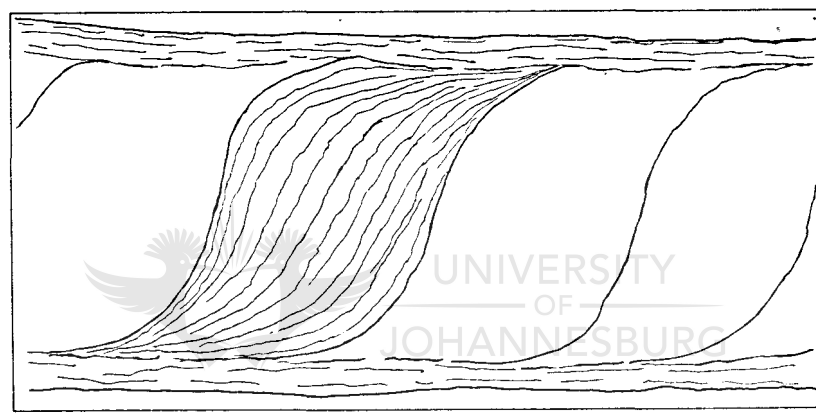

Figure 38 : Field sketch of uniform, foliated horses within a bedding parallel fault zone, on 1 Circular Shaft. The thick lines represent the s-plane of the foliation, which is the ramp plane for these horses. The thin and broken lines indicate the foliation within the horses. Note the parallel roof and floor detachments.

These foliation duplexes are extremely difficult to identify, as the ramp plane is often formed by the s-planes of the ductile shear zone (Fig. 36,37,38). This implies that movement can occur along the foliation planes, i.e. the plane of local flattening. Movement on these planes, together with the lack of markers, in many areas results in failure to recognize many ramps and associated duplexes within the fault zones,

particularly within the shale units. This is, further, a good example of the use of pre-existing planes in ramp development.

Zones >40cm in thickness may also contain duplexes constrained in fault zones. The angle between foliation and the fault planes (in this case the plane of bedding) in such zones usually ranges from <4° at the walls of the zone of shear, to 35° in the centre of the zone, resulting in a sigmoidal shape for the individual horses. Generally, the presence of ramps results in a steepening of this angle, behind the ramp, by up to 60°. The angle of the ramps varies greatly, as duplexes and horses do not stack uniformly. Individual horses vary in size, override one another by varying amounts and give rise to a more complex arrangement (Fig. 36). Larger duplexes are not only constrained to the fault zone, and do not only affect deformed material, but also carry undeformed horses. These horses are most commonly isolated and only distinguishable by the orientation of fault planes. Sharp deviation of a fault plane from its customary angle of dip and the anastomosing and reuniting of such planes define the horse. Where marker horizons are visible in beds within or immediately overlying undeformed pods, their orientation should reflect the presence of ramps. Although the angle of bedding in horses which have overriden each other varies depending on the amount of overlap of duplexes and original ramp angle, the ramps to such duplexes most commonly dip at 40° to 60° S.

As major ramps are approached, rocks in the Kimberley Formation display the geometrically necessary anticlinal folds of hanging wall strata, and show multiple duplexes. In addition, the footwall is often synclinally warped by the presence of horses

formed by footwall plucking. The duplexes behind these decametre scale ramps are particularly good examples of the phenomenon of larger duplexes which are internally duplexed (Fig. 25, above b).

As especially large ramp planes are approached, the angle of foliation and the dip of beds within duplexes may exceed an angle of 60°, approaching vertical and sometimes becoming overturned. In Figure 25, a curved dimensional view of two major ramps is shown. The SE portion contains duplexes in which a MK1 pebble layer is rotated through 110° from a shallow SW dip through the vertical to a dip of 50° to the E. Slickenfibres on the ramp plane and the angle between the foliation and shear plane indicate an oblique movement towards the NE on this plane (position a in Fig. 25). A similar steepening of the angle of the dip of the duplexes against the ramp plane, is seen at the left hand side of this profile, but the movement indicated on this ramp is towards the NNE (position b in Fig. 25). The true dip of the beds increases from behind the major ramp as the ramp is neared, and then decreases with distance in front of this ramp, tending again to the customary angle of dip of the beds in this area. When examining this profile, it must be borne in mind that the apparently flat dipping ramps are due to the down-dip view exposed on the curve of the tunnel.

In the thrust system shown in Figure 40, each horse comprises a lithology different to that in the overlying and underlying duplex. Zones of ductile deformation are thus confined to the bedding planes between contrasting lithologies. The thickness of these fault zones is usually 5 - 10cm, but may be as little as 2mm or as much as 50cm. Again a steepening of the angle of

fault plane and bedding is seen against the frontal ramp plane (position a in Fig. 40) (Fig. 39), and slickenfibres on this plane indicate a slightly oblique movement towards the NW. This ramp plane was previously interpreted as the undercut bank of an MK1 channel. Whilst this may have represented a channel originally, the present morphology of this "bank", and the beds within the "channel", are due to the deformation undergone by these beds.

Figure 39 : The "undercut bank" ramp structure seen in Figure 40, at position a. N is to the left of the photograph.

4.3.4.1 Movement on the ramp plane

The surfaces of the ramps are typically highly polished and may bear well developed slickensides. Slickenfibre growth is not unknown, and on the frontal ramp in Figure 40 such fibres indicate movement to the NNW. Large ramps examined commonly contain fault rock, and this may be accompanied by vein quartz.

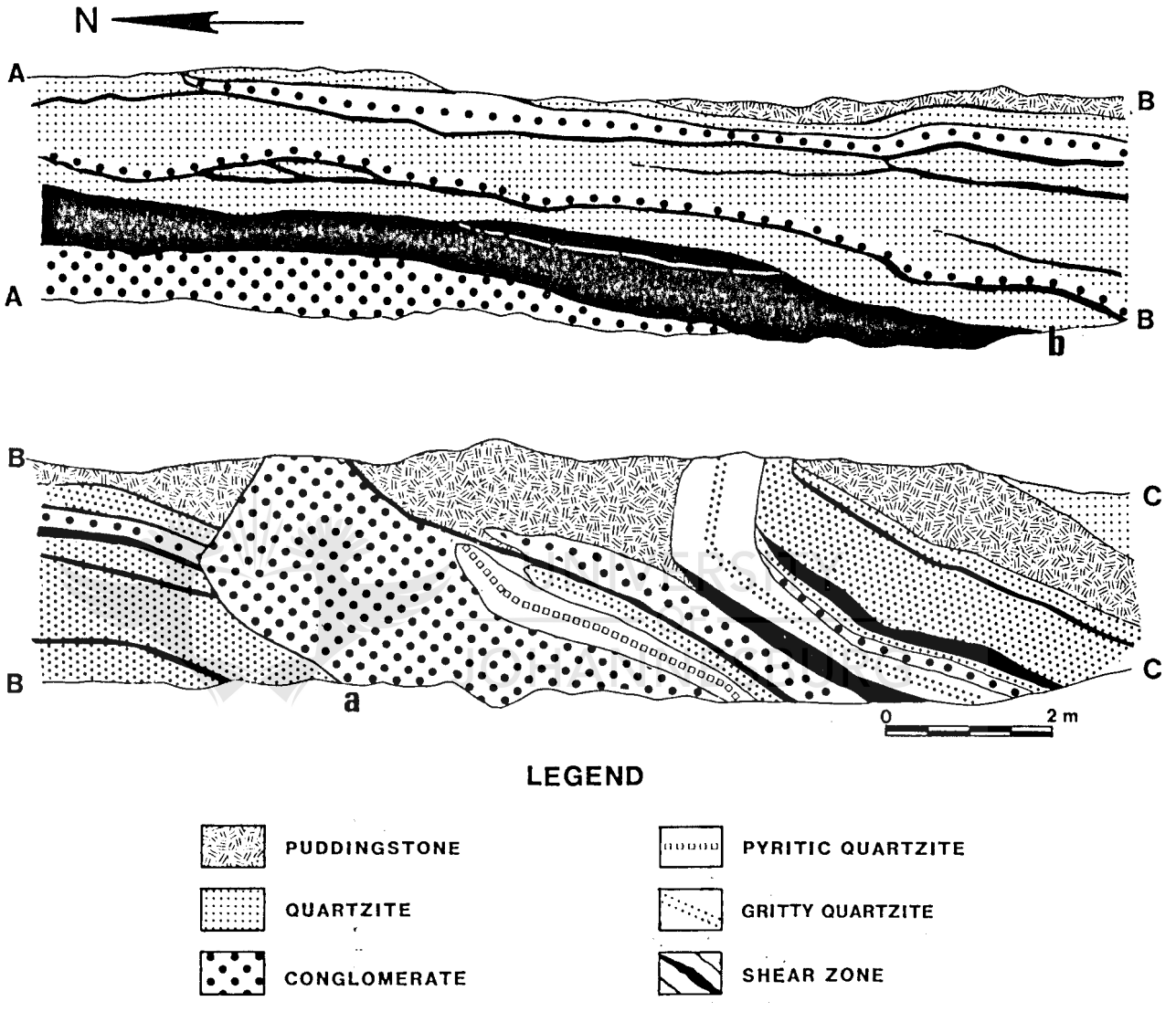

Figure 40 : Profile through an MK1 channel in 3W9A cross-cut N, 14 Shaft. The "undercut bank" of the channel forms a pre-existing plane used in ramping. Duplexes steepen and overturn against this plane. Solid lines between beds represent fault zones, drawn to scale.

Measurements of the dip and strike of ramps of all scales indicate no significant variation between groups of differing sizes. All measurements were made underground in the rocks of the Turffontein and Johannesburg Subgroups. Insufficient ramps are visible in the surface exposures of the West Rand Group to justify a similar treatment, but all those measured fall within the modes determined for the underground exposures.

Among the three major shafts exposing the Kimberley Formation there is little variation in the pattern of populations of movement directions measured on the ramp planes (Fig. 41). Those small variations which do exist are not significant. They may be attributed to the presence of footwall undulations at the time of formation of the ramp, their varying geographical position about the broad warp in this Goldfield and the tendency of these shear planes to exploit pre-existing fault and joint planes to facilitate ramping. Movement directions from all three localities display a broad scatter about N, with the predominant modes lying within 10 degrees either side of N. An additional mode is noted at 030-040° and the lack of scattered readings between this directional mode and the N mode suggests that it is a distinctly separate mode. Isolated measurements lying elsewhere may correspond with ramps associated with back-thrusts.

4.3.5 Quartz Veins

Veins associated with bedding plane faults fall within the "fault related" category as defined in section 4.2.2. The frequency of veins spatially related to the bedding parallel faults is dependent on the host lithology and proximity to

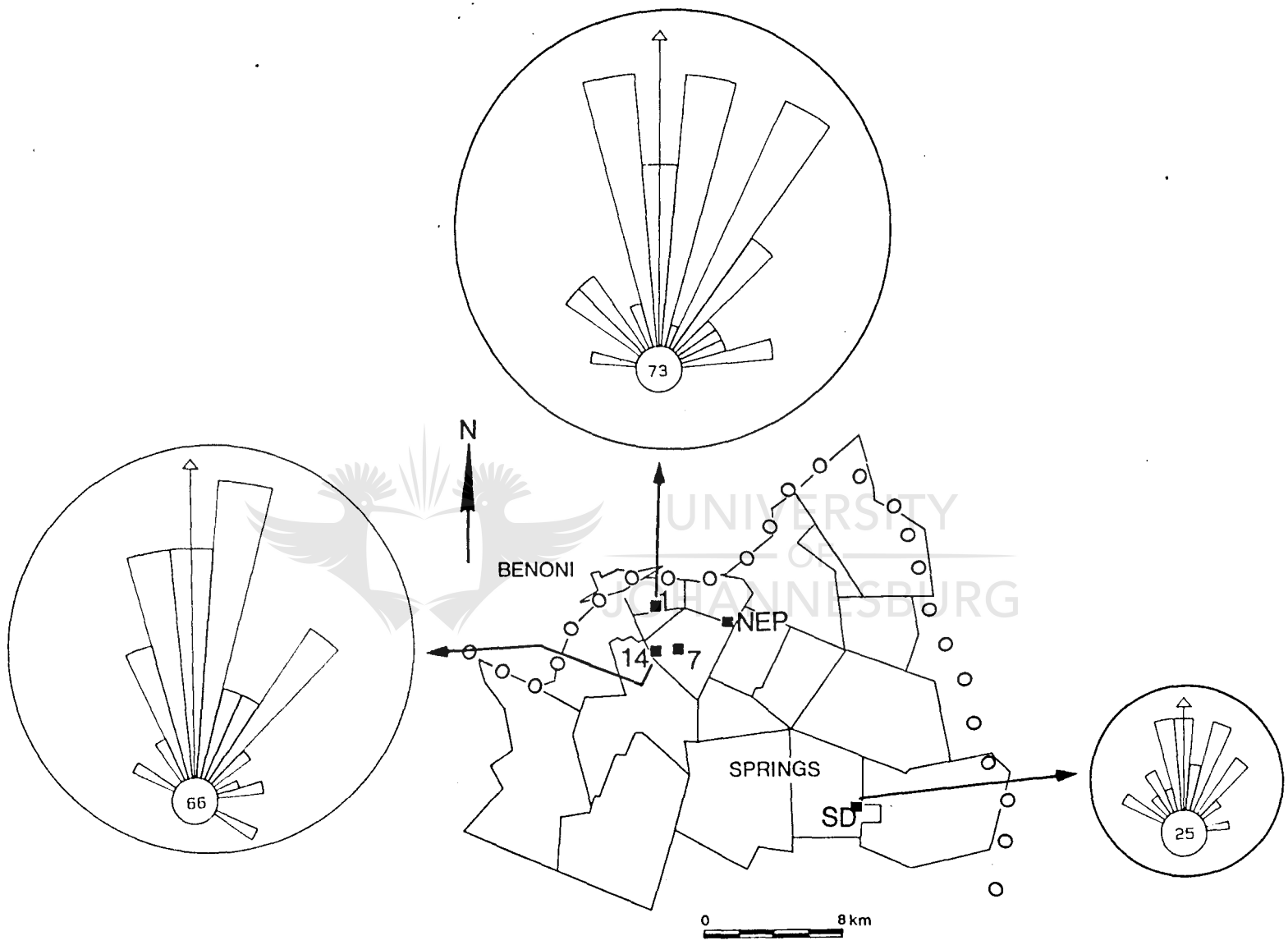

Figure 41 : The directions of movement on bedding plane faults obtained from measurements of slip movement lineations on ramp planes in the Central Rand Group on 1 Circular, 14 and SD shafts.

faults. As major bedding plane faults are approached within the Kimberley Formation, the number of parallel bounded, similarly oriented veins increases dramatically. On SD shaft, for example, the percentage of vein material in the rocks constituting the tunnel walls increases from <2% at 70m from the structure seen in Figure 25, to >60% 10 m away from the edge of this feature. Where the vein material exceeds 35% of the exposure, it is largely present as 5 or fewer extremely thick veins. Small, hairline planes of shear are commonly - but not always - visible along the walls of such quartz veins. These veins might, therefore, form along very much smaller fracture planes which parallel and form a prelude to a major fault plane. This phenomenon of similarly oriented very thin planes of failure increasing in frequency as major structures are approached is also witnessed where quartz veins are not as prevalent.

In siliceous lithologies, veins with a close spatial relationship to faults are present in far greater numbers than in less siliceous units. (This is also partially true of quartz-filled extension fractures). The influence of this control is most strongly demonstrated by zones of shear which parallel the bedding plane, as seen in the UK9B and MK3 quartzites.

Large (>10cm thick) veins lying on thin (<1cm) fault planes form a small numerical percentage of the quartz veins found within bedding plane faults. The vast majority of such veins are, instead, <10 cm wide and do not only lie on very thin fault planes, but are restricted to ductile shear zones. Although generally confined to the top and, or, bottom walls of ductile

zones (Figs. 17,37), they do also form within the central portions of thick (> 50cm) fault zones. In these larger fault zones, the angle of the foliation to the fault or bedding plane steepens from near-parallel at the zone walls to up to 35° in the centre of the zone. Immediately behind ramps the foliation may even be at angle of 60° to the bedding plane or upper detachment. Where the foliation is approximately parallel to the fault plane, the long axes of the veins lie within the shear plane (Fig. 17); where the foliation is inclined to the upper detachment, these veins are similarly inclined and may even serve to define horses (Fig. 20). They were thus generally aligned along planes parallel to the foliation, in the plane of flattening and extension within the zone of ductile shear.

The exact length of many fault restricted and fault associated veins is not measurable, as they typically exceed the length of exposure. In addition, many veins have a lensoidal shape resulting from mild boudinaging, and lenses are often interconnected by so thin a layer of vein material as to render the cut-off points on any given vein obscure. (A small minority of shorter veins due exist, especially along steep foliations and in shale units, where they are aligned on cleavage.) The length of these veins are up to 1000 times greater than the thickness of the fault on which they lie, in the case of the thick veins adjacent to faults (Fig. 42), and may be up to 10 to 100 times longer than the thickness of the faults in the case of fault restricted veins (Fig. 43).

Veins spatially constrained to the bedding parallel faults are commonly rimmed (Section 4.3.1) (Fig. 21). Although pennite, siderite and microcline are often developed in faults devoid of

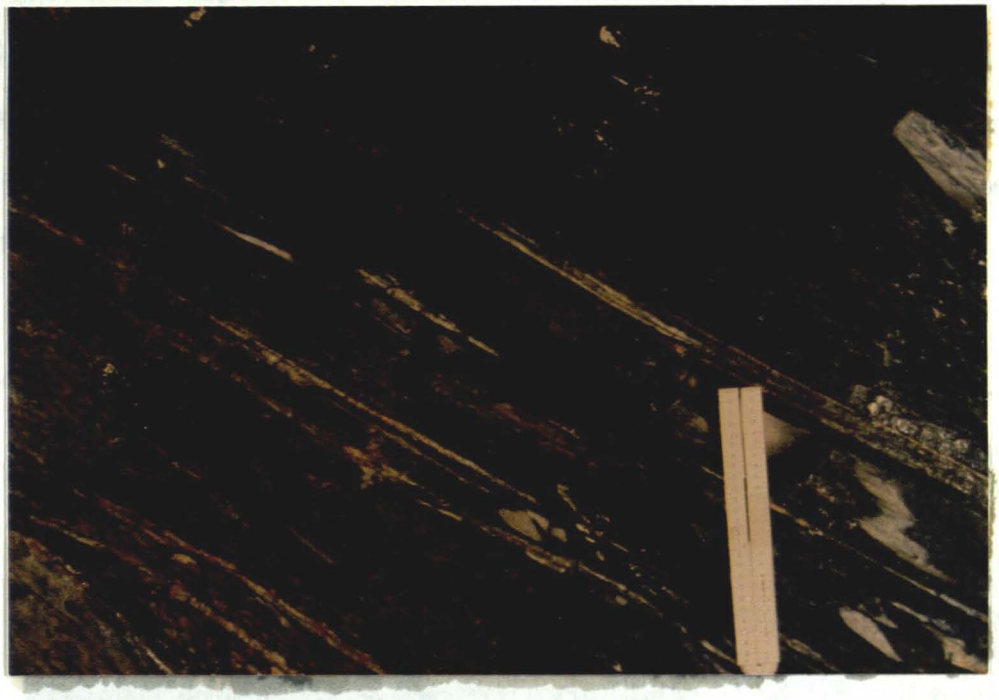

Figure 42 : Quartz veins within and on bedding plane faults of the LK2 unit, 1 Circular Shaft. Many veins exceed 2m in length and lie within faults of 1cm or less in width. Displacement is clearly of reverse sense.

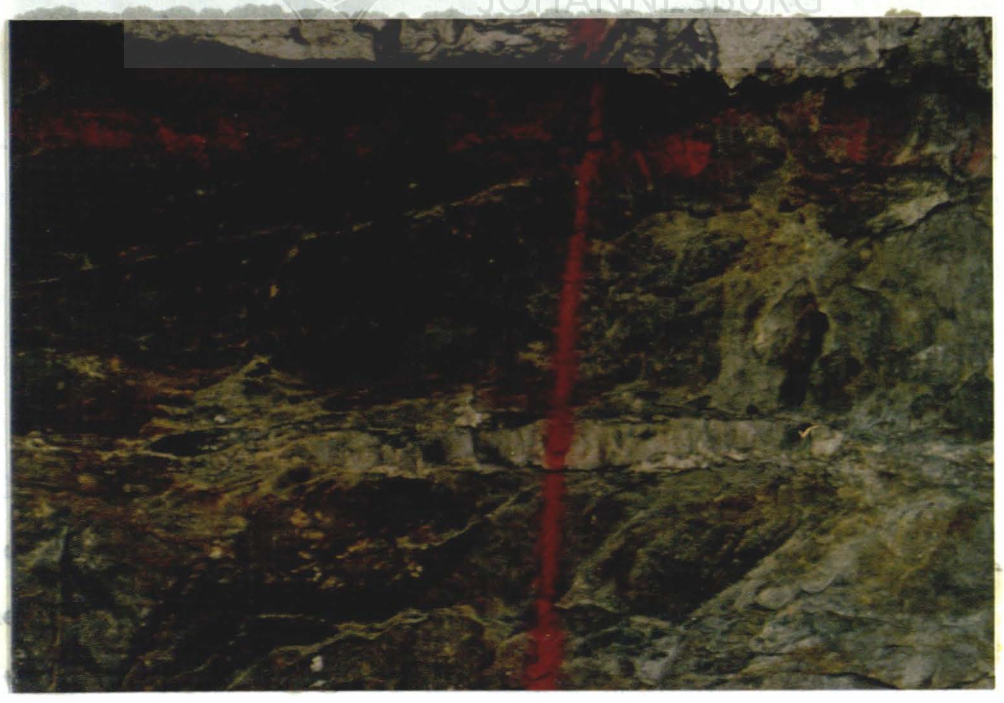

Figure 43 : A fault related vein on an MK1 bedding plane fault, SD shaft. The quartz vein is roughly 40cm long, the fault on which it lies is less than 5mm thick.

vein quartz, the presence of pyrite, chalcopyrite and pyrrhotite appears to be dependent on the occurrence of veins. The amount, position and presence of these sulphides sometimes serve to characterise individual bedding parallel faults sufficiently well to make it possible, by also taking into account their thickness, to identify and map them across a shaft.

Figure 44 : Quartz veins in a bedding plane fault of the MK3, 1 Circular Shaft. The veins have undergone some necking and later shear motion, resulting in their present morphology. Note the behaviour of the cleavage around the veins close to the boundary of the fault zone. Movement is towards the left-hand side of the photograph, which is to the N.

4.3.6 Boudins and intra-folial folds

Rotation of both quartz veins and quartz vein fragments is seen in some bedding plane faults with kinematic indicators indicating reverse sense of movement towards the N (Fig. 44). This phenomenon is frequently accompanied by boudinaging of these veins (Fig. 37). Boudins of vein quartz are necked and

thinned perpendicular to sub-perpendicular to the plane of the foliation and, where rotated, show the same sense of movement. The maximum thickness of such veins lies between 2 and 10 cm. The ductile fabric in these faults "flows" around boudins, the more ductile host occupying the volume created by the veins upon necking (Fig. 45).

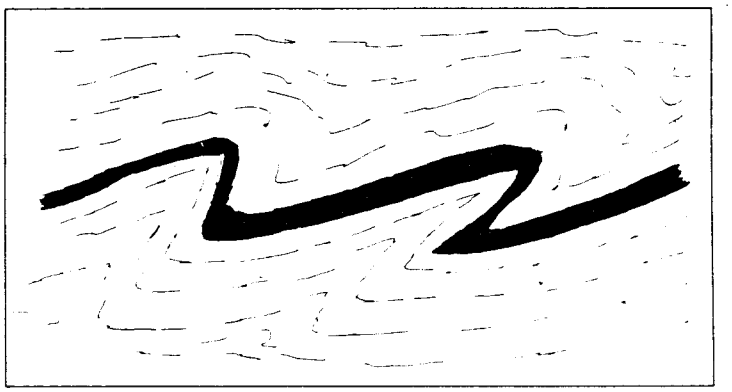

Figure 45 : Field sketch of folded vein quartz (solid black) within a bedding parallel fault. The broken lines represent the foliation, which locally parallels the veins.

4.3.7 Summary of features of the bedding plane faults

The bedding plane faults are extremely pervasive in the East Rand Goldfield. They are not restricted in geographical or lithological extent, and are the dominant structural feature noted in all the rocks. Although generally sited along the bedding planes, they may also lie within a single bed.

The fault rock is characterised by a strong tectonic foliation and is commonly altered. Most of this material is mylonitic. Slickenfibres on these planes lie on a broad N-S trend and

differing orientations on identical planes indicate that movement took place on more than one orientation.

Tectonic foliations and s-c fabrics in shear zones in the rocks of the Central Rand Group display at least two distinct populations of movement directions; to the NE and the N-NW. Data defining the latter mode are broad and diffuse and may represent two overlapping modes; to the N and the NW. Similar fabrics at the West Rand Group localities commonly indicate only the NE direction of movement.

Small-scale ramp and duplex structures are ubiquitous in the rocks of the Turffontein Subgroup. Horses in any particular zone of duplexes are not usually of the same shape and size, and therefore override material in front of the ramp by varying amounts. They are commonly internally duplexed.

Sigmoidal horses and duplexes of foliated rocks commonly lie behind ramps which are developed along the s-plane of shear, and are therefore difficult to define in the absence of markers. Movement along the cleavage planes, although unusual, has also been documented by Roering and Smit (1987). Ramp planes are both smoothly sigmoidal, and staircase in shape.

The dip of horses, and the beds within them, may be steepened against ramps, approaching vertical, and sometimes even becoming overturned. This is especially common where steep ramp planes and, or, oblique movements on the ramps are evidenced. Measurements of movement directions on the ramps indicates at least two distinct directions, to the NE and the N-NW.

Quartz veins associated with bedding plane shears generally parallel the plane of foliation. Their lengths generally exceed the thickness of the shear zone in which they lie by one to two orders of magnitude. As such, they do not represent tensile fractures which have been rotated into the plane of flattening by progressive shearing, but formed *in situ*. This requires that the fluids be pressurised in order to overcome the effect of the lithostatic load. Orientations of rotated quartz veins indicate movement broadly to the N. Cleavage "flow" about these veins are evidence of localized shear strain, i.e. ductile deformation.

These mesoscale features, and in particular the implications as regards ramp formation and the behaviour of the rocks against these ramps, may act as a key to the understanding of the larger, less- and unexposed structures in this goldfield.

4.4 Relationships between bedding plane faults and other faults.

The bulk plots of poles to faults on Schmidt stereographic projections of pre- and post- bedding plane fault ages produces a confusion of overlapping modes (Figs. 46,47). In addition, a number of faults show contradictory relationships. Normal faults are seen to have displaced only one fault in a package of parallel bedding plane faults. These normal faults may then have been displaced by a bedding parallel fault from this self-same package.

Many of the dykes observed display the same apparent contradictions in age with respect to the bedding plane faults.

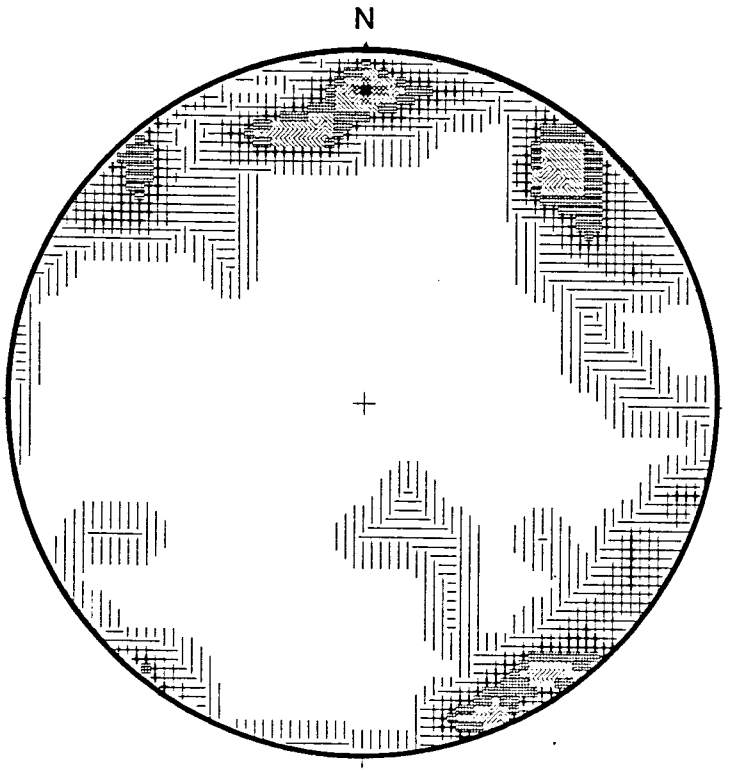

Figure 46 : Contoured plot of the poles to fault planes whose field relationships suggest they are older than the bedding plane faults. (Schmidt stereographic projection). Total number of readings = 55. Contoured at 1% level.

One bedding parallel fault plane will pass through a dyke - possibly altering its orientation within the dyke - and another of equal magnitude be cut off by the dyke. For this reason individual planes of bedding parallel faults were examined with respect to their relationship with these structures and the movement direction on the bedding plane faults to determine if this confusion resulted from more than one age of bedding plane fault formation, or more than one age of movement on other fault planes, or a combination of the two.

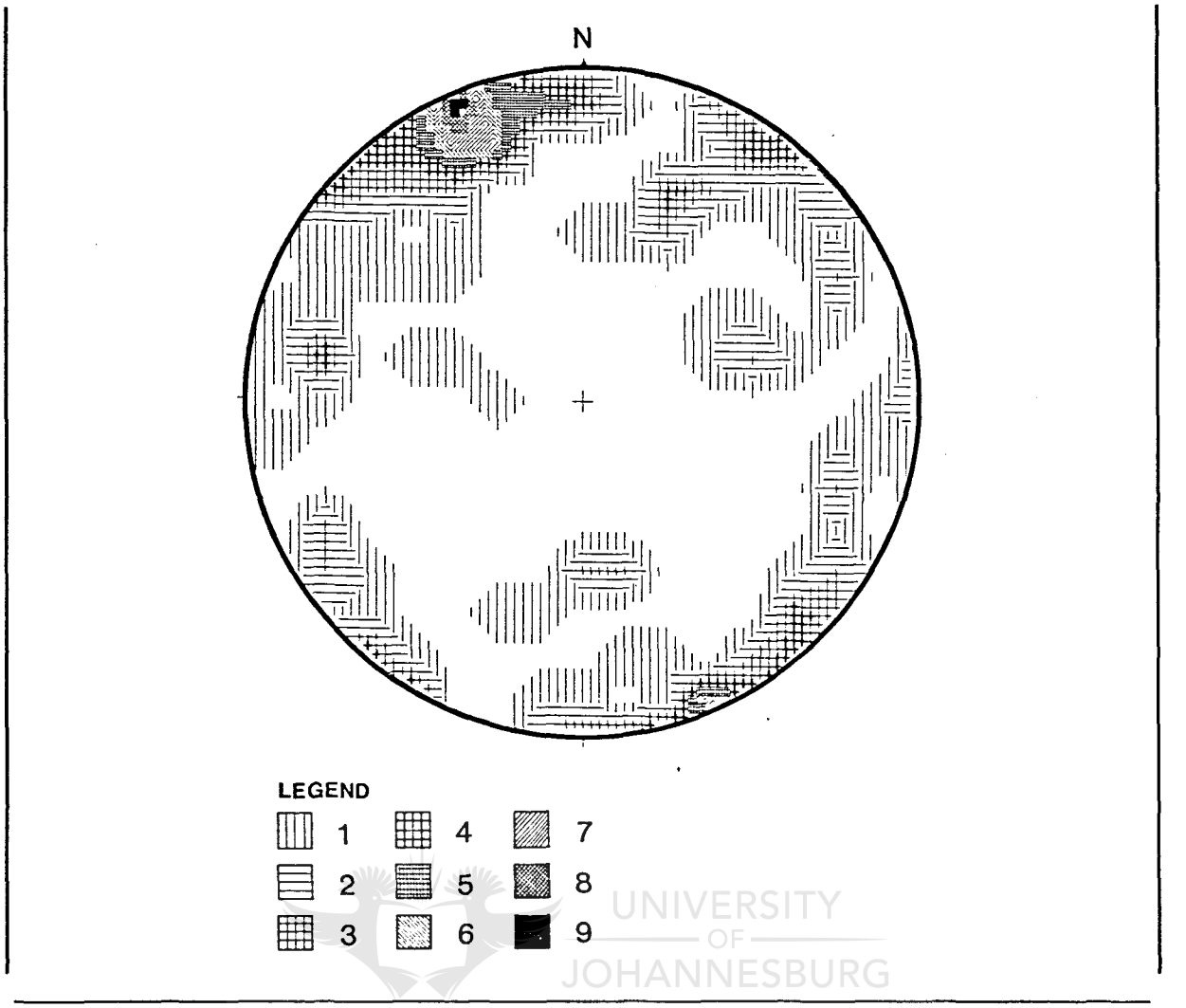

Figure 47 : Contoured plot of the poles to fault planes whose field relationships suggest they are younger than the bedding plane faults. (Schmidt stereographic projection). Total number of readings = 74. Contoured at 1% level.

The Karoo Dolerites are generally not associated with faulting, and no displacement of beds across them is seen. Although the bedding plane faults are similarly not displaced across these dykes, they also do not pass through the dykes, which normally obliterate these faults. Similarly, the Green Syenites, as described in section 3.3, cut all bedding plane faults, but the bedding plane faults and these dykes are displaced by the later E-W and NW-SE faults.

The Ilmenite Diabase dykes have a more complex relationship with the bedding plane faults. Bedding plane faults whose s-c intersections yield a N to NW movement direction pass through these intrusives (Fig. 48). These faults may give rise to minor displacements of the contacts between the dykes and host rocks, but later faulting of these dykes by N-S oblique and strike-slip faulting and E-W strike-slip motion often obscures this relationship. Bedding plane faults, which moved towards the NE, do not, in contrast, pass through these dykes, and on a local scale may even have acted as barriers to dyke intrusion and related alteration of the host rock. The movement directions on the bedding plane faults are at ±40 to 90° to the dyke contacts.

Figure 48 : An Ilmenite Diabase dyke exposed on 1 Circular Shaft. The chilled contact of the dyke is sheared by a fault dipping 72N on 321. This fault plane bears slickenfibres which plunge 06SE on 120. Fine bedding plane faults, with apparent N movement, pass through the fault with minimal vertical separation, and continue within the dyke.

Only one exposure of an intersection was observed between a Ventersdorp age dyke, and a bedding plane fault. This fault strikes NW-SE, and movement on the ramps within the shear zone is towards the NE. The dyke is cut off and displaced along this fault by an unknown amount, as its displaced portion has not been exposed within the current mining operations.

The fault events for which age relationships could be resolved by comparison with dykes and other faults of assumed age are the steep to vertical group of N-S faults, the steeply dipping, E-W faults with horizontal displacements, and the NW-SE strike-slip faults. The N-S faults consistently displace bedding plane faults with NE displacements, and are deformed in turn by bedding plane faults which moved to the N. This set of N-S faults is pre-BRQF in age. The ESE-WNW strike-slip faults similarly displace the bedding parallel faults which moved to the NE, and are cut off by those which moved to the N (Fig. 49). The NW-SE strike-slip faults display precisely the same relationship to the bedding plane thrusts. The re-activation of the other fault events makes it impossible to further resolve their age relationship to the bedding plane faults.

4.5 Folds

Although the folds in the rocks of the Witwatersrand Supergroup in the East Rand Goldfield is the aspect of tectonics normally referenced in any discussion of this region, it is neither the most striking or best understood of the structural features present. Evidence suggesting several ages of fold formation has been presented by various authors. A compressional event which

Figure 49 : Fault planes (with slickenfibres) which dip steeply on an ESE strike (vertical in the photograph) are displaced by a N directed bedding plane fault (horizontal in the photograph) within the MK3 unit, 1 Circular Shaft.

folded the Footwall Reef Beds and bedding plane faults within the footwall shale to these beds, prior to the deposition of the Main Reef Leader, is one of the earliest structural events documented (Carleton-Jones, 1936; Whiteside, 1950; Kupisiewicz, 1954-1956; Antrobus and Whiteside, 1964). This folding occurred along roughly E-W to ESE-WNW axes (Kupisiewicz, 1954-1956), and plunges to the NW (De Jager, 1964). A similar feature is noted in the pre-UK9A channels. Folding of the pre-UK9A beds is generally considered to be about a NW-SE axis (Cluver, 1957; Antrobus and Whiteside, 1964; De Jager, 1964), but suggestions have been made that this axis may actually be N-S (Armstrong, 1968).

On the regional scale (Fig. 50), three NW-SE trending anticlines have been recognised in the East Rand Goldfield (Cluver, 1957).

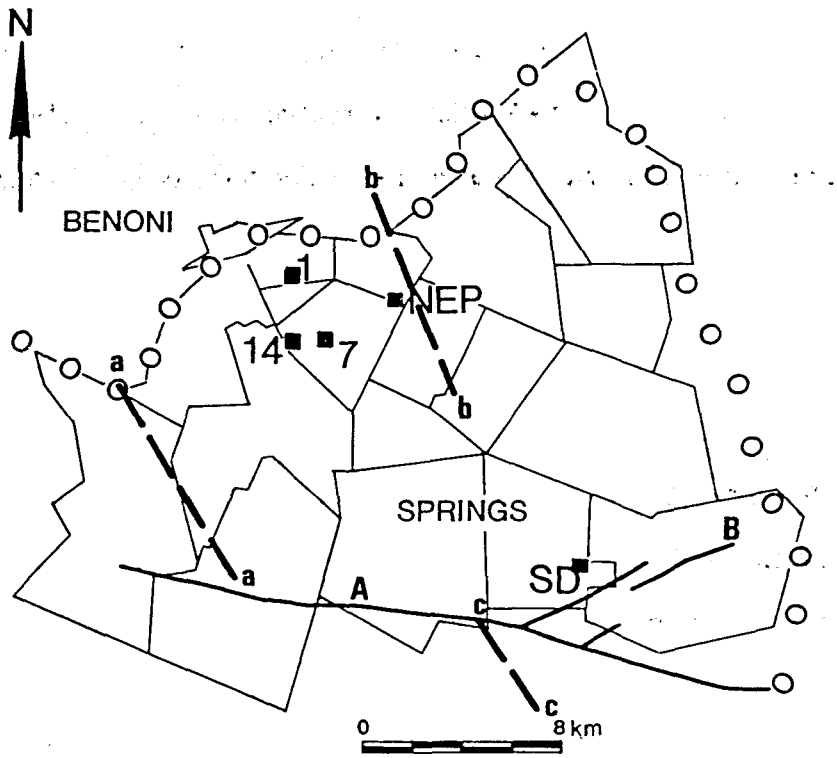

Figure 50 : Orientation and location of fold axes traces of anticlines in the East Rand Goldfield (After Cluver, 1957). A = Vogel's Tear; B = Jeffrey's Tear; a = Van Dyk Anticline; b = Geduld-Modder Bee Anticline; c = Springs Monocline.

Cluver's study involved the mapping of the lithologies underground, and was largely restricted to the level of the Main Reef Leader. He nevertheless believed that the UK9A reef displayed the same broad regional structures. One of the folds which he was able to study at higher stratigraphic levels appeared to die out towards the upper contact of the Central Rand Group. The anticline in the Geduld-Modder Bee area (NEP shaft) was characterised by the lack of a SW syncline, and on this flank it opens into a broad "gentle, undulating plane". Many of these folds are asymmetrical, and Cluver recorded that their axial planes dip steeply towards the NE and plunge S in the N portion of the Goldfield, and N in the S portion of the

Goldfield.

The timing of the large scale folding is unclear. Cluver (1957) documented that the pay shoots of the Central Rand Group cross the anticlines and concluded that these anticlines were of post-Central Rand Group age. Antrobus and Whiteside (1964) noted pay shoots which both cross the anticlines and follow synclinal traces, and they concluded that minor folding was initiated during deposition of the rocks of the Central Rand Group and continued during the deposition of the rocks of the Ventersdorp Supergroup. Greenberg (1963) and Lenthall (1972) examined pay shoot trends and heavy mineral distribution in the Central Rand Group respectively, and suggested that the folding was active during deposition.

Armstrong (1968) in his examination of the sedimentology of the East Rand Goldfield stated that the erosion of the pre-UK9A beds did not permit satisfactory conclusions to be drawn about the timing of folding.

Bedding data collected within the Turffontein Subgroup in this study were used to determine the π girdle and derived axes of the folds affecting each shaft (Fig. 51). The MK1 channels were examined to elucidate on the folding previously documented within other channels.

Open folding makes determination of the fold axes difficult to ascertain, particularly if the π girdles are used in isolation (Fig. 51). These girdles are, however, compatible with the ±N-S axis proposed by Armstrong (1968) and plunge to the ±S attributed to them by Cluver (1957).

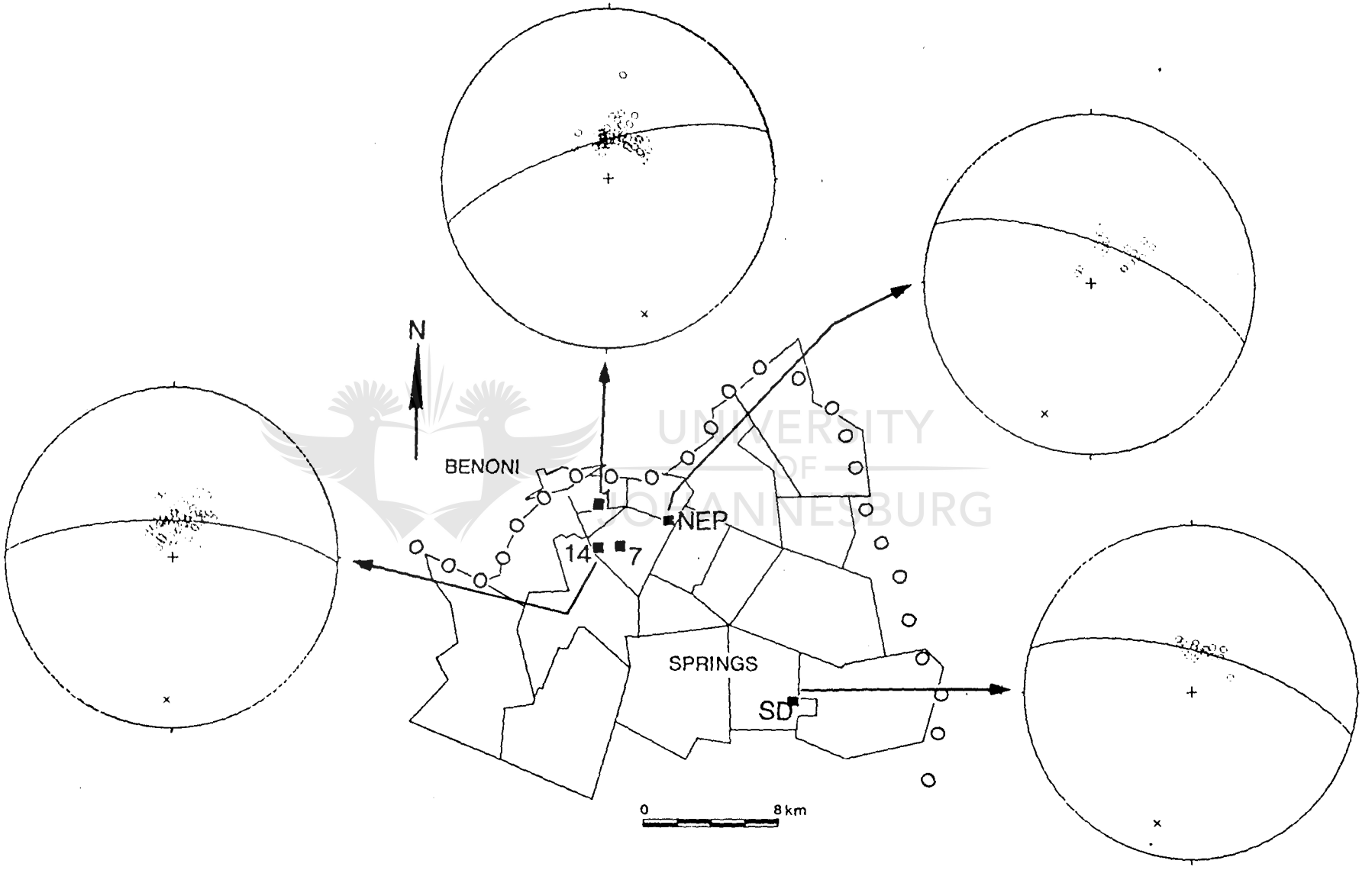

Figure 51 : Pi axes determined from bedding dip and strike data at each shaft of CMM, except 7.

The MK1 beds examined are characterised by bedding plane faults, ramps and duplex formation. These duplexes often appear to be folded in response to the compression which caused these faults, but evidence of progressive steepening of the bedding to overturned (Figs. 25,39), is related to the action of ramping on steep pre-existing planes and/or oblique movement on these ramp planes.

5. STRAIN EVALUATION

5.1 Introduction

Effects of bedding parallel thrusting cannot always be directly observed, since movement does not commonly juxtapose obviously different lithologies. This fact necessitates an investigation of the amount of strain - and thus displacement - associated with thrust movement along bedding plane faults. The primary methods used in this analysis are those described by Ramsay (1980). Shortening calculations employing the form and geometry of duplexes (Boyer and Elliot, 1976) were used to supplement these data. Although small scale repetition of stratigraphy is evident, large scale duplication has not been recorded within the studied sequence in this area. Since no large ramps are exposed in the region between the Main Reef Leader suboutcrop in the north, and SD shaft in the south, it is assumed that this study has been conducted within a single nappe.

The relationship of linear markers and the angle they make relative to a fault prior to (α) and following deformation (α') could not be widely applied in this study. The method utilizing the angular relationship of the shear plane and foliation within the shear (θ') was, however, useful in the examination of bedding parallel faults, because the ductile behaviour of these rocks produced a distinct fabric within fault zones. γ is calculated from this angle by the formula (Ramsay, 1980):

$$\gamma = 2/\tan 2\theta'$$

As previously noted, fault zones vary considerably in thickness,

ranging from microscale to > 5m. When measuring θ', mesoscopic faults (< 2cm) are problematic because they are too narrow to permit measurement of the orientation of the foliation plane. Similarly, measurement of θ' is difficult in those faults where orientation of the foliation is closely parallel to the shear plane.

Disagreement exists as to the minimum angle between the shear plane and foliation which can be accurately measured. Roering and Smit (1987) suggested that a 5° difference is necessary to permit accurate measurement and that any angle of less than 5° be considered as a 5° angle. They also suggested that any fault zone of less than 5cm width be regarded as "unmeasurable". The final γ proposed by them, however, based on additional data from the shortening deduced from duplexes on "unmeasurable" fault zones, corresponds to an average θ' for unmeasurable fault zones of 3°. S. White (pers. comm., 1988) suggests that no angle < 10° should be considered valid. In this work, three γ values are presented for the strain calculations to allow for those zones in which foliation closely parallels the shear plane. The values are for cut-off angles of 3°, 5° and 10° . (Note that those θ' angles which do not fall below a given cut-off angle have retained their measured θ' value, θ_m'.)

5.2 Method of Study

A number of structural profiles were constructed through the Kimberley Formation on 1 Circular, 14 and SD Shafts. The underlying Bird quartzites and Bird Amygdaloid lava were examined on NEP shaft. The Booysens Shale (LK2) was also

examined on 1 Circular, NEP and SD Shafts. Short profiles within the Promise, Brixton and Roodepoort Formations were mapped on surface in the Clinic, Danie Taljaard Park and Middle Lake areas.

The dimensions of duplexes encountered were largely measured on exposures. The tips of large scale duplexes (Figs. 26,41), whose complete extent is not exposed, were constructed from their available mapped limits and then measured on the mapped profiles.

θ' was measured directly on exposures, in the plane of the section. Where possible, the orientation of foliation and bedding plane fault were measured. The data were subsequently plotted on a stereographic projection to verify the measured θ' value.

The intensity and frequency of shearing appeared to be dependent on lithology and measurements are shown in Table 3. γ values were calculated for individual lithostratigraphic units when the stratigraphic position of an exposure was accurately known. In addition, the intensity, width and density of fault zones commonly increase with proximity to any lithological contact. This relationship necessitates that measurements be taken through a complete section of each unit to ensure against errors of underestimation or overestimation.

A complete stratigraphic exposure of the Kimberley Formation is not available at any single shaft. The LK1 - UK9 units could be studied on 1 Circular Shaft, while units above UK9 and below LK1 were only sufficiently exposed on SD and NEP Shafts. Since a

low angle unconformity cuts out the stratigraphic interval between the LK2 and UK9 beds at SD, the strain that should have been experienced by this interval at 1 Circular Shaft is considered to have been taken up elsewhere in the stratigraphy. This model suggests that units in the succession at SD will display higher strain values than their equivalents to the NW. Since the rocks of the Kimberley Formation overlie the Booysens Shale, however, it has been assumed that the remaining strain was taken up in the ductile shale rather than the relatively brittle quartzite units. Increased frequency of faults and deformation of the Booysens Shale at SD supports this assumption.

The pervasive evidence of bedding plane faults in all exposures within the Witwatersrand Supergroup indicates that this entire sequence of rocks has experienced shear deformation.

Since many of the East Rand units are not represented in available exposures, γ values used for these units are those predicted in this study. Such predicted values were derived through comparison with the characteristics of the measured beds. The γ^5 (see p. 102) value of a measured bed, which most closely matches the physical nature of an unmeasured bed, was then applied to the unexposed strata. This approach was supported by the extremely compatible γ values calculated for the lithologically comparable UK9 and UK7 units (Table 4). These two groups of values are in close agreement at the 3, 5 and 10° levels. Multi-lithological units have been subdivided into their component lithologies and each component then compared to measured beds (Table 5). Further, this assumption may be permitted since the bedding plane thrusts are pervasive

Figure 52 : Panoramic photograph of duplexes developed within the MK3 at 1 Circular Shaft. The ramps are of a low angle. Note that the nearly parallel roof and floor detachments to these duplexes result in little deformation of the hanging wall.

Lithology	*Bedding Plane Faults (/m)*	*% Of Stratigraphy*		*% Shears Unmeasurable As Thickness Of*	
		Ave.	*Extreme*	*Shears*	*Stratigraphy*
WEST RAND GROUP					
Brixton Fm.					
Roodepoort Fm.	4.0	13		0	0
	4.6	20		3	1
CENTRAL RAND GROUP					
Bird Quartzites					
Bird Lava	5.4	9	17	84	68
LK2	9.4	17		36	6
LK1	7.0	22		54	11
MK3	3.3	10	19	94	13
MK2	1.6	12	23	42	4
MK1	2.6	17	36	55	7
UK9	1.6	18	30	35	3
UK8	3.6	14	62	70	10
UK7	1.3	14		ID	ID
	3.1	18		20	3

Table 3 : Relationship between rock type and frequency of faults as measured by : the number of visible faults per metre; the percentage they constitute of the stratigraphy. The percentage of these faults which are characterised by an angle of less than 5° is presented in terms of the percentage of faults present and the percentage they form of the stratigraphy. (ID = insufficient data)

Unit	*Gamma values*		*Displacements (m)*		*Difference*
	1.	2.	1.	2.	
UK7	2.0	1.4	30	21	30%
UK9	2.4	1.4	36	21	42%
MK1	1.1	0.8	20	14	30%
MK2	2.0	1.0	48	24	50%
MK3	1.4	1.1	119	94	21%
LK1	1.8	1.2	45	30	33%
LK2	2.8	2.0	336	240	29%

Table 4 : The difference between the gamma and displacement values calculated when using: 1. A cut-off angle of 3°, and 2. A cut-off angle of 5°, and the percentage difference between the two displacement values thus determined for each unit.

throughout the exposures of the Witwatersrand Supergroup in the study area.

5.3 Strain Data

5.3.1 Duplexes

The panoramic photograph of small scale duplexes (Fig. 52) displays their typical flat, elongated form. It is important to note that the formation of duplexes will not always result in the deformation of the roof thrust, and thus of the overlying sediments. Upper and lower detachments which are therefore closely parallel will result (Jones, 1987). The duplexes presented in Figure 52 are an example of this type of geometry, and may therefore be difficult to identify.

An attempt to balance the profile of duplexed beds mapped at SD proved impossible, as movement on the S plane, against which overturning of beds occurred, was neither in the plane of the section, nor in the same plane as that of the N ramp. In such localities, the Boyer and Elliot (1976) method for shortening calculations proved valid.

Calculated localized shortening achieved through the formation of duplexes as noted at various localities is listed in Table 6. An average additional localized shortening of approximately 65% is derived from several discreet exposures of the Central Rand Group.

LITHOSTRATIGRAPHY	COMPARABLE UNITS FOR PORTIONS OF SHALE	QTZITE	CONGLM	LAVA	THICKNESS (/m) OF FRACTIONS OF SHALE	QTZITE	CONGLM	LAVA	DISPLACEMENT/m
WEST RAND GROUP									
Hospital Hill S.G.									
Orange Grove	LK2	LK1	-	-	70	100	-	-	**260**
Parktown Fm.	LK2	LK1	-	-	630	100	-	-	**380**
Brixton Fm.	LK2	M	-	-	360	330	-	-	**116**
Government S.G.	LK2	M	UK7	-	930	1150	12	-	**3125**
Jeppestown S.G.									
Florida Fm.	LK2	MK2a	-	-	230	360	-	-	**288**
Crown Lava	-	-	-	BIRD	-	-	-	30	**42**
Roodepoort Fm.	LK2	M	-	-	120	180	-	-	**420**
CENTRAL RAND GROUP									
Johannesburg S.G.									
Main Reef Leader	-	-	UK9A	-	-	-	0.6	-	**1**
Upper Leaders & Q	-	UK9	UK9	-	-	16	2	-	**25**
Q	-	M	-	-	-	46	-	-	**46**
Fine-grained green Q	-	LK1	-	-	-	30	-	-	**36**
Q	-	M	-	-	-	46	-	-	**46**
Argillaceous Q	-	M	-	-	-	30	-	-	**48**
Q	-	M	-	-	-	46	-	-	**46**
Bird Reefs	-	UK9	UK9	-	-	-	21	-	**29**
Q	-	M	-	-	-	6	-	-	**6**
Bird Amygdaloid	-	-	-	M	-	-	-	46	**64**
Q	-	M	-	-	-	6	-	-	**6**
Bird Reef Marker	-	UK9	UK9	-	-	-	3	-	**4**
Q	-	M	-	-	-	67	-	-	**67**
Booysens = LK3	-	LK1	-	-	-	30	-	-	**36**
LK2	M	-	-	-	120	-	-	-	**240**
Turffontein S.G.									
Doornkop Q = LK1	-	M	-	-	-	25	-	-	**30**
Kimberley Fm.									
MK3	-	M	-	-	-	85	-	-	**94**
MK2	-	M	M	-	-	24	-	-	**24**
MK1	-	M	M	-	-	18	-	-	**14**
UK9	-	M	M	-	-	15	-	-	**21**
UK8	-	MK2a	-	-	-	30	-	-	**69**
UK7	-	M	M	-	-	15	-	-	**21**
UK6	-	MK2	MK2	-	-	50	-	-	**50**
UK5	-	UK7	UK7	-	-	-		-	**84**
UK4	-	MK2	MK2	-	-	60	-	-	**60**
UK3	-	UK9	UK9	-	-	-		-	**46**
Elsburg Fm.									
UK2	-	MK2	-	-	-	146	-	-	**146**
UK1	-	MK2	MK2	-	-	15	-	-	**15**
					2460	3051	132	76	**9042**

Table 5 : Division of units into their lithological components for comparison of unmeasured beds with measured beds to predict gamma and displacement values for the units. (M = measured, a = argillaceous, Q = quartzite)

UNIT	*H'*	*L'*	*Lo*	*t*	*S*	*S%*
MK3	55	242	503	25	261	54
MK3	88	140	385	32	245	64
MK3	9	12	36	3	24	67
MK2	40	320	457	28	137	30
MK2	40	81	96	34	15	16
MK2	65	84	260	21	176	68
MK2	95	110	435	24	325	75
MK2	79	38	69	11	31	45
MK2	355	410	910	160	500	55
MK2	275	340	1170	80	830	71
MK2	72	147	504	21	357	71
MK2	28	59	138	12	79	57
MK1	135	500	844	80	344	41
MK1	45	400	900	20	500	56
MK1	25	135	225	15	90	40
MK1	20	125	167	15	42	25
UK9	30	185	241	23	56	23
UK7	33	40	110	12	70	64
UK7	40	45	180	10	135	75
UK7	48	50	180	13	130	72

Table 6 : Examples of duplex dimensions measured in the Kimberley Formation and the local percentage shortening due to duplexing thereby calculated. The average over all 68 duplexes measured = 50 - 65%. Method and symbols used as in Boyer and Elliot (1982).

5.3.2 Shear Fabric Angles

Within metres of any reading, almost all fault zones observed in the studied rocks vary in width and associated θ' angle. In order to arrive at a mean value for these measurements and to examine the effect of variations on calculated γ values, lateral variation was investigated in the profiles mapped (Fig. 53). Results indicate that both strain and displacement are heterogeneous along most fault planes, but that the difference between localities generally does not vary by more than approximately 10% to 15% within the exposure. For this reason, multiple sections and profiles were used to arrive at each calculated γ value. The average for any particular unit was calculated by weighting each average γ derived for that unit in

proportion to the relative thickness of the sections.

In order to ensure that the relative contribution of any fault plane and its associated γ are retained, strain and associated displacement for each fault was computed. The displacement along each shear was integrated over the width of the stratigraphic interval under examination, as shown in the example below. The same method was applied to the calculation of the total displacement and average γ value for the entire thickness of the Witwatersrand Supergroup.

$$\text{i. e.} \quad \gamma_5 = \sum (\gamma_n \times z_n) \; / \; Z$$

$$= \sum S_n \; / \; Z$$

(Where γ_5 is the γ value obtained at the 5° cut-off level)

Example :

θ'_m	z/cm	γ_3	γ_5	γ_{10}	S_5
3	0.3	19.0	11.3	5.5	3.4
7	19.2	8.0	8.0	5.5	56.0
2	0.5	19.0	11.3	5.5	5.7
3	14.5	19.0	11.3	5.5	163.8
6	3.6	9.4	9.4	5.5	33.8
8	16.0	7.0	7.0	5.5	112.0
11	2.4	5.0	5.0	5.0	12.0

Total thickness of stratigraphy containing these faults = Total Z = 143.0cm

Total displacement across this stratigraphic interval = Total S = 393.9cm

Resulting average γ across this stratigraphic interval = Ave. γ_5 = 2.7

An almost continuous profile through the UK9, MK1 and MK2 beds was mapped in 1E7S cross-cut on 1 Circular Shaft (Fig. 53). The position of the thickness and θ' values measured are shown in

No.	z	a	No.	z	a	No.	z	a	No.	z	a	No.	z	a	No.	z	a
1	3.2	2	31	2.2	2	61	10.2	4	91	5.8	3	121	0.2	1	151	0.5	30
2	2.0	1	32	3.1	4	62	7.3	3	92	8.8	5	122	0.2	1	152	0.8	2
3	0.6	4	33	3.9	5	63	4.7	3	93	8.9	5	123	7.2	8	153	1.0	0
4	1.1	0	34	8.0	2	64	3.4	0	94	11.8	6	124	0.8	1	154	4.1	2
5	0.5	0	35	8.2	2	65	0.7	0	95	8.3	5	125	12.3	12	155	1.5	1
6	0.5	0	36	19.5	12	66	9.9	8	96	4.1	1	126	0.7	5	156	1.4	1
7	0.3	0	37	1.8	2	67	4.1	4	97	9.0	5	127	0.8	5	157	8.6	7
8	0.5	0	38	4.0	3	68	7.9	7	98	4.7	2	128	4.2	6	158	3.2	4
9	14.1	4	39	10.2	8	69	2.5	3	99	5.2	2	129	8.9	11	159	4.7	6
10	0.6	2	40	2.5	2	70	5.7	5	100	8.9	6	130	14.8	14	160	2.3	4
11	2.0	2	41	3.8	3	71	5.4	5	101	9.1	5	131	0.5	5	161	1.0	3
12	8.1	4	42	3.6	2	72	3.1	2	102	9.9	7	132	0.9	6	162	7.7	7
13	2.2	2	43	1.2	2	73	2.2	3	103	14.3	8	133	0.5	5	163	4.9	4
14	0.9	2	44	1.3	3	74	1.9	4	104	3.7	5	134	0.4	4	164	3.3	2
15	2.1	2	45	0.8	1	75	2.8	2	105	3.6	3	135	0.6	5	165	12.1	8
16	15.1	6	46	18.1	9	76	4.0	2	106	4.1	4	136	0.6	6	166	10.3	6
17	8.0	2	47	20.2	6	77	4.8	0	107	15.0	10	137	2.7	4	167	8.7	6
18	1.1	2	48	19.5	3	78	4.4	1	108	5.4	5	138	2.8	5	168	9.8	6
19	1.0	1	49	21.5	8	79	7.3	3	109	2.1	2	139	0.5	1	169	15.3	6
20	1.2	3	50	28.7	7	80	2.7	4	110	6.1	5	140	0.4	5	170	8.4	5
21	3.1	6	51	3.4	4	81	3.9	3	111	0.8	2	141	0.5	4	171	1.6	9
22	1.4	3	52	17.3	22	82	0.7	0	112	3.6	5	142	0.6	4	172	2.1	10
23	1.6	1	53	20.1	7	83	1.8	1	113	6.2	3	143	1.2	3	173	7.9	24
24	0.8	0	54	0.8	5	84	1.3	0	114	6.3	0	144	2.7	8	174	3.2	3
25	3.2	2	55	0.9	2	85	3.9	1	115	2.0	1	145	0.8	3	175	1.5	8
26	1.3	1	56	0.9	2	86	4.1	0	116	1.2	0	146	2.3	5	176	6.0	5
27	6.0	3	57	3.7	3	87	8.8	8	117	1.7	2	147	2.2	2			
28	5.2	6	58	1.1	2	88	4.1	2	118	1.1	2	148	2.2	2			
29	9.9	8	59	8.9	2	89	5.2	6	119	0.6	1	149	1.4	2			
30	6.2	6	60	11.7	3	90	6.9	4	120	0.4	0	150	4.7	5			

Table 7 : The thickness and angles measured on shear zones in the strain profile mapped through the MK2, MK1 and UK9 beds on 1 Circular Shaft. The number of each reading represented on this profile corresponds to the number of each reading in this table.

Figure 53 : a) Structural profile mapped through the UK9, MK1 and MK2 units on 1 Circular Shaft. The shear thicknesses are not drawn to scale, but each reading indicated is listed, together with the measured θ value in Table 7.
b) The lithological mapping of the same profile.

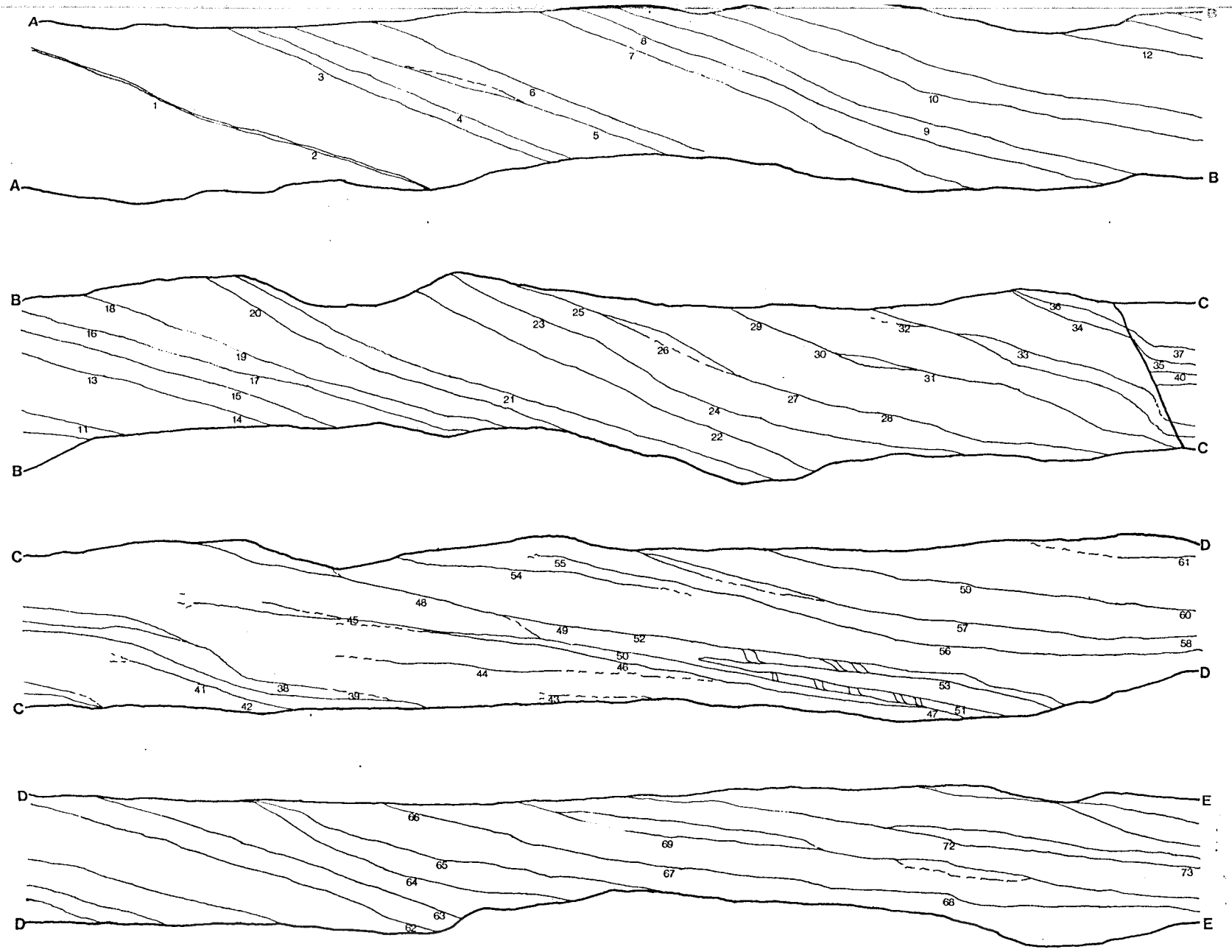
A
A
B
B
C
C
D
D
E
E
F
F
G
G
H
H
Loss of exposure
for 10 m
Loss of exposure
for 6 m
Dyke for
8m

b

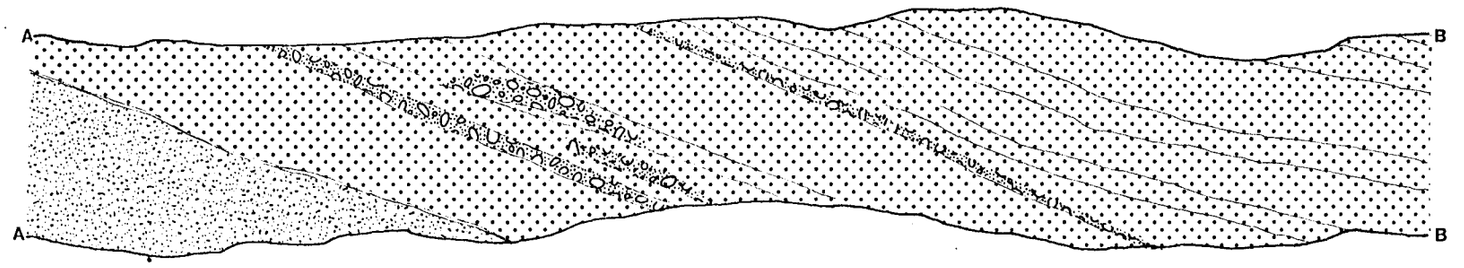

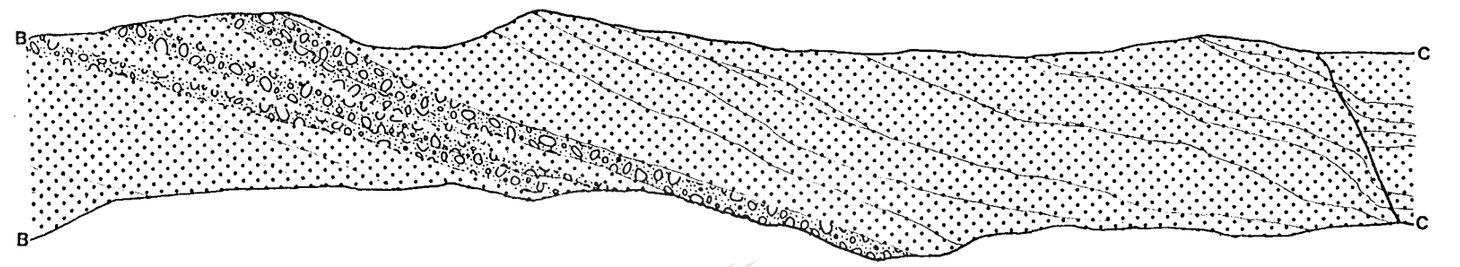

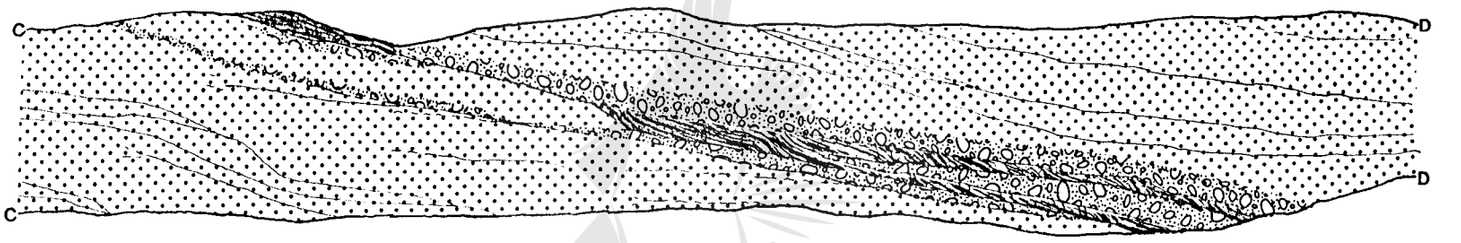

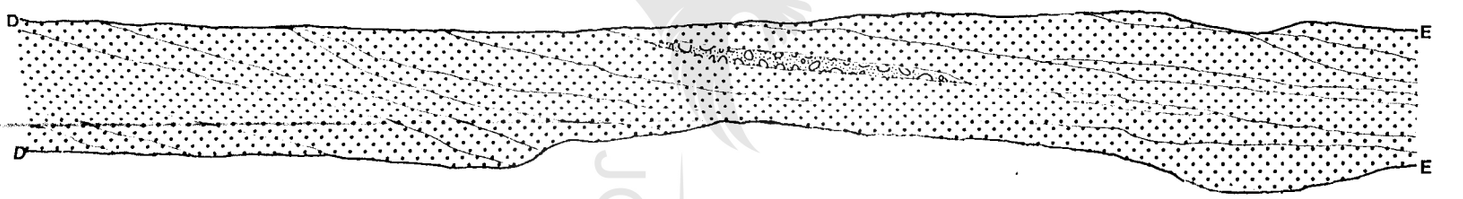

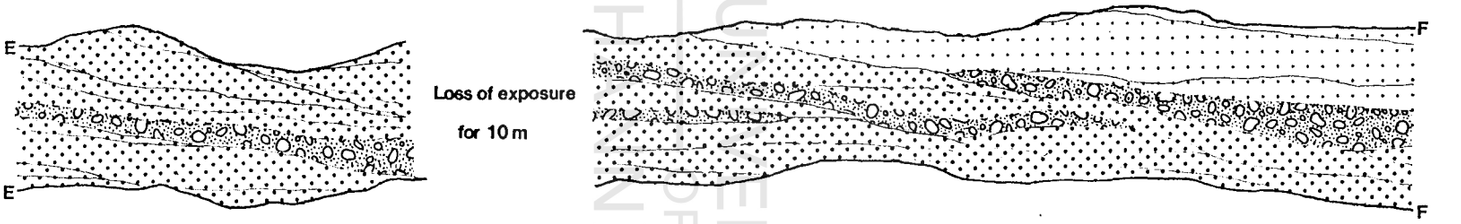

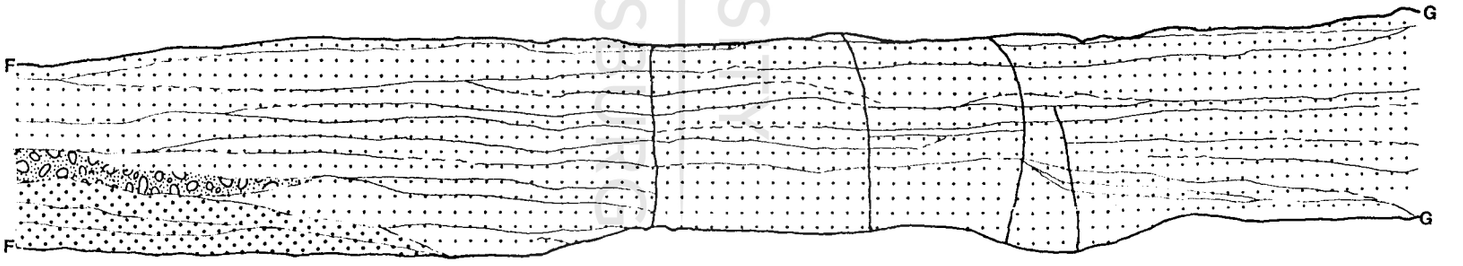

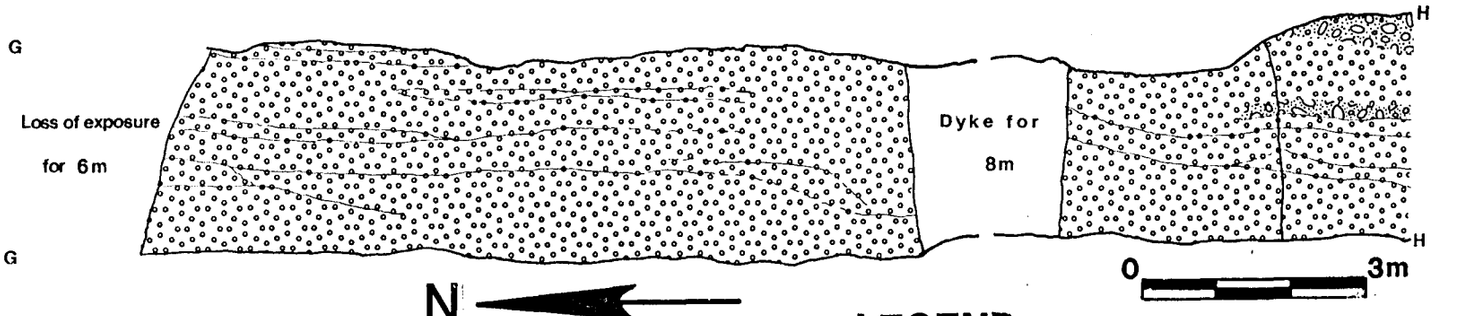

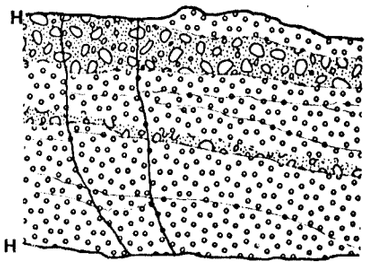

N

LEGEND

UK9QUARTZITE

MK1QUARTZITE

MK2QUARTZITE

MK3QUARTZITE

CONGLOMERATIC BEDS

SHEAR ZONES

this Figure, and the values at each point are listed in Table 7. From this profile the lateral variation of these values can be seen, particularly where a single fault bifurcates to envelop a horse of undeformed material. Despite this variation, an

overall conservation of strain is indicated if the γ values of the upper and lower faults of a bifurcated fault are added, which suggests that the shear strain is distributed between the upper and lower faults through the bifurcation of the original parent shear.

Sections through the large fault zone at the MK3-MK2 contact constructed in adjacent cross-cuts on 1 Circular Shaft show a similar variation in z and θ'values, and, in addition, a change in the number of zones of shear which constitute this fault zone. Again, the strain values do not differ by more than 30%.

5.3.3 Results of calculations

Formation thicknesses used for the West Rand Group on the East Rand are those quoted by Tankard, et al, (1982). Central Rand Group thicknesses are those of Sharpe (1944) and Antrobus and Whiteside (1964). The total thickness of the Witwatersrand Supergroup in the East Rand Goldfield is taken as approximately 5700m.

The total predicted displacement over this thickness is approximately 9000m. Calculations indicate that the average γ^5 is 1.6 (Table 5).

The influence of the "cut-off" angle on the displacement

calculated for individual units is listed in Table 4. The difference between displacements calculated at the 3° and 5° values ranges from 0-50%, with a mean value between 20-30%. The γ employed for the predicted displacement over the Witwatersrand Supergroup was determined assuming a minimum θ' of 5° (Table 5). If γ_3 (minimum θ' = 3°) is used in this computation, the resultant displacement is approximately 12km, with an average γ of 2.1. This is within the same order of magnitude as that determined using a minimum θ' value of 5°, but suggests that an underestimation of the final value by 30% is possible.

UNIT	*1.*	*2.*	*Percentage Difference*
MK3	14.3	11.3	20
MK2	32.3	8.0	75
MK2	13.0	9.4	34
MK1	17.9	9.4	47
MK1	9.5	8.0	16
UK9	12.7	11.3	10

Table 8 : Examples of the gamma values determined for a given shear using:
1. The shortening accomplished through duplexing and thus displacement on the overriding or roof shear, and
2. The measured θ' value of this shear, and the percentage difference between the two gamma values thus calculated.
The average difference between the two methods used, over all 33 duplexes and associated shears thus compared, is 30 - 40%.

Further, the difference in displacement calculated from the θ' angle, and that measured on underlying duplexes whose fault planes merge with the measured roof thrust (Jones, 1987), is approximately 30% (Table 8). Considering this, together with the fact that this calculation has not taken into account the contribution to the overall displacement of microscopic scale shear planes, major ramps, duplexes or fault zones in which the foliation parallels the shear plane, it would appear that this final value is underestimated by an unknown, but possibly

significant amount. Predicted displacement should, therefore, only serve as a guideline to the possible extent of displacement from bedding parallel thrusting. It should be borne in mind that despite the predominance of exceedingly narrow faults within the quartzites, relatively substantial movement can still be accomodated along such faults.

5.4 Summary of strain quantification

1. The entire sequence of Witwatersrand Supergroup rocks have experienced shear strain.
2. The pervasive shear-related fabric is used to derive an estimate of the shear strain and associated displacement which has taken place on bedding parallel planes.
3. The inherent problems associated with measuring fabrics nearly parallel to shear planes, and fault zones which are extremely narrow result in a underestimation of the total strain.
4. There is a lithological dependence evidenced in the number, distribution and intensity of ductile bedding plane faults.
5. Strain values for units which are not sufficiently exposed in the study area are predicted through comparison with similar lithologies for which data could be gathered.
6. Localised shortening achieved through the formation of duplexes is approximately 65%.
7. The minimum average γ calculated for the entire Witwatersrand Supergroup in the East Rand Goldfield is 1.6. This corresponds to a minimum displacement of 9km across the thickness of this sequence.

6.DEFORMATION IN THE BLACK REEF QUARTZITE FORMATION.

Deformation in the BRQF was studied for comparison. The hangingwall quartzites, reef zone and footwall quartzites are exposed on the 7 and NEP shafts of CMM. The unconformable contact with the underlying Central Rand Group indicates a difference in the dip of bedding between the Witwatersrand and Transvaal Supergroups in this area of more than 10°.

6.1 Faulting

Fault measurements indicate that the extensional faults in this area which have a vertical or sub-vertical dip and strike NW-SE, NE-SW, N-S, and WNW-ESE are present in the BRQF (Fig. 54). All these generations pass through the northerly bedding parallel faults without being disrupted, and may displace these bedding parallel faults. E-W striking faults form a very small proportion of the faults present, but evidence of horizontal movement on planes of this orientation have been observed.

Bedding parallel faults are present in these rocks. The angular unconformity between the underlying Witwatersrand Supergroup and the BRQF is mirrored in the bedding plane faulting, and the faults within the rocks of the Witwatersrand Supergroup are truncated at this contact (Fig. 55). The foliation of this brittle - ductile event indicate that the faults are thrusts and displace overlying strata towards the NW. Slickenfibres and slickensides on these fault surfaces are rare, but where present lie along a NW-SE direction. Sections within the BRQF reveal that the faults are more localised than usually is the case in the underlying Witwatersrand strata. Whilst graphitic beds

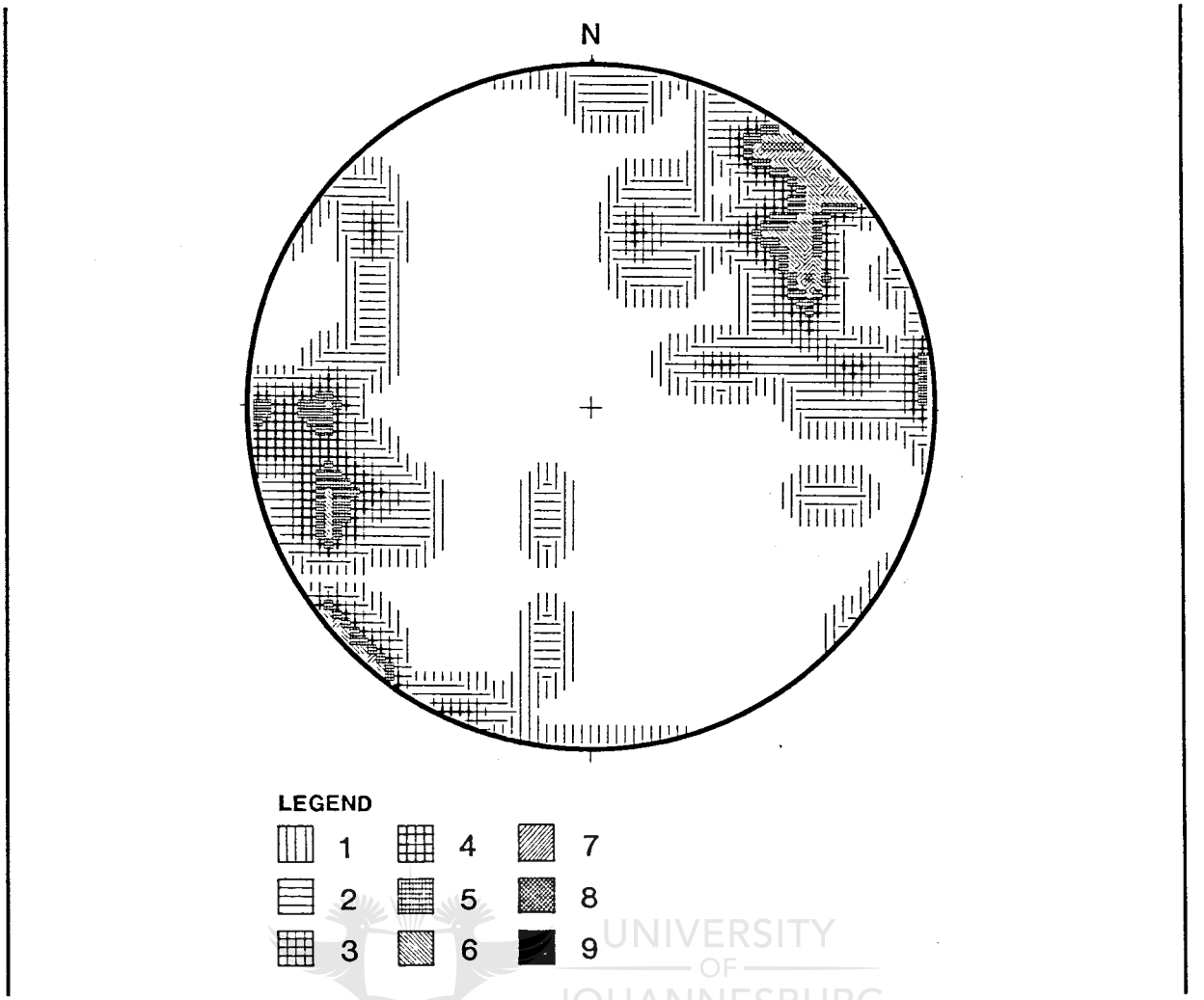

Figure 54 : Contoured plot of the orientation of the poles to fault planes of all non-bedding parallel faults measured within the BRQF in the East Rand Goldfield. (Schmidt stereographic projection). Total number of readings = 51. Contoured at 1% level.

display a ductile shear fabric, non-graphitic quartzites appear to be almost entirely unfoliated and contain fewer faults by volume than lithologically comparable Witwatersrand strata. The fault rock is usually a graphite-rich cataclasite. In addition, faults with width less than 10cm within non-graphitic quartzitic layers do not display the lateral continuity seen in rocks of the Central Rand Group. Instead, they generally terminate in splays of multiple untraceable failure planes of less than 0.2mm in width. These faults are again most commonly positioned at

Figure 55 : The contact between the Witwatersrand Supergroup and BRQF on NEP shaft. The angular unconformity between the rocks is mirrored in the unconformity between the bedding plane faults of the two differing ages of rocks. The bedding plane faults of the Witwaters-rand Supergroup at this locality have moved to the NE; that of the BRQF along this contact to the N. The fabric of the NE mode does not progressively rotate into the overlying fault, nor pass through it, but stops against this faulted contact.

contacts between differing lithologies.

The fault zones are generally uniform in thickness, varying from microscale to 15cm, and often contain intraformational duplexes and ramps which may thicken an individual fault zone by 50% to 100%.

Unlike the bedding plane faults in lithologies of the Witwatersrand Supergroup, the graphite bearing faults of the BRQF do not display a simple relationship to the quartz vein-filled extension fractures which they cut. At intersections

between these extension fractures and the bedding plane faults, the fault plane and the fault rock appear to climb the walls of the fractures and erode the vein material. This vein material is then incorporated into the fault zones and forms asymmetric "intrafolial folds" which verge towards the NW (Fig. 56).

Figure 56 : A bedding plane fault within the BRQF, 7 Shaft. The fault rock appears to actively erode the quartz veins which cross cut its path, producing a local thickening of an otherwise uniform fault zone. Folds are present in the quartz veins within the faults. N is to the right of the photograph.

6.2 Ramps and Duplexes

Intraformational ramping and duplexing predominates, with few isolated horses present and a small amount of footwall plucking evidenced. Directions of movement up ramps are scattered about a dominantly NW mode (Fig. 57). No distinct mode to the NE is evidenced. The angle between the bedding plane and the ramps is

generally < 40°, but may be as much as 50°.

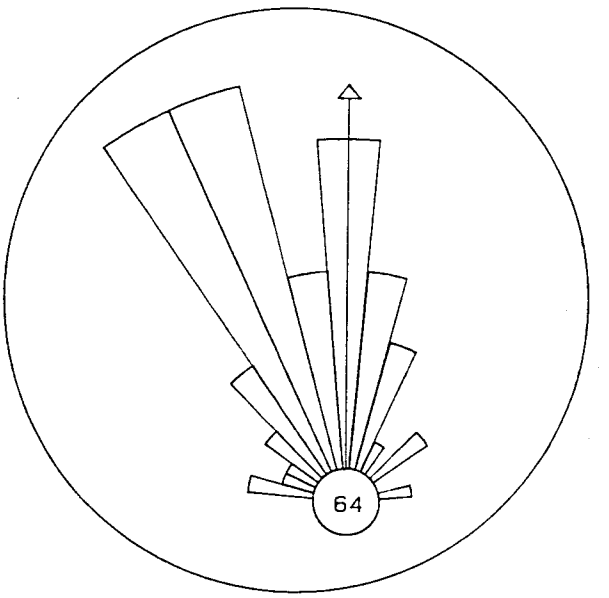

Figure 57 : Rose diagram of movement directions obtained from the movement lineations on ramps within bedding plane faults in the BRQF, 7 Shaft.

6.3 Extension Fractures

At least two generations of vein-filled extension fractures are present in the BRQF, with strike modes of 060-085° and 130-150°. The first generally form en echelon arrays and individual fractures may exceed 5cm in width and 50cm in length. It is disrupted and eroded by the bedding parallel faults and progressive rotation of some veins has occurred, from a strike of 050° in the centre of the length to 130° at the tips. The second, 130°-150°, generation passes undisturbed through bedding parallel faults and may result in up to 1cm of displacement of the faults across the fracture. This relationship suggests that the two generations of veins may be close in age, and may have formed with the progressive rotation of the stress axes.

6.4 Quartz Veins

Sinuous streaky quartz veins and irregular massive blocks of vein quartz are rarely observed, but quartz in extension fractures is present as frequently as in the Witwatersrand Supergroup. There are fewer veins restricted to the bedding parallel faults and where present they are between 0.5cm and 5cm in thickness. These veins may outline duplexes, lie along and beneath intraformational ramp planes and form intrafolial folds, but they are not seen defining the boundaries of these fault zones as commonly as they do in the Central Rand Group. Brecciated vein material is included in these zones, and appears to be particularly derived from the "eroded" extension fractures. This material is generally elongated and lies in the plane of the foliation.

6.5 Strain Evaluation

Both the shortening evidenced by the duplexes and the orientation of the fabric in the faults relative to the shear plane were employed to derive an estimate of the strain and displacement associated with the bedding plane faults. Duplexes within mapped sections suggest that a local shortening of at least 60% has occurred. The localisation of shear zones in thin, less competent graphitic and argillaceous layers results in a wide range of γ values in various sections. Strain values lie between 0.5 and 2.4, dependent almost entirely on the mineralogy of the beds, but a realistic mean value for the formation is approximately $\gamma^5 = 1.2$. For the 25m local thickness of the BRQF, this corresponds to a displacement of 30m.

Both bulk deformation (folding and cleavage formation), and sliding on discrete surfaces (bedding plane shears) have occurred in the East Rand Goldfield.

The bedding parallel fault rocks of the Witwatersrand Supergroup are strongly foliated altered quartz schists, in which the quartz grains show a typical mylonitic fabric and the phyllosilicates, particularly pyrophyllite, define the foliation. The mylonitic schists, and the localised flow of the foliation around quartz veins within the faults all indicate that the bedding parallel deformation occurred in an essentially ductile environment. Pervasive chloritic alteration, accompanied by the precipitation of sulphide minerals, suggest that the shear zones have acted as conduits for fluid movement during their history, often post-foliation.

In contrast, most of the fault rock in the bedding plane faults in the BRQF are cataclasites. This variation in the nature of the fault rock could be due to a differing rates of strain in the faults, or differing metamorphic conditions during deformation. Since there appears to be a distinct correlation between lithology and γ value for the thrust faults, and the quartzites of the BRQF are similar to those of the Witwatersrand Supergroup, it is assumed that the rate of strain in both groups of rocks did not differ significantly for any single event. It is therefore suggested that the metamorphic conditions associated with the thrust faults in the Witwatersrand Supergroup and the BRQF differ considerably, with that of the former occurring at significantly greater pressures, and thus at

a greater depth.

Most of the quartz veins associated with these faults are parallel to the foliation. They are syntectonic in age, as their lengths generally greatly exceed the thickness of the shear zone, thereby precluding the possibility of their being extension fractures which have been rotated within the shear zone into the plane of the foliation. In addition, where sampled in the Central Rand Goldfield, these veins contain pyrophyllite and kyanite (Coetzee, pers. comm., 1989), which indicates that they formed synchronous with the metamorphism. In order for these veins to form in this plane, the fluids from which they formed were probably at a pressure exceeding the lithostatic pressure. It would appear that these veins formed by the same filter-press mechanism proposed by Roering and Smit (1987) for similar shear restricted veins in rocks of the Witwatersrand Supergroup on the Central Rand. It can be expected that their presence reduced the effect of overburden and thus enhanced movement along these planes (Hubbert and Rubey, 1959).

The small population of non-parallel veins found in close association with bedding plane faults appears to represent an earlier population of veins which were boudinaged and folded during progressive deformation. The precise age of formation of these veins cannot be deduced. Progressive deformation of veins in this manner has been modelled by Platt (1983) and Hudleston (1989).

Within the bedding plane shears, s-c fabrics (Simpson and Schmid, 1983; Lister and Snoke, 1984), movement parallel

lineations on the ramps and flats of bedding plane shears, orientation of intrafolial folds (Mawer, 1987) and rotation of resistant clasts such as boudins (Ghosh, 1975; Malavieille, 1987), all indicate broad northerly movement. This sense of motion with overlying strata moving relatively N suggests that the bedding plane faults are related to a period(s) of contractional faulting.

The orientation of foliations and movement lineations suggest that only NE movement occurred along these thrust faults within the West Rand Group. Similar data from the rocks of the Central Rand Group, however, display more than one mode of movement directions, viz.: NE and N-NW. These modes are seen within single cross-cuts on each shaft when the kinematic data of different shears are plotted. The NE mode is not represented in the sediments of the BRQF, suggesting that the compression which resulted in this movement acted prior to the deposition of the BRQF. The N mode is broad and diffuse and may represent two overlapping modes, to the N and NW. The lack of post-Transvaal pre-Karoo intrusive phases, and the uncertain age of the emplacement of the Green Syenite dykes, do not constrain the relative ages of the N and NW events. The NE and N modes can also be temporally separated based on their relationships with dykes and other fault events.

The NE directed thrust faults are characterised by the development of mesoscale ramps and duplexes. Plots of the slickensides and slickenfibres developed on the ramp planes present in the rocks of the Central Rand Group display the same pattern of directions as those of the s-c intersection directions. At least two distinct populations are evident, to

invoked to account for their steep nature. Back tilting could, however, be achieved through ramp development on steep, pre-existing planes of anisotropism such as the banks of sedimentary channels and older faults. Such response is enhanced by oblique movement along the steep anisotropism.

Thus the presence of the NNE trending Van Ryn Fault, and the NE trending Homestead Fault, together with the overturning of the beds to the S, appear to represent large-scale examples of the morphologies here attributed to mesoscale oblique and steep ramp planes.

At the Clinic locality (Map 1), the timing of the steeply plunging slickenfibres is ambiguous, although they may have formed simultaneously to the steepening and overturning of the strata, as back tilting and rotation of the beds could result in the progressive rotation of the slickenfibres. Such a progressive change from upright to oblique movement of the beds against the ramp plane and the resulting differential displacement could result in relative anticlockwise rotation of the beds, and thus account for the current juxtaposition of the strike and dip orientations of the beds on the N and S sides of both the Van Ryn and Homestead Faults.

Both earlier and later faulting along these planes is possible. Due to the paucity of outcrop, however, identification of these events is not possible. Possible explanations include early normal faulting with associated roll-over of the beds (Fig. 58). Platberg age faults which elsewhere occur on a similar orientation (Roering, *et al*, 1990) might equally well be responsible. An early thrust ramp and formation of anticlinally

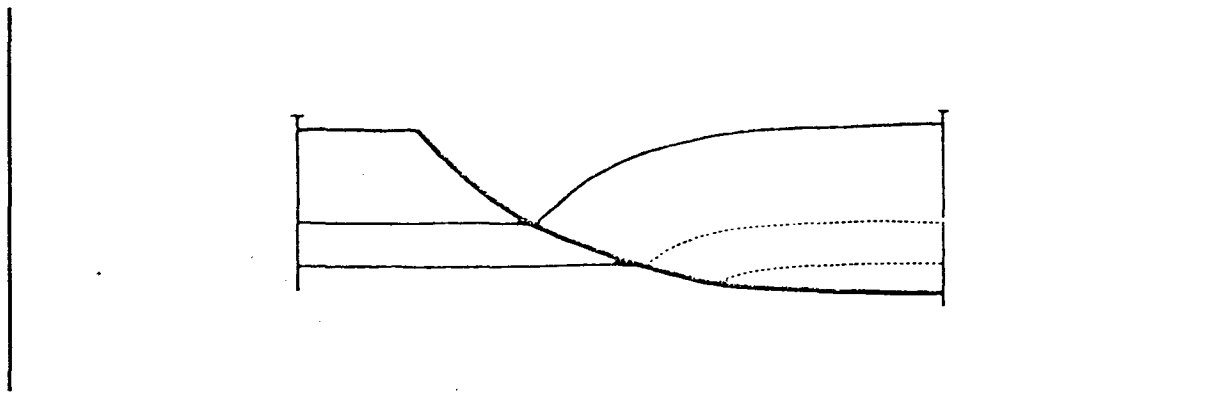

Figure 58 : The geometry of a roll-over fold developed during normal listric faulting, as might be invoked to explain the overturning of beds adjacent to a fault. (After Coward, 1987).

folded duplexes, once eroded would produce a similar surface morphology (Fig. 59). The pervasive evidence for re-activation of fault planes in this area suggests, however, that no single explanation should be invoked to account for these features. A complete resolution of this problem will only be possible once the distribution of lithologies with depth is known. It would appear, however, that the major mode of deformation in the vicinity of these fault planes is one of oblique ramping, irrespective of when the ramp formed.

There are many possible explanations for the lack of cleavage in the rocks of the West Rand Group in the East Rand Goldfield during the N directed thrust event. Most of the ramps observed in this Goldfield follow a smooth sigmoidal trajectory of the nature proposed by Cooper and Trayner (1986), but staircase forms (Boyer and Elliot, 1976) are also present. The latter variety will result in an undeformed footwall (Cooper and Trayner, 1986). A similar lack of cleavage development may result during layer parallel shortening if this shortening is accomodated by the thickening of the sequence (Cooper, *et al*,

1983).

Alternatively, there may have been a décollement between the rocks of the West Rand and Central Rand Groups which protected the lower rocks during the second thrust event. Field evidence suggests that a thrust ramp is present in the Van Ryn area. The dip of "shales" in the Jeppestown Subgroup steepen dramatically from the N towards the contact between the rocks of the Central and West Rand Groups (Map 1). The overlying beds similarly steepen from the S (± 18°S on CMM) towards this contact. The dip and strike directions of the hanging and footwall beds of the contact are not conformable, and a local difference of up to 60° has been recorded (Antrobus and Whiteside, 1964). The presence of a thick mylonite zone observed at the base of the quartzites, accompanied by a strongly deformed footwall and extensive bedding parallel quartz veins testifying to movement along this plane, also imply that this contact is tectonic. In addition, the large scale Van Ryn Fault (Map 1) cannot be traced into the rocks of the Central Rand Group lying S of the contact,

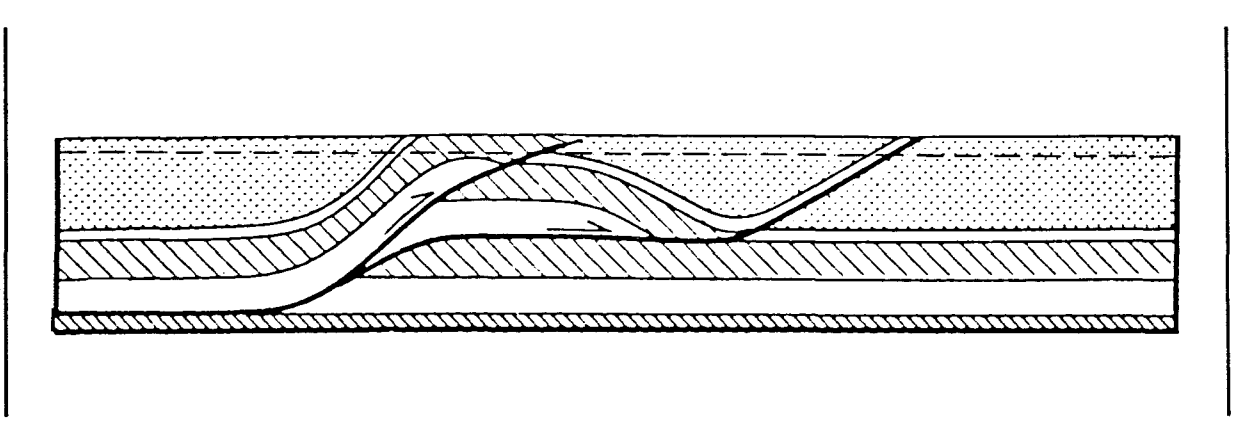

Figure 59 : The possible ramp and horse formation against the Van Ryn and Homestead faults. The extensive soil cover prohibits verification of several of the features on this model. The dashed line represents the proposed present erosion level. (After Jones, 1987).

despite the considerable displacements along it less than 2km to the N. The angular unconformity which this contact represents is also evident in the extreme and unsystematic variation of the distances on surface between the Main Reef Leader and various beds within the West Rand Group across this Goldfield (Map 1).

A significant number of faults and fractures with either strike-slip or normal displacements are present in the Central Rand Group near its contact with the West Rand Group (Map 1). Separation on any individual fault is usually less than 200m. The distribution of fractures associated with quartz veins of up to 0.5m in thickness is particularly intense approximately 3km E of the Van Ryn Mine (locality F). At this same locality, kink bands are developed in deformed footwall quartzites to the Main Reef Leader. These bands deform a pre-existing E-W foliation which formed during the ductile bedding plane faulting.

All this would suggest that the contact, and underlying phyllonites of the Jeppestown Subgroup, acted as a sizeable detachment zone during thrust faulting, and that ramp formation took place in the Van Ryn region. The quartzites of the Johannesburg Subgroup overlying this contact are not as finely bedded as the underlying phyllonite, and would therefore have acted as a relatively stiffer, massive sequence which was unable to maintain the same amount of interstratal slip as the phyllonites during ramping. Extensive fracturing of the more competent unit (Jones, 1987) (Fig. 60) would be expected in this situation and is compatible with the fractures and normal faults observed in this area. Heterogeneous displacement of portions of the thrust nappe would give rise to ± N-S strike-slip faults. This, too, is compatible with the features developed in the

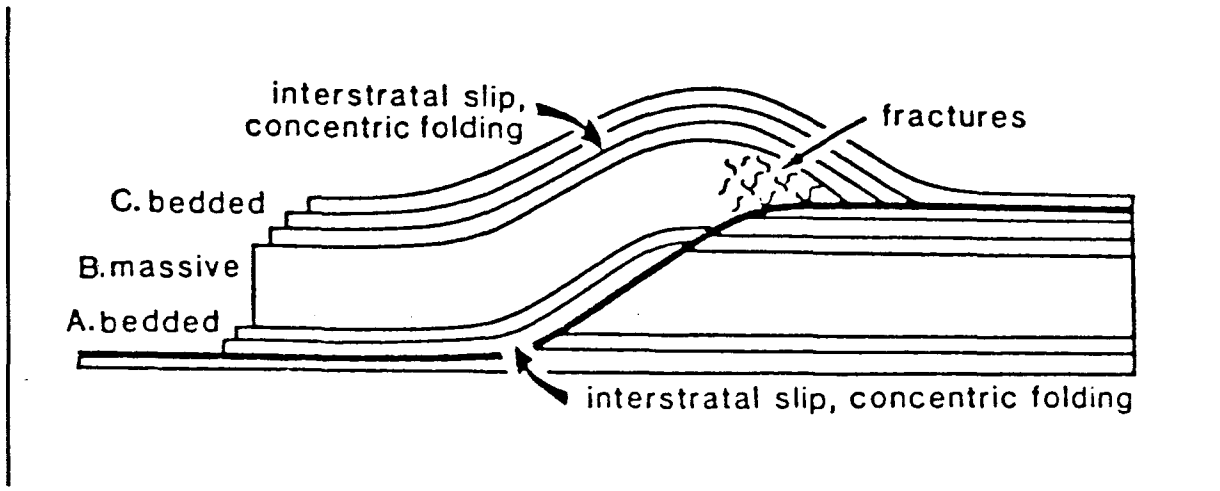

Figure 60 : Fractures developed in the relatively massive beds of a ramp-induced fold. (After Jones, 1987).

Central Rand Group in the Van Ryn area. Whilst it seems unlikely that a ramp (as opposed to a flat) would form within the relatively incompetent phyllonite, similar phenomena have been reported elsewhere in the world (Bombolakis, 1989).

The wide range in inclination of the axial planes of kinks to σ_1, as reported by Verbeek (1987), makes it difficult to conclusively determine the orientation of the stress field responsible for the development of the kinks in the Van Ryn region. If the possible angles of inclination of σ_1 to the anisotropic plane are also considered, however, a horizontal to sub-horizontal E to SE plunging σ_1 is indicated. The movements to the N, NE and E indicated by slickenfibres developed on the long limbs of the kinks suggests that episodic and progressively rotated movement has taken place. It might be anticipated that the significent uplift of the beds through ramp development would raise the rocks through a ductility transition to a shallower and more brittle environment. Late stage localised compression of the beds on an E-W trend could then result in N-S

trending kink bands with axial planes which dip steeply E. The continued episodic propogation of a thrust nappe into the region of the Van Ryn Fault may have inhibited the forward movement of the nappe and establish localised, shallow, relatively brittle deformation of the beds like that evidenced in the Van Ryn region.

7.3 Folds

All folds in the East Rand Goldfield lie along the same broad trends. Thrust ramps, indicative of a compressional event, are evident in the MK1 channels at 14 and SD Shafts. Flat faulting and "folding" of the channel beds, is documented by Kupisiewicz (1954-56) and Whiteside (1950) in the Footwall Reef Beds below the Central Rand Group unconformity. It would appear that the reported folding of these beds is actually the overturning of the beds against a ramp plane. As discussed above, this would be more easily achieved where ramping occurred on steep pre-existing planes such as channel banks, and where slightly oblique movement had occurred on these planes.

The development of the Springs Monocline on a NW-SE trend (Fig. 50) appears to be responsible for the current steep dip of the beds. The beds in the monocline are displaced by a NW-SE reverse fault with downthrow to the SW. The differential folding of beds of the monocline on either side of the ± E-W trending Vogel's Strike-slip Fault was cited by Ellis (1943) as evidence of folding on this axis both prior to and following the fault movement. Antrobus and Whiteside (1964) interpreted these features as being a result of recurrent growth of the fold, with

only minor fold development during syn-Central Rand Group times, and the major fold growth occurring during the emplacement of Ventersdorp Supergroup.

These folds (Fig. 50) were, therefore, probably initiated by the onset of a NE directed SW-NE compression during the closing stages of Central Rand Group sedimentation. Continued compression on this trend may have produced large scale blind thrust faults that accentuated the monocline.

The precise mode of formation of the other NW-SE trending folds (Van Dyk and Geduld-Modder Bee Anticlines) is difficult to ascertain due to the paucity of information available, i.e. no axial planar foliations, lineations or data on the beds at depth beneath these folds. They are, however, broad, open folds, which increases the problem of fold analysis.

The NE dip of the axial planes, as reported in the literature (Cluver, 1957), and determined using the axial traces of the folds together with the π girdles (section 4.5), does not appear to fit the thrust-fold models generally described in the literature (e.g. Gibson and Gray, 1985; Morley, 1986) (Fig. 61). Small scale structures in this Goldfield suggest, however, that a dip towards the foreland or hinterland of the axial planes is possible, and that the only restriction on the orientation of the axial planes of these folds is that, during development, their strike should be perpendicular to the direction of movement or propogation of the thrust fault. Fold growth due to faulting of this type will be a spasmodic response to seismic slip on the flat of the fault (Bombolakis, 1989) with an exponentially decreasing rate of growth for a short period

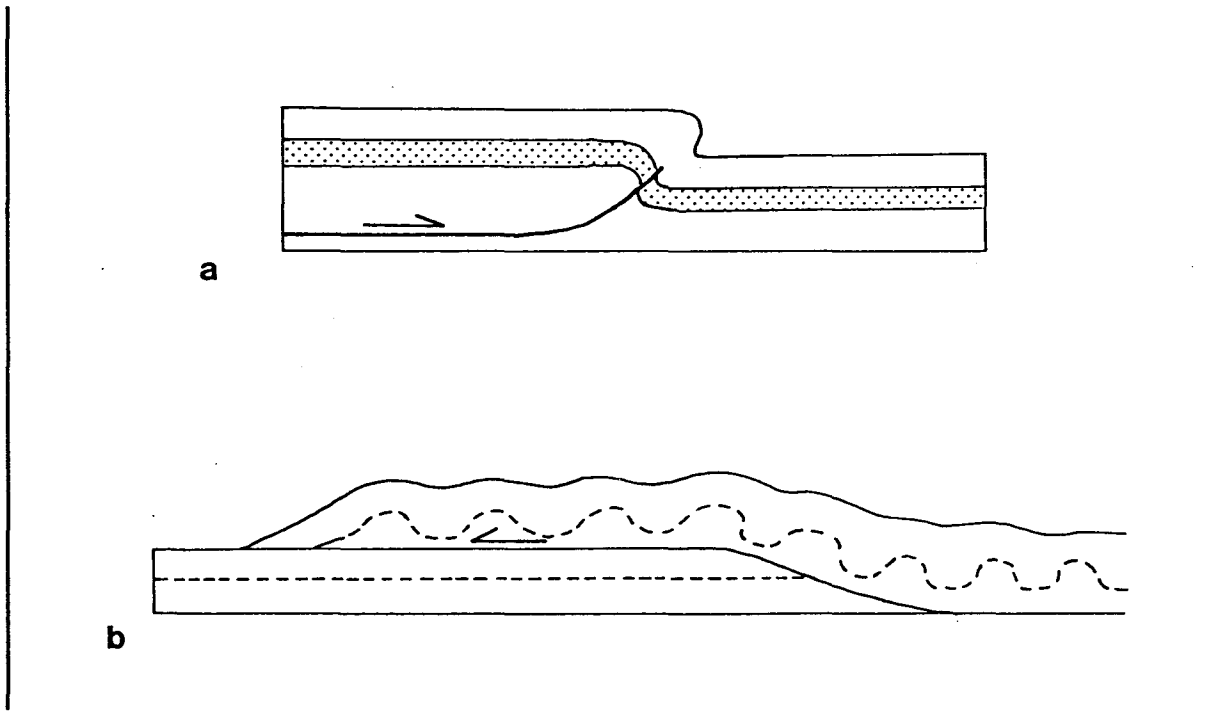

Figure 61 : a) The development of a monocline above a blind thrust (Morley, 1986). This alternative model for the formation of the NW-SE folds would be particularly applicable to folds of the nature of the Springs Monocline.
b) The tip-line fold pair model of Morley (1986), which may represent the mechanism of formation of the NW-SE fold axes during NE directed thrust faulting.

thereafter. Recurring slip on the thrust flat is thus manifested as recurring growth, and further results in a broadening of the fold (Bombolakis, 1989).

During the development of the Post-Transvaal, N directed compression, the orientation of the strike of these axial planes would have approximately paralleled that of the shear direction, and therefore have experienced little rotation but may have undergone further growth.

The surface and sub-surface strike of the Main Reef Leader appears to be broadly folded. Differential movement of

individual thrust sheets in a thrust fault system and the rapid sideways propogation of individual faults result in an interlocked apparently singular fault plane. The differential movement of the interlocked sheets become substantial at shortening of greater than 25-40% and results in a distinctly lobate and "folded" thrust front (Mulugeta and Koyi, 1987). The possible inhibition on forward movement of the thrust sheet by a barrier such as the Van Ryn Fault would further enhance differential movement - possibly leading to ramp development - and form a folded tongue of the thrust front away from the barrier. This morphology is demonstrated by the trace of the rocks of the Central Rand Group some distance to the NE of the Van Ryn Fault (Fig. 1).

7.5 Strain

The definition of the strain values associated with each individual compressional event was not within the scope of this investigation. For this reason, the overall resultant strain and displacement have been computed and are assumed to represent the cumulative effects of each successive event.

It is clear from the above discussion of the possible presence of a décollement during the N thrust event, that the rocks of the West and Central Rand Group do not form a single nappe. This fact suggests that the extrapolation of strain values for the Central Rand Group to the rocks of the West Rand Group would be erroneous. Short profiles mapped within the Jeppestown and Government Subgroups are, however, in close agreement with the values predicted for such lithologies by comparison with similar lithologies in the Turffontein Subgroup. It would appear,

therefore, that the strain experienced by both the Central and West Rand Groups was of the same order of magnitude, implying the NE thrust event had the most significant displacement.

The 9km displacement calculated is well within the range of total displacements of major overthrusts in various parts of the world (Gretener, 1972). In addition, a γ value of 1,25 has been calculated for rocks of the Witwatersrand Supergroup exposed on East Driefontein (Vermaakt, *et al*, in prep.), γ = 2,07 was found for the Parktown Shale Formation at Swartkops north of Johannesburg (Roering, 1985), and γ = 1 was predicted by Roering and Smit (1987) for the rocks of the entire Witwatersrand Supergroup. Shortening calculated through the restoration of N verging duplexes of the West Rand Group at Swartkops, is approximately 60% (Roering, 1985). Similar calculations applied to the lavas of the Klipriviersberg Formation (Ventersdorp Supergroup) reveal that a shortening of over 200% has been achieved through imbricate thrust faulting to the N (T. Hewitt, pers. comm., 1989). The strain and displacement reported here is thus of the order of the minimum strain due to thrust faulting reported elsewhere in the Witwatersrand Goldfield, and indicates that this style of faulting is not limited to the East Rand Goldfield. As the lower portion of the major ductile zone within the Jeppestown Subgroup is not exposed, this figure may be significantly underestimated; since it may be expected that the movement and strain will be greater within the lower portion of a thrust fault than in the upper portion (Elliot, 1976; Sanderson, 1982). Formation of many of the duplexes did not significantly deform the hangingwall, but, instead, they have almost parallel upper and lower detachments within the limits of the exposure. This

morphology of the duplexes has been predicted by both kinematic and mechanical models for ramps of low angle (Cruikshank *et al.*, 1989), and reported from elsewhere by Jones (1987) and Cooper *et al.*, (1983). This greatly inhibits the identification of markerless duplexes, and, in particular, of "foliation" duplexes. Underestimation of shortening on these planes is therefore likely. This, together with the reasons cited in section 5.3.3, suggest that this predicted displacement should be treated as an absolute minimum.

7.6 Chronology

The re-activation of shear planes by later stresses is a common phenomenon in the East Rand Goldfield. The orientation of later stresses do not, however, have to directly parallel the earlier stress systems, as deformation softening of planes will promote the use of pre-existing fault planes (Cobbold and Gapais, 1987). This makes the assignment of faults of any one strike orientation into a particular deformational period problematic. The present work yields a relative chronology of the history of this area which is similar, but not entirely compatible, with that of Antrobus and Whiteside (1964). Those events, such as specific dyke intrusions, which were not encountered in the exposures examined in this study, but which were documented by Kupisiewicz (1945-1956) and Antrobus and Whiteside (1964), have not been included in the proposed chronology, unless similar evidence was found in the study area. They are indicated by asterisks. The following relative chronology is proposed:

1. Deposition of the West Rand Group. (Post-3060 Ma).
2. Compressional deformation of the Footwall Reef Beds.

3. Disconformity.
4. Deposition of the pre-UK9A beds.
5. Disconformity.
6. Compressional deformation of the MK1 channel beds.
7. Initiation of a SW-NE compression and associated folding on a NW-SE trend.
8. Completion of the deposition of the Witwatersrand Supergroup.
9. Intrusion of the Ventersdorp dykes. (± 2700 Ma).
10. Extensional faulting of possible syn-Ventersdorp Supergroup age.
11. Major period of SW-NE compression resulting in NE directed thrust faults and the major growth period of associated folds with NW-SE axes.
12. ± E-W (strike 115 °) left-lateral strike-slip movement of the Vogel's Tear type. *
13. Intrusion of the Ilmenite Diabase dykes.
14. Right lateral NE-SW strike-slip faults.)unclear
    Steeply dipping ESE-WNW right lateral strike-slip faults.)relative
    NW-SE, moderate dip, strike-slip faults)ages
15. Moderate to steeply dipping N-S faults with oblique and normal movement.
16. Deposition of the Transvaal Sequence. (2500-2300 Ma).
17. N directed thrust fault movement.
18. Moderate N-S oblique movement)unclear
    NE-SW normal faulting)ages
19. Proposed NW thrust fault movement and tilting of steep NW-SE fold axes.
20. Intrusion of the Green Syenite dykes, of Bushveld Igneous Intrusion (2060 Ma) (Antrobus and Whiteside,

1964) or Pilansberg age (± 1300 Ma) (Grohmann, 1989).

21. Moderately dipping NW-SE strike-slip faulting.
22. Steep, right-lateral, E-W strike-slip faulting. *
23. Intrusion of the Karoo dolerites (± 200Ma).

The East Rand Goldfield has clearly been subjected to a complex, multi-deformational history. This history is characterised by alternating periods of compression and extension. The long time span (3060 Ma to 1400 Ma) over which these events took place accounts for the often apparently contradictory directions of movement, since successive faults do not necessarily relate to the same stress system. The reactivation of numerous pre-existing structures has been outlined in this study. Not only have pre-existing faults been reactivated by suitably oriented stress fields, but pre-existing folds have been accentuated by later stress fields. (It should be borne in mind that a force angled at 30° to a fault plane, or 90° to a fold axis, is "ideally oriented", and "suitably oriented" can diverge significantly from this angle.)

In particular, the confusing history and/or morphology of the following structures may be ascribed to reactivation :

- the folds and ramps of the Footwall Reef Beds and the MK1 channels,
- growth of the Springs Monocline during and after the deposition of the Central Rand Group sediments,
- shallow dips (± 45°) of the strike-slip faults of the Vogel's Tear type,
- the second generation of NW-SE and E-W strike-slip faults,
- N-S oblique and NE-SW normal faults.

The unusually shallow dip of the Vogel's Tear and related strike-slip faults suggests that this movement took place on previously formed normal or reverse faults. Ample evidence of earlier normal faults of this orientation in adjacent goldfields has been recorded (Spencer, 1986; Tweedie, 1986; Vermaakt, 1986). A plane of this orientation could also have acted as - or been initiated as - an oblique ramp during the preceding thrust faulting.

It is proposed by the author, as similarly suggested by Grohmann (1989) for the Central Rand Goldfield, that the apparent movement towards the NW on bedding parallel planes took place in response to compressive stresses active during the emplacement of the Bushveld Igneous Intrusion to the N. The ± E to W compression which these rocks must have undergone may also have tilted the steep NW-SE fold axes.

1. Most of the non-bedding parallel fault planes have experienced more than one period of movement.
2. These faults accommodated normal, reverse and strike-slip motions.
3. Bedding parallel faults are concentrated along the bedding contacts.
4. Such shears are manifested in all lithologies, but the frequency of shears and amount of strain recorded is dependent on the rock type. The shale units have, in particular, acted as a locus for such shearing. Their highly deformed character suggests that they should be regarded as phyllonites.
5. Bedding parallel shears are characterised by the presence of quartz schists, mylonite, quartz veins and phyllosilicate alteration.
6. Shear restricted quartz veins in the bedding plane shears parallel the foliation, developed in the plane of flattening, are syntectonic in origin and aided the movement of overlying strata during shearing.
7. All kinematic indicators imply a broad N movement on the S dipping bedding parallel shears, these shears are therefore thrust faults.
8. Directionally specific kinematic indicators display at least two thrust fault movement directions on bedding parallel shear planes in the Central Rand Group, one to the NE and a second to the N to NW. The second probably represents two overlapping directions of movement.
9. Only one direction of thrust fault movement is indicated in the West Rand Group, this is to the NE.

10. The NE thrust event is post-Ventersdorp dyke emplacement and pre-BRQF in age.
11. The N event is post-BRQF and pre-Karoo in age.
12. A possible third event of Bushveld intrusion age (2060 Ma) may be manifested as a NW thrust fault.
13. The contact between the Central Rand and West Rand Groups has acted as a major décollement during the second thrust fault event.
14. The folds in this region probably developed as result of the NE thrust faulting in pre-Transvaal times.
15. Minor additional growth of the folds during the N event seems likely.
16. Tilting of the fold axes during the postulated third thrust event is possible.
17. The resultant displacement across the Witwatersrand Supergroup arising from the thrust faulting is of the order of 9km, with an additional local shortening of up to 65% being achieved through duplex formation.

9. ACKNOWLEDGEMENTS

I wish to thank the CSIR, FRD and the RAU for funding this project. A great debt is owed to the staff of Consolidated Modderfontein Mines (1979) Ltd., particularly the geologists past and present: M. Austin, A. Auchterlonie, H. Clough, R. Linkogel, R. Sloman, J. Wilson and D. du Plessis.

Benoni Municipality and Dries van Heerden's surface blasting company were exceedingly co-operative and willingly granted access to sub-surface exposures!

Prof. C. Roering and **Prof. J. M. Barton Jnr.** initiated and supervised this project. I'll never understand where they found the patience. Thank you. The staff and post-graduate students of the RAU geology department contributed tireless discussion and support, and provided many answers to the unanswerable.

Thanks are especially due to my parents, **Lynn and Iain Pitts, my family and Tim Hewitt**; all of whom believed in me, even when they should have known better.

10. REFERENCES

Aleksandrowski, P. 1985. Graphical determination of principal stress directions for slickenside lineation populations: an attempt to modify Arthaud's method. *J. Struc. Geol.*, 7, 73-82.

Antrobus, E.S.A.; Whiteside, H.C.M. 1964. The geology of certain mines in the East Rand. *In* S.H. Haughton, Ed. *"The geology of some ore deposits of Southern Africa. Vol.1"*. Geol. Soc. S. Afr., Johannesburg, 125-160.

Armstrong, G.C. 1968. Sedimentological control of gold mineralization in the Kimberley Reefs of the East Rand Goldfield. *Information Circular*, Econ. Geol. Res. Unit, Univ. Witwatersrand, 47, 40 p.

Auchterlonie, D.A. 1987. A sedimentological and stratigraphic investigation of the Middle Kimberley Reef on Consolidated Modderfontein Mines (1979) Ltd. Unpubl. Hons. thesis, Univ. Witwatersrand, 120 p.

Bombolakis, E.G. 1989. Thrust fault mechanics and dynamics during a developmental stage of a foreland belt. *J.Struc. Geol.*, 11, 439-455.

Boyer, S.E.; Elliott, D. 1982. Thrust Systems. *Bull. Am. Assoc. Petrol. Geol.*, 66, 1196-1230.

Brandt, R.T. 1950. The geology of certain intrusive rocks in the Far East Rand, Transvaal. Unpubl. MSc. thesis, Univ.

Witwatersrand, 110 p.

Brock, B. B.; Pretorius,D. A. 1964a. An introduction to the stratigraphy and sedimentation of the Rand Goldfield. *In* S.H. Haughton, Ed. *"The geology of some ore deposits of Southern Africa. Vol.1"*. Geol. Soc. S. Afr., Johannesburg, 25-61.

Brock, B. B.; Pretorius, D. A. 1964b. Rand Basin sedimentation and tectonics. *In* S.H. Haughton, Ed. *"The geology of some ore deposits of Southern Africa. Vol.1"*. Geol. Soc. S. Afr., Johannesburg, 549-599.

Carleton-Jones, G. 1936. Correlation and other aspects of the exploited auriferous horizons on the Witwaterand Mining Field. (Pres. Address). *Trans. Geol. Soc. S.Afr.*, 39, 23-58.

Cluver, A.F. 1957. On the tectonic history and some related sedimentological aspects of the Witwatersrand and Ventersdorp Systems in the Far East Rand, during Upper - Witwatersrand, Pre-Transvaal System time. *Ann. Univ. Stellenbosch*, 33, Sect.A, 71-123.

Cobbold, P.R.; Gapais, D. 1987. Shear criteria in rocks: an introductory review. *J. Struc. Geol.*, 9, 521-524.

Cooper, M.A.; Garton, M.R.; Hossack, J.R. 1983. The origin of the Basse Normandie duplex, Boulonnais, France. *J. Struc. Geol.*, 5, 139-152.

Cooper, M.A.; Trayner, P.M. 1986. Thrust-surface geometry: implications for thrust-belt evolution and section-balancing

techniques. *J. Struc. Geol.*, **8**, 305-312.

Cousins, C.A. 1965. Disconformities in the Main Reef zone of the Witwatersrand System, and their bearing on reef correlation, with particular reference to the East, Central and West Witwatersrand. *Trans. Geol. Soc. S.Afr.*, **68**, 121-142.

Coward, M.P. 1987. The geometry of normal faults: Short Course Notes. Tect. Div. Geol. Soc. S. Afr., 371 p.

Coward, M.P.; White, S.H. 1988. The role of shear zones in the deformation and mineralization of the Archaean in Southern Africa: Short Course Notes. Tect. Div. Geol. Soc. S. Afr., 450 p.

Cruikshank, K.M.; Neavel, K.E.; Zhao, G.Z. 1989. Computer simulation of growth of duplex structures. *Tectonophysics*, **164**, No. 1, 1-12.

De Jager, F.S.J. 1964. The Witwatersrand System in the Springs-Nigel-Heidelberg sector of the East Rand Basin. *In* S.H. Haughton, Ed. *"The geology of some ore deposits of Southern Africa. Vol.1"*. Geol. Soc. S. Afr., Johannesburg, 161-190.

De Jager, F.S.J. 1986. The East Rand Goldfield and South Rand Goldfield. *In* E.S.A. Antrobus, Ed., *"Witwatersrand Gold - 100 Years"*.Geol Soc. S. Afr., Johannesburg, 111-167.

du Toit, A.L. 1954. Geology of South Africa. Oliver and Boyd, London, 611 p.

Elliot, D. 1976. The energy balance and deformation mechanisms of thrust sheets. *Phil. Trans. Roy. Soc. Lond.*, **283A**, 289-312.

Ellis, J. 1943. A tear fault in the Far East Rand. *Trans. Geol. Soc. S.Afr.*, **46**, 75-89.

Ellis, J. 1946. The simple dykes and sills of the Far East Rand. *Trans. Geol. Soc. S.Afr.*, **49**, 213-239.

Ellis, J. 1947. The Marievale Granophyre - a metamporhic rock. *Trans. Geol. Soc. S.Afr.*, **50**, 121-160.

Gibson, R.G.; Gray, D.R. 1985. Ductile - to - brittle transition in shear during thrust sheet emplacement, Southern Appalachian thrust belt. *J. Struc. Geol.*, 7, 513-525.

Ghosh, S.K. 1975. Distortion of planar structures around rigid spherical bodies. *Tectonophysics*, **28**, 185-208.

Greenberg, R. 1963. Structure-gold relationships as revealed by some Witwatersrand mine survey plans. *Trans. Instn. Min. Metall., London*, **73** (Bull. 683), 1 - 10.

Gretener, P.E. 1972. Thoughts on overthrust faulting in a layered sequence. *Bull. Can. Pet. Geol.*, **20**, 583-607.

Grohmann, G. 1989. Faulting and Dyking in the mines of the Central Rand Goldfield . *Information Circular*, Econ. Geol. Res. Unit, Univ. Witwatersrand, **204**, 39 p.

Hubbert, M.K.; Rubey, W.W. 1959. Role of fluid pressure in mechanics of overthrust faulting. *Geol. Soc. Am. Bull.*, 70, 115-166.

Hudleston, P.J. 1989. The association of folds and veins in shear zones. *J. Sruc. Geol.*, 11, 949-957.

Jones, P.B. 1987. Quantitative Geometry of Thrust and Fold Belt Structures. AAPG, Oklahoma, 26 p.

Kassner, T. 1933. Map of the East Rand. Hortors, Ltd. Johannesburg.

Krause, H.L. 1913. A contribution to the structural geology of the East Rand. *Trans. Geol. Soc. S.Afr.*, 15, 93-99.

Kupisiewicz, Z. 1954-1956. Unpublished mine reports, Anglo American Corporation of South Africa.

Lenthall, D.H. 1972. Quantitative compositional variations in Witwatersrand conglomerates in the East Rand - Delmas area, Transvaal. *Information Circular*, Econ. Geol. Res. Unit, Univ. Witwatersrand, 68, 43 p.

Lister, G.S.; Snoke, A.W. 1984. S-C mylonites. *J. Struc. Geol.*, 6, 617-638.

Lurie, J. 1981. *South African Geology*. 3rd Revised Edition. McGraw-Hill, Johannesburg. 189 p.

Malavieille, J. 1987. Kinematics of compressional and

extensional ductile shearing deformation in a metamorphic core complex of the northeastern Basin and Range. *J. Struc. Geol.*, 9, 541-554.

Mawer, C.K. 1987. Shear criteria in the Grenville Province, Ontario, Canada. *J. Struc. Geol.*, 9, 531-539.

McCarthy, T. S.; Charlesworth, E. G.; Stanistreet, I. G. 1986. Post-Transvaal structural features of the northern portion of the Witwatersrand Basin. *Information Circular*, Econ. Geol. Res. Unit, Univ. Witwatersrand, 191, 21 p.

Mellor, E.T. 1915a. The East Rand.*Trans. Geol. Soc. S.Afr.*, 18, 57-71.

Mellor, E.T. 1915b. The Upper Witwatersrand System.*Trans. Geol. Soc. S.Afr.*, 18, 11-56.

Morley, C.K. 1986. A classification of thrust fronts. *Bull. Am. Assoc. Petrol. Geol.*, 70, 12-25.

Mulugeta, G.; Koyi, H. 1987. Three-dimensional geometry and kinematics of experimental piggyback thrusting. *Geology*, 15, 1052-1056.

Nicholson, R.; Pollard, D.D. 1985. Dilation and linkage of echelon cracks. *J. Struc. Geol.*, 7, No. 5, 583-590.

Platt, J.P. 1983. Progressive refolding in ductile shear zones. *J. Struc. Geol.*, 5, 619-622.

Pretorius, D.A. 1964. The geology of the Central Rand Goldfield. *In* S.H. Haughton, Ed. *"The geology of some ore deposits of Southern Africa. Vol.1"*. Geol. Soc. S. Afr., Johannesburg, 63-108.

Pretorius, D.A. 1974. The nature of Witwatersrand gold deposits. *Information Circular*, Econ. Geol. Res. Unit, Univ. Witwatersrand, 86, 43 p.

Ralston, I.T. 1953. The complex intrusives of the Far East Rand. Unpubl. MSc. thesis. Univ. of Pretoria. 118 p.

Ramsay,J.G. 1980. Shear zone geometry: a review.*J. Struc. Geol.*, 2, 83-99.

Ramsay, J.G. 1967. *Folding and fracturing of rocks*. McGraw-Hill, New York. 568 p.

Raybould, J.G. 1975. Tectonic control on the formation of some fibrous quartz veins, Mid-Wales. *Geol. Mag.*, 112, 81-90.

Roering, C. 1984. The Witwatersrand Supergroup at Swartkops: A re-examination of the structural geology. *Trans. Geol. Soc. S. Afr.*, 87, 87-99.

Roering, C.; Smit, C. A. 1987. Bedding - parallel shear, thrusting and quartz vein formation in Witwatersrand quartzites. *J. Struc. Geol.*, 9, 419-427.

Roering, C.; Barton, J.M.; Winter, H. de la R. 1990. The Vredefort structure: a perspective with regard to new

tectonic data from adjoining terranes. *Tectonophysics*, ,

Roering, C.; Berlenbach, J.; Schweitzer, J. (in prep.) A guideline to the classification of fault rock. COMRO, 20 p.

Sanderson, D.J. 1982. Models of strain variation in nappes and thrust sheets: a review. *Tectonophysics*, **88**, 201-223.

Sharpe, J.W.N. 1943. Footwall and Kimberley Reefs on Government Gold Mining Areas. *Trans. Ass. Mine Mgrs. Transv.*, **2**, 851-873.

Sharpe, J.W.N. 1949. The economic auriferous bankets of the Upper Witwatersrand beds and their relationship to sedimentation features. *Trans. Geol. Soc. S. Afr.*, **52**, 265-288.

Simpson, C.; Schmid, S.M. 1983. An evaluation of criteria to deduce the sense of movement in sheared rocks. *Geol. Soc. of Amer. Bull.* **94**, 1281-1288.

Smith, G. 1964. Unpublished map of the East Rand. Anglo American Corp.

South African Committee for Stratigraphy (SACS). 1980. Stratigraphy of South Africa. Part 1. (Comp. L. E. Kent). Lithostratigraphy of the Republic of South Africa, South West Africa/Namibia, and the republics of Bophuthatswana, Transkei and Venda. *Handbk. Geol. Surv. S. Afr.*, **8**, 690 p.

Tankard, A.J.; Jackson, M.P.A.; Eriksson, K.A.; Hobday, D.K.;

Hobday, D.K.; Hunter, D.R.; Minter, W.E.L. 1982. Crustal Evolution of Southern Africa. Springer-Verlag, New York. 523 p.

Verbeek, E.R. 1987. Comment on "Kink folding in an extended terrane: Tortilla Mountains, southeastern Arizona". *Geology*, 15, 870-871.

Vermaakt, D.T.; Barnard, H.C.; Lambert, P.E. (in prep.) Evidence of northwards thrusting on East Driefontein Gold Mining Company Ltd. 17 p.

Vermaakt, D.T. 1986. The Sugarbush Fault: a structural analysis. Ext. Abstr. Geocongress '86.

Viring, R.G. 1986. The mineralisation and sedimentation of the MK1 Basal at Consolidated Modderfontein Mines (1979) Ltd. Unpubl mine report, CMM. 20 p.

Wagener, G.F. 1975. Sedimentary tectonics of the East Rand Basin with special reference to the Brakpan Formation. *Ann. Univ. Stellenbosch, Ser. A1*, 1, 233-286.

Walraven, F.; Armstrong, R.A.; Kruger, F.J. 1990. A chronostratigraphic framework for the north-central Kaapvaal craton, the Bushveld Complex and the Vredefort structure. *Tectonophysics*, 171, 1-26.

Whiteside, H.C.M. 1944. Discussion on "A tear fault in the Far East Rand". *Proc. Geol. Soc. S. Afr.*, 46, 56-59.

Whiteside, H.C.M. 1950. Geology of part of the Far East Rand basin. unpubl. Ph.D. thesis, London Univ., 190 p.

Wise, D.U.; Dunn, D.E.; Engelder, J.T.; Geiser, P.A.; Hatcher, R.D.; Kish, S.A.; Odom, A.L.; Schamel, S. 1984. Fault-related rocks: some suggestions for terminology. *Geology*, 12, 391-394.

MAP 1: LOCALITY MAP OF SURFACE EXPOSURES OF THE WITWATERSRAND SUPERGROUP IN THE GREATER BENONI AREA.